Master's thesis

NTNU
Norwegian University of Science and Technology
Faculty of Natural Sciences
Department of Chemical Engineering

Håvard Martin Fromreide

Dynamic Modelling and Control of a Silver-Catalysed Formaldehyde Production Plant

Master's thesis in Chemical Engineering and Biotechnology
Supervisor: Sigurd Skogestad, IKP
Co-supervisor: Nils Arne Susort, Dynea
June 2025

NTNU
Norwegian University of
Science and Technology

Håvard Martin Fromreide

Dynamic Modelling and Control of a Silver-Catalysed Formaldehyde Production Plant

Master's thesis in Chemical Engineering and Biotechnology
Supervisor: Sigurd Skogestad, IKP
Co-supervisor: Nils Arne Susort, Dynea
June 2025

Norwegian University of Science and Technology
Faculty of Natural Sciences
Department of Chemical Engineering

NTNU
Norwegian University of
Science and Technology

ABSTRACT

The development of plant-wide models for chemical processes has become an important tool available for chemical engineers in the design and operation of chemical process plants. With the advancement of chemical modelling, its range of application has also increased. These include in-depth analysis of the plant's response to proposed upgrades, determining optimal operation parameters, and exploring optimal process control structures. With the ability to provide accurate calculations and depictions of the system's dynamics, these models have proven to reduce design times and enhance plant performance.

In this thesis, a plant-wide model of a silver-catalysed formaldehyde production plant was developed based on an existing plant operated by Dynea. The process comprises a vaporiser, a reactor, and an absorption column used to convert methanol and oxygen into a liquid formaldehyde product. To represent the chemical behaviour in each unit, a variety of mathematical models were implemented into the model. Upon completion, the model was used to analyse the effects of introducing gas recycle as a potential control parameter for product quality. Additionally, the system's response to variations in the methanol concentration of the liquid feed was also investigated. All modelling and simulations were carried out using *MATLAB R2024b*

From the analysis, the methanol/oxygen ratio in the vapour feed to the reactor was identified as a key parameter for the quality of the final product. The implementation of gas recycling will affect this ratio and is a potential control parameter for the product composition. However, it was found that this also required the additional control of several other factors, such as the total gas flow and possibly reactor temperature.

SAMMENDRAG

Utviklingen av helhetlige modeller for kjemiske prosessanlegg har blitt et viktig verktøy for prosessingeniører i forbindelse med utforming og drift av slike anlegg. Fremskritt innen kjemisk modellering har også utvidet bruksområdet betydelig.

Dette inkluderer grundige analyser av prosessens respons på foreslåtte oppgraderinger, bestemmelse av optimale driftsparametere og utforsking av optimale prosesskontrollstrukturer. Med evnen til å gi nøyaktige beregninger og beskrivelser av systemets dynamikk, har slike modeller vist seg å kunne redusere designtid og forbedre anleggets effektivitet.

I denne oppgaven ble det utviklet en helhetlig modell av et sølvkatalysert formaldehydproduksjonsanlegg, basert på et eksisterende anlegg drevet av Dynea. Prosessen består av en fordamper, en reaktor og en absorpsjonskolonne, som benyttes til å omdanne metanol og oksygen til et flytende formaldehydprodukt. For å beskrive de kjemiske prosessene og dynamikken i de ulike enhetene, ble en rekke matematiske modeller implementert. Etter at modellen var ferdigstilt, ble den brukt til å analysere effekten av å introdusere gassresirkulering som en potensiell kontrollparameter for produktkvalitet. I tillegg ble systemets respons på variasjoner i metanolkonsentrasjonen i væskestrømmen også undersøkt. All modellering og simulering ble utført i *MATLAB R2024b*.

Fra analysen ble forholdet mellom metanol og oksygen i dampstrømmen til reaktoren identifisert som en nøkkelparameter for kvaliteten på sluttproduktet. Implementering av gassresirkulering vil påvirke dette forholdet og kan være en mulig kontrollparameter for produktets sammensetning. Det ble imidlertid funnet at dette også krever ekstra kontroll av flere andre faktorer, som total gassmengde og reaktortemperatur.

PREFACE

This thesis is the final work of the master's program in Chemical Engineering at the Norwegian University of Science and Technology in Trondheim, Norway.

I would like to thank my supervisor, Sigurd Skogestad, for his assistance in completing this project and for providing valuable feedback during the development of the model. I would also like to thank him for his patience and for sharing his extensive knowledge.

I would also like to thank my Co-supervisor, Nils Arne Susort, for his time and feedback, both during my specialisation project and master's thesis. His extensive knowledge of the process plant and control structure. His assistance with both plant data, PFDs, and general descriptions of the process has been an enormous help in the modelling process. I would also like to thank him for allowing me to work on this project, which has been highly interesting and educational as the final part of my studies.

Finally, I would like to thank my loved ones who made great efforts to support and assist me while working on this thesis. Their continued support and encouragement have been a major help in completing this project.

CONTENTS

LIST OF FIGURES

LIST OF TABLES

LIST OF ABBREVIATIONS AND SYMBOLS

Abbreviations

CV	Controlled Variable
FA	Formaldehyde
HF	Hemiformal
HEX	Heat Exchanger
$\mathbf{H_{Vap}}$	Enthalpy of Vaporization
$\mathbf{K_c}$	Controller Gain
L	Liquid
MG	Methylene Glycol
Me	Methanol
MPC	Model Predictive Control
MV	Manipulated Variable
PFD	Process Flow Diagram
P&ID	Process and Instrumentation Diagram
TMP	Throughput Performance Manipulator
UA	Overall Heat Transfer Coefficient
V	Vapor
VLE	Vapor-Liquid Equilibrium
WA	Water

Symbols

$\mathbf{C_p}$	Heat Capacity
$\overline{\mathbf{C}}_\mathbf{p}$	Mean Heat Capacity
$\mathbf{C_v}$	Valve Coefficient
$\mathbf{F}$	Flow of Vapor
$\mathbf{G}$	Gibbs Free Energy
$\mathbf{K}$	Equilibrium Constant
$\dot{\mathbf{m}}$	Mass Flow
$\mathbf{P}$	Vapor Pressure
$\dot{\mathbf{Q}}$	Heat Supplied
$\mathbf{R}$	Ideal Gas Constant
$\mathbf{s}$	Weighted Coefficient
$\mathbf{S}$	Entropy
$\mathbf{T}$	Temperature
$\overline{\mathbf{T}}$	Mean Temperature
$\tilde{\mathbf{x}}$	Overall Mole Fraction in Liquid Phase
$\mathbf{x_i}$	Mole Fraction of Component i in Liquid Phase
$\mathbf{y_i}$	Mole Fraction of Component i in Vapor Phase
$\boldsymbol{\delta}$	Stoichiometric Coefficient
$\boldsymbol{\gamma}$	Activity Coefficient
$\boldsymbol{\tau}_\mathbf{c}$	Closed-Loop Time Constant
$\boldsymbol{\tau}_\mathbf{L}$	Residence Time
$\boldsymbol{\xi}$	Extent of Reaction

CHAPTER

ONE

INTRODUCTION

Modelling and simulation of process systems are valuable assets for chemical engineers to determine possible optimisations and control schemes for the system. The potential for optimisation is always present in the process industry. This is especially true for older systems, which often depend on operational experience rather than on calculated optimal parameters or simulations. For new plants, the design basis for equipment and process parameters is primarily based on simulations and mass and energy balances for the system, depending on the specific requirements. While the development of extensive and accurate models is expensive and requires constant updates, they have proved invaluable for the process industry.

Each process plant is unique, and therefore, no uniform process model exists even for similar systems. However, research on the modelling of chemical processes and phenomena is continually evolving, providing readily available modelling approaches for typical processes that can be adapted for further work.

Tertiary systems of formaldehyde, methanol, and water have been extensively studied to determine accurate interaction parameters for such systems. The most widely accepted model was introduced by Maurer and is considered to capture these interactions accurately [1]. With advances in analytical techniques over the years, the model has undergone several updates since its original publication. Although it focuses solely on the vapour–liquid equilibrium and thermodynamics of the system, it provides a solid foundation for more comprehensive modelling of formaldehyde production plants.

1.1 Motivation

Dynea's formaldehyde production plant, located outside of Lillestrøm, may be categorised as an older plant. As a result, Dynea is frequently looking to improve its formaldehyde process. While models of the individual parts of the process have previously been the subject of several master's theses, these did not involve a complete process model. Optimising smaller sections, such as the control parameters of individual units, is an essential part of the optimisation process. However, for full-scale optimisations or investigations of the effect of changing parameters on the total process, a complete model is required.

In recent years, reducing emissions of greenhouse gases such as carbon dioxide and carbon monoxide has become increasingly important. For many chemical processes, such gases are often generated either through direct combustion or as by-products from other side reactions, such as the water-gas shift. In formaldehyde production, both carbon dioxide and carbon monoxide are formed through these reactions. Additionally, the tail gas contains high concentrations of nitrogen and hydrogen, resulting from the oxidation of methanol and the generation of hydrogen during product formation. The tail gas is therefore often used as fuel for steam generation, which is in turn utilised for process heating or external processes. While nitrogen and hydrogen serve a functional purpose, carbon dioxide and carbon monoxide are purely considered as emissions.

Gas recycling could reduce the initial formation of these emissions by shifting the chemical equilibrium in the formation reactions away from the production of these greenhouse gases. Since the tail gas inevitably contains some unreacted formaldehyde and methanol, recycling it increases the overall conversion of methanol and enables more formaldehyde to re-enter the process, ultimately ending up in the product.

The reduction of feedstock consumption is always essential in chemical processes, as this reduces the operational costs of the process. A key optimisation factor is therefore to minimise feedstock usage, while maintaining the product within the specifications. In formaldehyde production, the methanol feed is often combined with a separate water flow. Finding the optimal ratio between the two streams can reduce methanol use, resulting in a more economically efficient process while maintaining the same product quality.

1.2 Objective

The objective of this thesis was to develop a complete model of the formaldehyde process section of the Dynea plant, including the process control scheme used. This included the modelling of the vaporiser, reactor and absorption column.

The model was then used to investigate the impact of recycle gas on the process, where a portion of the tail gas from the absorption column was combined with the air feed. Additionally, the split ratio between the methanol and liquid feeds to the vaporiser was examined. The goal of these investigations was to determine a possible control structure for a newly installed in-line analysis meter on the product stream.

1.3 Previous work

In the specialisation project, parts of the plant were modelled. A dynamic model of the vaporiser was developed, while the reactor was modelled as a steady-state system using input from the vaporiser simulation. Both models were developed in *MATLAB R2024b*.

Controllers were also implemented for the vaporiser, including a level controller and a ratio controller for the liquid feeds.

The models were constructed using mass and energy balances for the system, based on thermodynamic data. The vaporiser included a vapour-liquid equilibrium model to determine the composition of the liquid and vapour phases. The reactor was made as a conversion model, in which a known fraction of oxygen was assumed to react in the oxygen-driven reactions. The equilibrium reactions were modelled using the Gibbs free energy of reaction to calculate the equilibrium constant. The reaction extent was then determined from these equilibrium constants, and the converted flows were calculated using reactive mass balances.

While the models aligned well with the dataset from the plant in certain aspects, there was still room for improvement in both models. These improvements include the implementation of a temperature controller to control reactor temperature and fine-tuning the level controller.

1.4 Thesis structure

The thesis is divided into six chapters. Chapter 1 provides a brief introduction to the thesis objectives and summarises the previously completed work carried out during the specialisation project.

Chapter 2 includes a description of the process, the design basis for the model, underlying assumptions, and the mathematical models used to represent the process. This chapter also presents process flow diagrams, chemical reactions and information about the thermodynamic coefficients used in the model.

Chapter 3 outlines the unit modelling process, including the implementation of the models described in Chapter 2 and the overall modelling structure. A description of the combined model structure, along with the process control structure, is also given.

Chapter 4 presents secondary findings for the model, such as results for model validation and tuning of controllers.

Chapter 5 presents the main findings from the simulations, along with the discussion and interpretation of these results

Chapter 6 contains the conclusion based on the analysis performed on the model

Chapter 7 Contains the recommendations for further work

CHAPTER

TWO

PROCESS DESIGN AND MODELLING

2.1 PFD

The process consists of a vaporiser with an external heating loop featuring a heat exchanger, a superheater that overheats the vapour from the vaporiser, a reactor and an absorption column. The process flow diagram of the modelled process is shown in Figure 2.1.1. As the heat exchangers in the absorption column are cooled by external cooling water, these were not included in the process model, instead, perfect temperature control was assumed in the column.

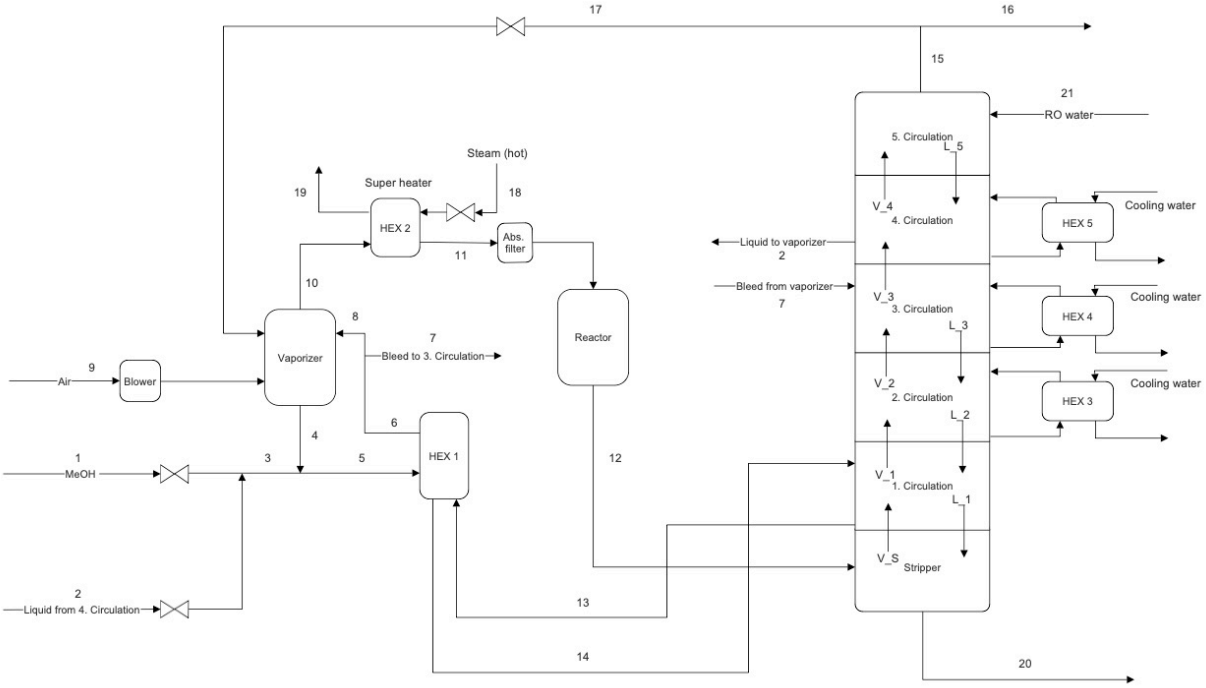

Figure 2.1.1: The process flow diagram for the whole system.

2.2 Process description

The process modelled in this master's thesis consists of three main parts. The first is a vaporiser, where a liquid mixture of water and methanol is vaporised and combined with an air feed containing oxygen and nitrogen. The resulting gas mixture is then fed into a reactor. The second part of the process is the reaction between vaporised methanol and oxygen from the air stream to form the desired product, formaldehyde. In addition to this main reaction, three side reactions also occur, consuming both oxygen and methanol. Reducing these side reactions is therefore critical to ensure that the majority of the feedstock is converted into the desired product. After the reaction, formaldehyde remains in the gas phase. To be recovered as a valuable product, the formaldehyde must be absorbed into a liquid phase. This occurs in the third part of the process, which consists of an absorption column. The gas stream from the reactor is introduced at the bottom of the absorption column, while water is fed into the top. The column operates using countercurrent absorption, enabling efficient transfer of formaldehyde from the gas to the liquid phase. The column is divided into several sections, allowing for improved control over the composition of the final liquid product collected at the bottom.

2.2.1 Vaporiser

The vaporiser in the system is designed as a large tank with a curved bottom and a conical top. Heating of the liquid inside the tank is primarily achieved through an external heating loop with a heat exchanger. Additional steam-heated coils are also installed inside the tank, allowing for supplemental heating using steam if the heat supplied by the exchanger is insufficient.

The liquid feed going to the vaporiser (Flow 3) consists of a liquid stream from the absorption column (Flow 2) and a pure methanol stream (Flow 1). The relationship between the liquid and pure methanol streams that make up the feed is controlled by a ratio controller. As sections 4 and 5 of the absorption column are gas cleaning sections, the liquid flow will include some methanol and formaldehyde in addition to water. This allows for a higher degree of methanol conversion as less methanol is lost in the tail gas from the top of the column, instead being recycled back to the vaporiser.

The feed enters the heating loop of the vaporiser, where it is combined with the liquid from the bottom of the vaporiser (Flow 4). The combined liquid (Flow 5) is circulated through a heat exchanger (HEX 1), where it heats the feed to the desired temperature. The heated liquid (Flow 6) is divided into the bleed to the 3rd section of the absorption column (Flow 7) and the liquid into the vaporiser (Flow 8). As previously described, the liquid from the 4th section of the absorption column is used as the feed to the vaporiser. The bleed to the 3rd section is therefore working as the absorption liquid for the lower parts of the column. A flow controller regulates the bleed and is typically set to a constant mass flow rate, determined by the production rate.

The feeds to the vaporiser also include an inlet of cleaned outside air (Flow 9), which makes up the oxygen used in the reactions to form formaldehyde. As a result, the stream is also composed of nitrogen, water and some carbon dioxide. Due to their low solubility in water, these gases make up most of the vapour phase and are included in the vapour stream to the reactor (Flow 10) along with the vaporised liquid. In addition to the airstream, the tail gas from the absorption column can be recycled to the vaporiser (Flow 17) to make up part of the total gas feed. Similar to the liquid from the 4th circulation, the recycled gas will also contain trace amounts of both formaldehyde and methanol. The use of gas recycling can therefore be employed to enhance the process efficiency.

The gas feeds to the vaporiser are led directly into the vaporiser through nozzles in the gas-feeding pipe, located below the liquid surface inside the tank. This increases the liquid's vapour pressure, allowing for a higher degree of vaporisation at lower temperatures. For this effect to take place, the liquid level must be maintained above the nozzles, forming a minimum point.

The vapour containing the gas feeds and vaporised liquid is led through a heat exchanger (HEX 2) in order to increase the temperature by 10 °C before entering the reactor. This ensures the complete vaporisation of the vapour stream, as any liquid droplets still present in the vapour will damage the silver catalyst. The heated vapour (Flow 11) is then fed into the reactor.

2.2.2 Reactor

The reactor is designed as a fixed-bed reactor, with a waste heat boiler located below to cool the gas and generate steam using the excess heat. The oxygen and methanol in the vapour feed (Flow 11) react over a silver catalyst bed. The desired formaldehyde product is produced through the partial oxidation of methanol, a reaction that occurs in this process. Although the catalyst is highly selective towards this reaction, complete oxidation of the methanol also occurs, producing carbon dioxide and water instead. Both of these reactions are exothermic and will increase the temperature in the reactor. In the absence of oxygen, an endothermic dehydrogenation of methanol will occur over the catalyst, resulting in the reduction of methanol to formaldehyde and hydrogen. With the presence of hydrogen, water and carbon dioxide, a fourth exothermic water-gas shift reaction occurs, producing carbon monoxide.

Other small-scale reactions, such as the formation of methylene glycol and hemiformal, will also take place. However, the main reactions in the process are assumed to include the four previously mentioned reactions. Partial oxidation and complete oxidation of methanol are given by Equation 2.1 and 2.2, respectively. These reactions are considered irreversible reactions and are limited by the amount of reactants available. Usually, the limiting reactant in the process is oxygen, as the dehydrogenation of methanol also produces formaldehyde. The equilibrium reactions for dehydrogenation of methanol and water gas shift are given in Equation 2.3 and 2.4.

$$\mathrm{CH_3OH} + \frac{1}{2} \cdot \mathrm{O_2} \longrightarrow \mathrm{HCHO} + \mathrm{H_2O} \Delta_\mathrm{r} \mathrm{H}_{298} = -158\,\mathrm{kJ/mol} \tag{2.1}$$

$$\mathrm{CH_3OH} + \frac{3}{2} \cdot \mathrm{O_2} \longrightarrow \mathrm{CO_2} + 2 \cdot \mathrm{H_2O} \Delta_\mathrm{r} \mathrm{H}_{298} = -726\,\mathrm{kJ/mol} \tag{2.2}$$

$$CH_3OH \rightleftharpoons HCHO + H_2 \Delta_r H_{298} = 85\,\mathrm{kJ/mol} \tag{2.3}$$

$$CO + H_2O \rightleftharpoons CO_2 + H_2 \Delta_r H_{298} = -41\,\mathrm{kJ/mol} \tag{2.4}$$

The oxidation of methanol, both complete and partial, are exothermic reactions and contributes significantly to the increase in reactor temperature. The temperature in the reactor is therefore mainly controlled by the oxygen-to-methanol ratio in the vapour feed. Both of these reactions are oxygen-driven, and an increase in oxygen content would consequently lead to an increase in reactor temperature. With the dehydrogenation of methanol in the deficit of oxygen being endothermic, reducing oxygen would instead lower the reactor temperature. The reactor temperature is therefore controlled based on the vaporisation of methanol by increasing or decreasing the heat supplied to the vaporiser.

Most of the oxygen in the vapour feed will be consumed during these reactions, and the converted gas stream (Flow 12) can be assumed to contain almost zero oxygen. Due to the oxygen-driven reactions being exothermic, the temperature set-point in the reactor is around 650 °C. This makes the partial oxidation of methanol more thermodynamically preferable due to the lower exothermic energy while still allowing for optimal conditions for the silver catalyst. The converted gas stream (Flow 12) is then cooled through a waste heat boiler before being fed to the top of the stripper section in the absorption column.

2.2.3 Absorption column

The absorption column is designed as a countercurrent column divided into several sections. These sections consist of three absorption sections, a stripper section at the bottom of the column, and two additional gas cleaning sections above. The lower sections get their liquid feed from the section above, except for the 3rd section, which receives liquid through a bleed from the vaporiser (Flow 7). In the column, there is no exchange of liquid between the 4th and 3rd sections, with the liquid from the 4th section instead acting as an additional liquid feed to the vaporiser (Flow 2). As a result, the vapour absorbed into the liquid in the gas cleaning sections does not end up in the product, instead, it is recycled back to the vaporiser. This reduces the loss of both methanol and formaldehyde, while allowing sections 4 and 5 to have a higher liquid flow than needed for the rest of the column. Ensuring a higher degree of absorption into the liquid and less product leaving the column as part of the tail gas (Flow 15). The liquid feed into the top of the column (Flow 21) is directed into the top of section 5 and consists of pure water. The liquid then flows down into the 4th section to act as the absorption liquid in both sections, in addition to the supplementary liquid feed to the vaporiser. The cleaned vapour leaving the column as tail gas can either be recycled (Flow 17) or be used as fuel in an external furnace to produce steam (Flow 16).

The vapour from the reactor (Flow 12) is fed into the top of the stripper section and rises upwards inside the column. The liquid bleed from the vaporiser (Flow 7) is flowing downwards from the 3rd section. In each section, some of the gas is absorbed into the liquid. The potential absorption in the column is increased by using packing in certain parts of the column. This increases the gas-liquid interface, leading to greater interaction between the liquid and vapour phases. While the other sections are composed of a packed part and a sump at the bottom, the stripper section is instead designed as a tray column. This allows some of the water, methanol, and formaldehyde to be re-vaporised, increasing the formaldehyde concentration of the product while also reducing the methanol content. The product stream (Flow 20) leaves the bottom of the column for further processing before being stored.

The absorption itself can be considered as a mildly exothermic reaction between the absorbed gas components and the liquid. There are also exothermic reactions between formaldehyde and water, as well as between formaldehyde and methanol. The reaction between formaldehyde and water leads to the formation of methylene glycol ($HO(CH_2O)H$) as shown in Equation 2.5. Further polymerization will form poly(oxymethylene) glycols ($HO(CH_2O)_iH$) given by Equation 2.6, for i > 1. The reactions between formaldehyde and methanol will instead form hemiformal ($HOCH_2OCH_3$), with further polymerisation leading to poly(oxymethylene) hemiformals ($HO(CH_2O)_iCH_3$) for i > 1. These reactions are given by Equation 2.7 and Equation 2.8, respectively.

$$\mathrm{H_2O + CH_2O \rightleftharpoons HO(CH_2O)H} \tag{2.5}$$

$$\mathrm{HO(CH_2O)_{\mathit{i}-1}H + HO(CH_2O)H \rightleftharpoons HO(CH_2O)_{\mathit{i}}H + H_2O} \tag{2.6}$$

$$\mathrm{CH_3OH + CH_2O \rightleftharpoons HO(CH_2O)CH_3} \tag{2.7}$$

$$\mathrm{HO(CH_2O)_{\mathit{i}-1}CH_3 + HO(CH_2O)CH_3 \rightleftharpoons HO(CH_2O)_{\mathit{i}}CH_3 + CH_3OH} \tag{2.8}$$

As a result of the increase in temperature caused by these reactions, the column must be cooled to maintain the temperature profile within the column. For sections 2 and 3, cooling is achieved by circulating the liquid through heat exchangers (HEX 3, HEX 4) using external cooling water. For section 1, however, the liquid serves as the heating medium in the heat exchanger, heating the vaporiser liquid (HEX 1) and providing heating for the vaporiser (Flow 13). The returning flow acts as a cooling medium for the section (Flow 14). As the stripper section only consists of trays, the liquid for this section is not cooled, instead, the temperature is determined by the temperature of the liquid from the sections above and the vapour from the reactor.

2.3 Design basis

The design basis for the modelled process was Dynea's silver-catalysed formaldehyde production plant in Lillestrøm. In order to make the model comparable to real values, a dataset was supplied by Dynea for comparison with the resulting model values. The data were based on measurements and internal calculations done by Dynea at a time of relative stability in production and are presented in Appendix F. The measured feed flows that were used as initial parameters for the model are given in Table 2.3.1, and their compositions are shown in Table 2.3.2.

Table 2.3.1: The flow and temperature of the feed flows to the vaporiser and the ratio of controllers as given by Dynea, used as initial simulation input.

Feed	**Flow [kg/h]**	**Temperature [°C]**
Methanol (Flow 1)	4793	3
Column bleed (Flow 2)	2780	26.3
Air (Flow 9)	7712	47

Table 2.3.2: The molar composition of the feed flows to the vaporiser as given by Dynea, used as the initial simulation input.

Component	**Methanol**	**Column bleed**	**Air**
Formaldehyde	0	0.034	0
Water	0	0.949	0.04
Methanol	1	0.017	0
Oxygen	0	0	0.208
Nitrogen	0	0	0.788

To ensure the model accurately represents the real process, the same specifications were applied as those used in the real process. These included the temperature of the reactor, the formaldehyde concentration in the product and the methanol concentration in the product. The mass flow of product was also used to validate the model. The process specifications are shown in Table 2.3.3. These specifications were used in order to validate the model.

Table 2.3.3: The specifications for the simulated values of reactor temperature, formaldehyde and methanol concentration in the product and the flow-rate of the product stream.

Parameter	**Value**
Reactor temperature	646 °C
Formaldehyde in product	52 %w/w
Methanol in product	1 %w/w
Product flow rate	7708 kg/h

Some of the process parameters were determined by the controllers implemented in order to maintain liquid levels and temperatures. The temperature set-points for the system are given in Table 2.3.4.

Table 2.3.4: The temperature set-points for the process units from measurements by Dynea, including each of the sections in the absorption column.

Process unit	**Temperature [°C]**
Reactor	646
Stripper	90
Section 1	80
Section 2	70
Section 3	55
Section 4	22
Section 5	22

Only the vaporiser level and the liquid level of the 4th and 5th sections of the absorption column are directly controlled. The rest of the sections were instead controlled by the approximated liquid flow dynamics through the section when the sump was full. The liquid volumes for the vaporiser and each section of the absorption column are given in Table 2.3.5.

Table 2.3.5: The liquid volumes for the units in the system, including the individual sections and stripper in the absorption column.

Process unit	**Liquid volume [m^3]**
Vaporiser	23.33
Stripper	1.39
Section 1	7.82
Section 2	5.33
Section 3	1.40
Section 4	0.70
Section 5	0.27

To determine the vapour flow out of the vaporiser and each section in the absorption column, a simplified valve equation was used. The vapour flow is calculated as a function of the pressure difference between the pressure in the unit and the downstream pressure. A coefficient C_v was defined experimentally to determine the vapour flow based on the calculated pressure in the units. The coefficient was fitted to ensure that the pressure in the vaporiser and column sections matched the Dynea measurements. The pressures for each unit given by Dynea are listed in Table 2.3.6.

Table 2.3.6: The measured pressure in the vaporiser and each part of the absorption column used to define the fictitious valve coefficient C_v to calculate vapour flows out of the units.

Process unit	**Pressure [Bar]**
Vaporiser	1.269
Stripper	1.105
Section 1	1.102
Section 2	1.100
Section 3	1.095
Section 4	1.092
Section 5	1.090

The reactions for the oxidation of methanol in the reactor are oxygen-driven, as further described in section 2.2.2. To model the conversion from each of these reactions, as given by Equations 2.1 and 2.2, a fraction of the oxygen reacting in the first reaction was used. The fraction was based on the calculations previously made by Fraihat in his master thesis [2], and is presented in Table 2.3.7. The remaining oxygen was assumed to be consumed in the second reaction.

Table 2.3.7: Fraction of oxygen reacting in the partial oxidation of methanol.

Parameter	**[-]**
Fraction of oxygen reacted	0.71

The level in the vaporiser is controlled by a level controller, as further described in Section 3.5.1. The controller determines the inflow of methanol feed, which is in ratio with the additional water feed. The ratio is defined as the mass of water divided by the mass of methanol. The set-points for both the liquid level and the ratio controller, as given by Dynea measurements, are presented in Table 2.3.8.

Table 2.3.8: Set-point for liquid level in the vaporiser and ratio controller for the water feed, with the ratio given as mass of water/mass of methanol.

Parameter	**Set-point**
Liquid level	23.33 m^3
Feed ratio	0.58 %

2.3.1 Modelling assumptions

When modelling the process, several assumptions were made in order to simplify the mathematical models. These assumptions are summarised in the section below.

2.3.1.1 Assumptions for the vaporiser model

For the vaporiser model, the following assumptions were made to simplify the calculations of the vapour and liquid composition, along with the hold-up and temperature inside the vaporiser.

- The vaporiser system is assumed to reach vapour-liquid equilibrium.
- The vaporiser system is assumed to maintain vapour-liquid equilibrium at all times.
- It is assumed that only Formaldehyde, Methanol, and Water exist in the liquid phase.
- Oxygen and Nitrogen only exist in the vapour phase.
- If utilising recycled gas from the absorption tower, hydrogen, carbon dioxide and carbon monoxide are also assumed to only exist in the vapour phase.
- The formaldehyde in the liquid will behave as water in the vapour-liquid equilibrium due to the very low concentration.
- The activity coefficients of the liquid components can be modelled as a binary mixture of methanol and water
- The downstream pressure drives the vapour flow out of the vaporiser.
- The vapour behaves as an ideal gas
- The integrated heating system of the steam coils and external cooling can be modelled as a changing UA value of the heat exchanger while keeping the flow and temperature of heating liquid from the absorption column constant.

2.3.1.2 Assumptions for the reactor model

- The oxygen will be consumed entirely in the first and second reactions given by Equation 2.1 and Equation 2.2.
- The third and forth reaction given by Equation 2.3 and Equation 2.4 are equilibrium reactions.
- There is no loss of heat to the surroundings, and the temperature can be found from the energy balance over the reaction.
- The gas mixture can be considered as an ideal gas.
- The reactions are instantaneous with no delaying dynamics.
- The pressure inside the reactor can be considered constant at all times.
- There is no work being done due to a difference in volume or pressure.
- The catalytic activity is constant.

2.3.1.3 Assumptions for the absorption column

For the absorption column, the following assumptions were made. Due to the column being modelled in two different approaches, one pure VLE model and one model based on Maurer's model with polymer reactions [1], the assumptions for each model are listed below.

For the column model, only considering VLE without any reactions, the following assumptions were made.

- Each section reaches vapour-liquid equilibrium.
- The vapour and liquid remains at equilibrium at all times.
- Liquid consists of only formaldehyde, water and methanol.
- The other components do not absorb into the liquid
- Temperature control is perfect, and temperature is constant.
- Absorption can be modelled as condensation of the gas phase.

For the column model, which includes the polymerisation of formaldehyde into methylene glycol and hemiformal, the following assumptions were made.

- Each section reaches vapour-liquid equilibrium
- Remains at equilibrium at all times
- Liquid consists of only formaldehyde, water and methanol.
- The other components do not absorb into the liquid
- Temperature control is perfect, and temperature is constant.

2.4 Mathematical models

2.4.1 Models used in the vaporiser

The calculations used to model the vaporiser system were adapted from a model previously developed during Fromreide's specialisation project. However, some modifications were made in order to compare different approaches to modelling formaldehyde in the liquid phase. These modifications involved differences in how the vapour-liquid equilibrium (VLE) was calculated inside the vaporiser. Mainly by including activity coefficients for the formaldehyde in the liquid and adjusting the Antoine's coefficient A to closer fit the dataset provided by Dynea

The VLE model was also extended to include all gases that may exist in the vapour phase, such as H_2, CO_2 and CO. This was done in order to allow the model to account for the presence of these gases in the vapour phase. This will be introduced when simulating the process with a recycled gas stream from the absorption column. However, the main approach for calculating the VLE, with its resulting vapour phase composition and total pressure, is identical to the previous model, and further described in section 2.4.1.1.

2.4.1.1 Vapour-liquid equilibrium model

To determine the composition of the liquid and vapour phase in the vaporiser, a simplified vapour-liquid equilibrium (VLE) was used. The VLE model was developed using the extended version of Raoult's law, which also implements activity coefficients to account for the non-ideality of the liquid mixture. Raoult's law states that the partial pressure of each component in the vapour phase equals the partial pressure of the pure component vapour in the liquid phase.

The pure component vapour pressure for the liquid components was determined based on Antoine coefficients shown in Table 2.4.1. The vapour pressures are found from Antoine's equation given by Equation 2.9 [3]. These coefficients will provide the pressure in torr when used in Equation 2.9. [3]

Table 2.4.1: Antoine coefficients for methanol and water [3].

Component	**A**	**B**	**C**
Methanol	8.07247	1574.99	238.86
Water	7.94917	1657.462	227.02

$$\log \mathrm{P_{vp}} = \mathrm{A} - \frac{\mathrm{B}}{\mathrm{T} - \mathrm{C}} \tag{2.9}$$

While Raoult's law is often used to describe the vapour-liquid equilibrium of ideal mixtures, it has proven to be less accurate for highly non-ideal systems with multiple components. For the vaporiser system, it is assumed that the liquid contains a tertiary mixture of methanol, water and formaldehyde. The liquid can therefore not be considered ideal. In order to account for the non-ideality of the liquid phase, the extended Raoult's law was employed. The extension involves implementing activity coefficients for each liquid component to describe the interaction between components in the calculation of the liquid's vapour pressure.

To determine the interaction between the components in the liquid, UNIQUAC activity coefficients (γ_i) were calculated [4]. The calculation of the coefficients is given in Appendix A. These coefficients are applicable for both vapour-liquid and vapour-vapour systems and can therefore be used to find the vapour composition.

Due to the low concentration of formaldehyde that is expected in the vaporiser system, it was assumed that the formaldehyde content in the liquid could be modelled as behaving similarly to water. As a result, the effect of the formaldehyde on the activity coefficients in the liquid was neglected, and only the activity coefficients of water and methanol were taken into account. The vapour composition of formaldehyde was then calculated using the same activity and vapour pressure as water. The system is therefore essentially modelled as a two-component binary mixture.

Using the pure component vapour pressures and activity coefficients, the vapour pressure of the binary mixture can be determined from Equation 2.10. Where $\mathrm{x_i}$ and γ_i denote the composition and activity coefficient of liquid component i, respectively.

$$\mathrm{P_{bin}} = \sum_{\mathrm{n=1}}^{\mathrm{n}} \mathrm{P_{vp,i}} \cdot \mathrm{x_i} \cdot \gamma_\mathrm{i} \tag{2.10}$$

The extended Raoult's law can then be applied to determine the resulting composition in the vapour phase based on their partial pressures in the liquid phase, as shown in Equation 2.11.

In the vaporiser system, certain components, oxygen, nitrogen, hydrogen, carbon dioxide, and carbon monoxide, were modelled as existing only in the vapour phase. The vapour compositions of these were calculated from the dynamic mass balances and vapour hold-up. To account for their presence, their contributions were subtracted from the total vapour composition available to the vaporised liquid components.

$$\mathrm{y_i} = \frac{\mathrm{P_{vp,i}} \cdot \mathrm{x_i} \cdot \gamma_\mathrm{i}}{\mathrm{P_{bin}}} \tag{2.11}$$

Following Dalton's law for the total pressure of a vapour system, which states that the total pressure of the vapour must equal the sum of the partial pressures of its components, the total pressure can be calculated. The pressure inside the vaporiser was thus determined from Equation 2.12. Here, $\mathrm{y_{vaporised}}$ refers only to the vapour-phase fractions of the components that contribute to $\mathrm{P_{bin}}$.

$$\mathrm{P} = \frac{\mathrm{P_{bin}}}{\sum_{\mathrm{n=1}}^{\mathrm{n}} \mathrm{y_{vaporised,i}}} \tag{2.12}$$

2.4.1.2 Vapour outflow

The vapour outflow from the vaporiser was modelled using a fictitious valve. A simplified valve equation is given in Equation 2.13. F represents the flow of the vapour, while $\mathrm{P_1}$ and $\mathrm{P_2}$ represent the measured downstream pressure above the reactor and the pressure inside the vaporiser found from the VLE calculations, respectively.

$$\mathrm{F} = \mathrm{C_v} \cdot \sqrt{\mathrm{P_2} - \mathrm{P_1}} \tag{2.13}$$

The C_v value was determined by adjusting simulated values to match the measured pressure inside the vaporiser when simulating the vaporiser to steady-state using input data from the Dynea dataset.

2.4.1.3 Enthalpy model

The energy calculation for the vaporiser was based on the dynamic energy balance of the system. To determine the balance, the enthalpy of the flows into and out of the system was calculated. To streamline this process, a simple enthalpy model was constructed, enabling the fast calculation of the enthalpy for any stream composition of both vapour and liquid streams.

The enthalpy was determined from the temperature of the stream in addition to its composition and state, making it usable for any part of the modelled process. The model is based on calculating the enthalpy of a gas or liquid stream, given its state, and only includes the vaporisation energy if the stream is defined as a gas. Since the energy balance is based on the difference in enthalpy, this captures the energy required to vaporise the liquid well, as the initial gas feed will include the vaporisation energy at all times.

To calculate the enthalpy, the system first needs to determine the mean heat capacity of the stream over the temperature interval, as further described in Section 2.4.1.4. The specific enthalpies of the gas and liquid streams are given by Equations 2.14 and 2.15, respectively. [5]

$$\Delta \mathrm{h_{gas}} = \mathrm{y_i} \cdot \mathrm{H_{Vap,i}} + \bar{\mathrm{C}}_{\mathrm{p,vi}} \cdot \mathrm{y_i} \cdot \Delta \mathrm{T} \tag{2.14}$$

$$\Delta \mathrm{h_{liquid}} = \bar{\mathrm{C}}_{\mathrm{p,li}} \cdot \mathrm{x_i} \cdot \Delta \mathrm{T} \tag{2.15}$$

In these expressions, h denotes the specific enthalpy of the stream (in J/mol), and $H_{Vap,i}$ represents the enthalpy of vaporisation of component i (also in J/mol). The terms $C_{p,li}$ and $C_{p,vi}$ correspond to the mean heat capacities of component i in the liquid and vapour phases, respectively. The variables x_i and y_i refer to the mole fractions of component i in the liquid and vapour streams.

The vaporisation enthalpies for the components that were used in the model are listed in Table 2.4.2.

Table 2.4.2: The vaporisation enthalpy for the components at 298 K [6].

Component	**Δ H_{vap}**
Formaldehyde	24.48
Water	40.68
Methanol	35.21
Oxygen	6.82
Nitrogen	5.58
Hydrogen	0.89
Carbon Dioxide	0
Carbon Monoxide	6.04

2.4.1.4 Heat capacity

From Equation 2.14 and Equation 2.15, it can be observed that the enthalpy model that was previously described in section 2.4.1.3 requires the heat capacity of the stream for its calculations. A model was constructed to define the mean heat capacity of the components over the temperature interval between the reference temperature (T_0) and the temperature of the stream (T).

As the process contains both gas and liquid phases in most processes, except for the reactor, the model includes calculations of the mean heat capacity for both states. Table 2.4.3 gives the ideal gas heat capacity coefficients for the components in the gas phase, with the heat capacity given from Equation 2.16. [7] The mean heat capacity for the components is determined from Equation 2.17. [5]

Table 2.4.3: Constants for the ideal gas heat capacity equation, C_p = J/mol K [7].

Component	**A**	**B**	**C**	**D**
Formaldehyde	23.475	3.1568E-02	2.9852E-05	-2.300E-08
Water	32.243	1.9238E-03	1.0555E-05	-3.596E-09
Methanol	21.152	7.0924E-02	2.5870E-05	-2.852E-08
Oxygen	28.106	-3.680E-06	1.7459E-05	-1.065E-08
Nitrogen	31.150	-1.357E-02	2.6796E-05	-1.168E-08
Hydrogen	27.143	9.2738E-03	-1.381E-05	7.6451E-09
Carbon Dioxide	19.795	7.3436E-02	-5.602E-05	1.7153E-08
Carbon Monoxide	30.869	-1.285E-02	2.7892E-05	-1.272E-08

$$C_p(T) = A + B \cdot T + C \cdot T^2 + D \cdot T^3 \tag{2.16}$$

$$\bar{C_p} = \frac{1}{(T - T_0)} \cdot \int_{T_0}^{T} C_p(T)\, dT \tag{2.17}$$

For the heat capacity of the liquid, only the coefficients for formaldehyde, water and methanol were included, as the rest of the components are assumed to only exist in the gas phase. The coefficients used in the model are shown in Table 2.4.4. The calculation of the mean heat capacity for the liquid components is identical to that for gas and follows Equation 2.17.

Table 2.4.4: Constants for the liquid heat capacity, C_p = J/mol K [8].

Component	**A**	**B**	**C**	**D**
Formaldehyde	23.475	3.1568E-02	2.9852E-05	-2.300E-08
Water	32.243	1.9238E-03	1.0555E-05	-3.596E-09
Methanol	21.152	7.0924E-02	2.5870E-05	-2.852E-08

2.4.1.5 Heat exchanger model

To simulate the heat supplied ($\dot{Q}$) to the vaporiser system during the dynamic simulation, a heat exchanger model was constructed. The heating supplied was calculated using Equation 2.18, where UA represents the overall heat transfer coefficient for the heat exchanger. $\overline{T}_H$ and T_C represent the mean temperature of the heating medium and the temperature of the vaporiser liquid phase, respectively.

$$\dot{Q} = UA \cdot (\overline{T}_H - T_C) \tag{2.18}$$

The overall heat coefficient, UA, was calculated using the flows and temperatures provided in the dataset for Dynea. Later, the UA value was instead used as the manipulative variable (MV) with the reactor temperature as the controlled variable (CV). UA would then adjust the value required to maintain the reactor temperature at the set-point. The nominal UA value was initially calculated from Equation 2.19, which was derived from the energy balance and the definition of $\dot{Q}$ given in Equation 2.18.

$$UA = \frac{\dot{m}_H \cdot C_{p,h} \cdot (T_{H,in} - T_{H,out})}{(\overline{T}_H - T_C)} \tag{2.19}$$

When UA was used as the MV for the reactor temperature, the temperature of the heating medium leaving the heat exchanger was instead calculated from Equation 2.20. While keeping the flow, heat capacity and temperature of the heating medium into the heat exchanger constant.

$$T_{h,out} = \frac{\dot{m}_{hot} \cdot C_{p,h} \cdot T_{h,in} - \frac{UA}{2} \cdot T_{h,in} + UA \cdot T}{\frac{UA}{2} + \dot{m}_{hot} \cdot C_{p,h}} \tag{2.20}$$

Knowing both T_{in} and T_{out} for the heating medium, the mean temperature over the heat exchanger can be found. Using Equation 2.18, $\dot{Q}$ can then be calculated for any UA value.

2.4.2 Models used in the reactor

2.4.2.1 Equilibrium constant

The modelled reactions taking place in the reactor are given in Equation 2.1 to Equation 2.4, shown in Section 2.2.2. While the first two reactions are dependent on the consumed oxygen fraction in the first reaction to determine the composition of the reacted gas flow, the last two are assumed to be equilibrium reactions. To calculate the composition of the product flow after these reactions, the reactor model must first determine the equilibrium constant (K) for these reactions.

The equilibrium constant for a reaction at temperature (T) can be defined according to Equation 2.21 [5].

$$\mathrm{K(T)} = \exp \frac{-\Delta \mathrm{G_{rx}}}{\mathrm{R} \cdot \mathrm{T}} \tag{2.21}$$

Here, the temperature T is given in Kelvin, R is the ideal gas constant and $\Delta \mathrm{G_{rx}}$ represents the change in Gibbs free energy over the reaction.

The Gibbs free energy of the reaction is found from the enthalpy ($\Delta \mathrm{H_{rx}}$) and entropy ($\Delta \mathrm{S_{rx}}$) for the reaction, as shown in Equation 2.22.

$$\Delta \mathrm{G_{rx}} = \Delta \mathrm{H_{rx}} - \mathrm{T} \cdot \Delta \mathrm{S_{rx}} \tag{2.22}$$

From Equation 2.22, it can be seen that in order to calculate the Gibbs energy of reaction, both the enthalpy and the entropy of the reaction are required. Theoretical values for both the formation enthalpy and Gibbs free energy of formation for the components are therefore used to calculate the entropy at a reference temperature ($\mathrm{T_{ref}}$). From the stoichiometric balance provided by the reaction equations, the enthalpy and entropy of the reactions are determined at this temperature. In the same way, the mean heat capacity of reaction ($\bar{\mathrm{C}}_{\mathrm{p,rx}}$) for a temperature interval between $\mathrm{T_{ref}}$ and the temperature of reaction $\mathrm{T_{rx}}$ is found. As both are derived from the mean heat capacity, the changes in enthalpy and entropy over the reaction are calculated as shown in Equations 2.23 and 2.24.

$$\Delta \mathrm{H_{rx}} = \mathrm{H_{rx,ref}} + \bar{\mathrm{C}}_{\mathrm{p,rx}} \cdot (\mathrm{T_{rx}} - \mathrm{T_{ref}}) \tag{2.23}$$

$$\Delta \mathrm{S_{rx}} = \mathrm{S_{rx,ref}} + \bar{\mathrm{C}}_{\mathrm{p,rx}} \cdot \log(\frac{\mathrm{T_{rx}}}{\mathrm{T_{ref}}}) \tag{2.24}$$

The theoretical values that were used as the formation enthalpy and Gibbs free energy of formation for the components are given in Table 2.4.5 and Table 2.4.6, respectively.

Table 2.4.5: Formation enthalpy for components in the gas phase at 298 K, 1 Bar, [kJ/mol] [6].

Component	$\Delta_f H$
Formaldehyde	-109
Water	-242
Methanol	-201
Oxygen	0
Nitrogen	0
Hydrogen	0
Carbon Dioxide	-394
Carbon Monoxide	-111

Table 2.4.6: Gibbs free energy of formation for components in the gas phase at 298 K, 1 Bar, [kJ/mol] [6].

Component	$\Delta_f G$
Formaldehyde	-102
Water	-229
Methanol	-163
Oxygen	0
Nitrogen	0
Hydrogen	0
Carbon Dioxide	-394
Carbon Monoxide	-137

2.4.2.2 Model for reactions

The reactions were modelled using the extent of reaction (ξ). For the first two reactions, given in Equation 2.1 and Equation 2.2, ξ was determined by the amount of moles O_2 that was consumed in each reaction. The fraction of O_2 that reacted in the first reaction was taken from the master thesis of Fraihat, in which an initial fraction of 0.71 was found for a similar reaction [2]. The rest of the O_2 was assumed to react in the second reaction. The stoichiometric coefficient (δ) for the components in the reactions was then used to determine ξ for the other components.

For the equilibrium reactions, ξ was instead found from the calculated K, which was described in Section 2.21. Assuming the reaction is at equilibrium and with a known equilibrium constant, K can be defined from the partial pressure of the reactants and products as shown in Equation 2.25.

$$K = \frac{\Sigma n_{i,reactants}}{\Sigma n_{i,product}} \cdot \frac{P}{n_{total}} \tag{2.25}$$

Through the use of a numerical solver, ξ for the equilibrium reactions can then be found by minimising the difference between the calculated K and the partial pressures. To this end, a *fmincon* solver was used to determine ξ by balancing Equation 2.25. *fmincon* solvers allow for the use of boundaries and inequality constraints, discarding non-realistic solutions such as negative molar flows after reaction. The solution is found through the minimisation of the residual between the partial pressures and K.

By using reactive mass balances for each component as shown in Equation 2.26, the component molar flow after reaction ($\mathrm{n_{i,rx}}$) was found from the initial molar flow ($\mathrm{n_{i,initial}}$) for the reaction.

$$\mathrm{n_{i,rx}} = \mathrm{n_{i,initial}} + \delta \cdot \xi \tag{2.26}$$

2.4.2.3 Reactor temperature

The temperature of the reactor was used to determine the heating supplied to the vaporiser as described in Section 2.4.1.5. To calculate the temperature, the absolute enthalpy of the system was derived from the energy balance over the reactor. The enthalpy over the reactor was defined using the flow and composition of the in- and outflow, in addition to the heat generated by the reactions.

The standard enthalpy of reaction was calculated based on reaction stoichiometry and the formation enthalpy of the products and reactants as shown in Equation 2.27. The formation enthalpy used in the calculations is shown in Table 2.4.5.

$$\Delta \mathrm{H_{rx}} = \sum_{\mathrm{n=1}}^{\mathrm{n}} \delta_{\mathrm{prod.}} \cdot \Delta_{\mathrm{f}} \mathrm{H_{prod.}} - \sum_{\mathrm{n=1}}^{\mathrm{n}} \delta_{\mathrm{react.}} \cdot \Delta_{\mathrm{f}} \mathrm{H_{react.}} \tag{2.27}$$

The heat generated from the conversion can then be determined from the standard enthalpy of reaction along with the reaction extent, as shown in Equation 2.28.

$$\mathrm{H_{rx}} = \Delta \mathrm{H_{rx}} \cdot \xi \tag{2.28}$$

To calculate the enthalpy of the feed gas from the vaporiser and the converted gas exiting the reactor, the formation enthalpy was used in conjunction with the composition of the streams. By defining the formation enthalpy of the stream at a reference temperature, the enthalpy of the stream at a temperature T can be determined from Equation 2.29.

$$\mathrm{H_{stream}} = \mathrm{n_{stream}} \cdot (\Delta_{\mathrm{f}} \mathrm{H} + \int_{\mathrm{298K}}^{\mathrm{T}} \mathrm{C_p} \, \mathrm{dT}) \tag{2.29}$$

The energy generated by the conversion in the reactor is found as the difference in enthalpy between the inflow and the outflow. As both flows consist only of components in the gas phase, this will account for the heat of reaction from the conversions. The temperature in the reactor can then be determined by solving the energy balance, as given by Equation 2.30, with respect to the temperature of the outflow from the reactor.

With the assumption that the outflow of gas will hold the same temperature as the inside of the Reactor.

$$\Delta \mathrm{H}_{\mathrm{Reactor}} = \mathrm{H}_{\mathrm{stream,in}} - \mathrm{H}_{\mathrm{stream,out}} \tag{2.30}$$

As a safeguard for non-realistic solutions, the partial enthalpy method was also used to describe the temperature in the same way. Both of these methods should yield an identical temperature and can therefore be used as an additional equation to be solved for greater numerical stability. The partial enthalpy method uses the heat generated from the reaction from Equation 2.28 directly. Instead solving the energy balance as the enthalpy of the streams based on the heat capacity and adding the heat of reaction to the enthalpy calculation for the product stream as shown in Equation 2.31.

$$\Delta \mathrm{H}_{\mathrm{Reactor}} = \mathrm{H}_{\mathrm{stream,in}} - (\mathrm{H}_{\mathrm{stream,out}} + \mathrm{H}_{\mathrm{rx}}) \tag{2.31}$$

2.4.3 Models used in the absorption column

The models used in the absorption column are a combination of previously described models used in the vaporiser and reactor. While the principle remains the same as in previous models, they have been modified to better capture the dynamics in the absorption column.

2.4.3.1 Vapour-liquid equilibrium model

The vapour liquid equilibrium for each section of the absorption tower was solved similarly to the VLE model for the vaporiser described in Section 2.4.1.1. However, in the absorption column, there will be a greater concentration of formaldehyde, up towards 40 mol%. The assumption that the formaldehyde will behave as water and have no effect on the activity of the water and methanol in liquid is therefore void. However, a model using the same VLE model as for the vaporiser was constructed in order to compare it with a more extensive VLE model.

The more extensive VLE model instead followed the VLE model proposed by Maurer, which describes the vapour liquid equilibrium for tertiary water, formaldehyde and methanol systems [1]. This VLE model also includes the vaporisation of polymers that form between formaldehyde and the other components, such as methylene glycol (MG) and hemiformal (HF). While the longer polymer chains are assumed to be confined to the liquid phase. [1] While including polymers in the vapour and liquid phase, the VLE model still uses the extended Raoult's law to determine composition of the vapour and liquid phases as described in Section 2.4.1.1. UNIFAC activity coefficients were used to describe the interaction between all species in the liquid and vapour phase using the UNIFAC group-contribution method. These coefficients are calculated as shown in Appendix B.

2.4.3.2 Oligomer formation

To define the liquid and vapour phases, the polymer reactions needed to be modelled. Following the equilibrium reactions given in Equation 2.5 to Equation 2.7, the reaction extent was calculated similarly to the equilibrium reactions in the reactor. Numerical values for the equilibrium constants are calculated using Equation 2.32. A and B are equilibrium coefficients shown in Table 2.4.7, and T is temperature in Kelvin.

$$\ln \mathrm{K} = \mathrm{A} + \mathrm{B}/\mathrm{T} \tag{2.32}$$

Table 2.4.7: Coefficients for calculating equilibrium constant (K) for reactions [1].

Equilibrium Constant	**A**	**B**
$\mathrm{K}_{\mathrm{MG\,gas}}$	-16.984	5233.2
$\mathrm{K}_{\mathrm{HF\,gas}}$	-14.755	5969.4
$\mathrm{K}_{\mathrm{MG\,2}}$	4.980×10^{-3}	869.5
$\mathrm{K}_{\mathrm{MG}}, \mathrm{n} > 2$	1.908×10^{-2}	544.5
$\mathrm{K}_{\mathrm{HF}}, \mathrm{n} > 1$	-4.966×10^{-1}	-491.3

To determine the chemical equilibrium for the liquid phase of MG and HF reactions, the K values for the gas reactions are converted to the liquid phase using the vapour pressure of the pure components ($\mathrm{P_s}$). These are found from the Antoine's coefficients listed in Table 2.4.8. The pure component vapour pressure is then found from Antoine's equation shown in Equation 2.33. The temperature (T) is given in Kelvin, and the resulting vapour pressure is given in kPa.

The equations for calculating the chemical equilibrium constant in the liquid are given in Equation 2.34 and Equation 2.35. With a reference pressure ($\mathrm{P_0}$) of 1 atm.

Table 2.4.8: Antoine equation coefficients for pure component vapour pressure calculation[1].

Component	**A**	**B**	**C**
Formaldehyde (FA)	14.4625	-2204.13	-30.15
Water (WA)	16.2886	-3816.44	-46.13
Methanol (Me)	16.5725	-3626.55	-34.29
Methylene glycol (MG)	18.3287	-5699.81	-2.20
Hemiformal (HF)	19.5344	-5637.26	0.00

$$\ln \mathrm{P_{s,i}} = \mathrm{A} + \mathrm{B}/(\mathrm{T} + \mathrm{C}) \tag{2.33}$$

$$\mathrm{K_{MG,liquid}} = \mathrm{K_{MG,gas}} \cdot \frac{\mathrm{P_{s,FA}} \cdot \mathrm{P_{s,WA}}}{\mathrm{P_{s,MG}} \cdot \mathrm{P_0}} \tag{2.34}$$

$$\mathrm{K_{HF,liquid}} = \mathrm{K_{HF,gas}} \cdot \frac{\mathrm{P_{s,FA} \cdot P_{s,ME}}}{\mathrm{P_{s,HF} \cdot P_0}} \tag{2.35}$$

To determine the fraction of each polymer in the liquid at chemical equilibrium, K was defined as the equilibrium constant, representing the ratio of the fractions of reactants to the fraction of product. K for the reactions are then given by Equation 2.36 to Equation 2.39.

$$\mathrm{K_{MG,liquid}} = \frac{\mathrm{x_{FA} \cdot x_{WA}}}{\mathrm{x_{MG}}} \cdot \frac{\gamma_{\mathrm{FA}} \cdot \gamma_{\mathrm{WA}}}{\gamma_{\mathrm{MG}}} \tag{2.36}$$

$$\mathrm{K_{HF,liquid}} = \frac{\mathrm{x_{FA} \cdot x_{ME}}}{\mathrm{x_{HF}}} \cdot \frac{\gamma_{\mathrm{FA}} \cdot \gamma_{\mathrm{ME}}}{\gamma_{\mathrm{HF}}} \tag{2.37}$$

$$\mathrm{K_{MG_i,liquid}} = \frac{\mathrm{x_{MG} \cdot x_{MG_{i-1}}}}{\mathrm{x_{MG_i}}} \cdot \frac{\gamma_{\mathrm{MG}} \cdot \gamma_{\mathrm{MG_{i-1}}}}{\gamma_{\mathrm{MG_i}}} \tag{2.38}$$

$$\mathrm{K_{HF_i,liquid}} = \frac{\mathrm{x_{HF} \cdot x_{HF_{i-1}}}}{\mathrm{x_{HF_i}}} \cdot \frac{\gamma_{\mathrm{HF}} \cdot \gamma_{\mathrm{HF_{i-1}}}}{\gamma_{\mathrm{HF_i}}} \tag{2.39}$$

By calculating the partial pressure and total pressure of the liquid mixture after reaction from extended Raoult's law, the pressure and composition of the vapour phase coexisting with the liquid are found. This is further described in Section 2.4.1.1, and the same method is used for the column.

2.4.3.3 Enthalpy of oligomers

In order to calculate the total energy balance for the column, the energy released during the exothermic polymerisation reactions was calculated. The enthalpy model used for the polymers was adapted from the model proposed by Maurer [1]. Here, the enthalpy of the polymers in the gas phase, methylene glycol (MG) and hemiformal (HF), was determined from the reaction enthalpy as shown in Equation 2.40 and Equation 2.41, respectively.

$$\mathrm{h^g_{MG}(T) = h^g_{FA}(T) + h^g_{W}(T) + \Delta_R h^g_{MG}(T)} \tag{2.40}$$

$$\mathrm{h^g_{HF}(T) = h^g_{FA}(T) + h^g_{Me}(T) + \Delta_R h^g_{HF}(T)} \tag{2.41}$$

The enthalpies of the pure components, formaldehyde, water, methanol, methylene glycol and hemiformal in the liquid phase are calculated from the enthalpies in the gas phase and the vaporisation enthalpies for the components.

Reaction enthalpy of the oligomers, which are modelled to only be present in the liquid phase, is found from the liquid enthalpy of the pure components. The reaction enthalpies for poly(oxymethylene) glycols and poly(oxymethylene) hemiformals are given in Equation 2.42 and Equation 2.43, respectively.

$$\mathrm{h^l_{MG_i}(T) = h^l_{MG_{i-1}}(T) + h^l_{MG}(T) - h^l_W + \Delta_R h^g_{MG_i}(T)} \tag{2.42}$$

$$\mathrm{h^l_{HF_i}(T) = h^l_{HF_{i-1}}(T) + h^l_{HF}(T) - h^l_{Me} + \Delta_R h^g_{HF_i}(T)} \tag{2.43}$$

For liquid mixtures, the molar enthalpy of the mixture is then found from Equation 2.44, while for gaseous mixtures, Equation 2.45 is instead used.

$$\mathrm{h^l(T) = \sum_i x_i \cdot h^l_i(T)} \tag{2.44}$$

$$\mathrm{h^g(T) = \sum_i y_i \cdot h^g_i(T)} \tag{2.45}$$

Vaporisation enthalpy is found from the vapour-pressure curves given by the Antoine coefficients (Table 2.4.8) as shown in Equation 2.46. While the reaction enthalpy can be found from the chemical equilibrium coefficients (Table 2.4.7) as shown in Equation 2.47. $\mathrm{B_V}$ denotes the Antoine coefficient B for the component, while $\mathrm{B_K}$ represents the chemical equilibrium B coefficient.

$$\mathrm{\Delta h_V(T) = \frac{R \cdot B_V}{(1 + \frac{C}{T})^2}} \tag{2.46}$$

$$\mathrm{\Delta_R h(T) = -R \cdot B_K} \tag{2.47}$$

The Antoine coefficients and the chemical equilibrium coefficients, as well as the information provided by the calculated vapour-liquid equilibrium, enable the calculation of reaction and vaporisation enthalpy. As a result, only the heat capacities of the pure components, formaldehyde, methanol and water, are required to find the enthalpy. The heat capacity used in the model was taken from the Maurer model [1], and is shown in Table 2.4.9.

Table 2.4.9: Ideal gas molar heat capacity coefficients for pure components, J/mol K [1].

Coefficient	Formaldehyde	Water	Methanol
A	33.14	39.00	21.15
B	$-1.183 \cdot 10^{-2}$	$-1.131 \cdot 10^{-1}$	$-7.092 \cdot 10^{-2}$
C	$6.653 \cdot 10^{-5}$	$6.434 \cdot 10^{-4}$	$2.588 \cdot 10^{-5}$
D	–	$-1.122 \cdot 10^{-6}$	$-2.852 \cdot 10^{-8}$

2.4.3.4 Liquid outflow model

For sections without level control implementation, the liquid outflow model is used to describe the liquid outflow. The model is based on an estimation of the liquid dynamics for the section. By estimating the residence time for the liquid through the section, a liquid flow parameter ($\mathrm{K_L}$) was found.

Utilising a similar method to that used for a proportional controller, the parameter was used as $\mathrm{K_C}$ for the controller. The liquid flow from the section was defined as zero when the liquid volume was below the calculated set-point. This allows the model to simulate the filling of the sumps and packed parts, ensuring that the sections do not run dry.

The $\mathrm{K_L}$ parameters were found from the hold-up of liquid in the section and the expected flow based on Dynea data. The hold-up was determined from the composition and molar volume of the liquid. The liquid volume was determined by combining the volume of the sump and the volume of liquid in the packing. In the absorption column, there is a circulation of liquid that cools each section. Although the cooling loop is not included in the model, the circulation flow must be accounted for in the total flow through the section. The residence time (τ_L) is calculated according to Equation 2.48, with $\mathrm{K_L}$ given by Equation 2.49.

$$\tau_\mathrm{L} = \mathrm{M_L} \cdot \mathrm{F_L} \tag{2.48}$$

$$\mathrm{K_L} = \frac{1}{\tau_\mathrm{L}} \tag{2.49}$$

The stripper section was an exception to this method. While employing a similar overall model philosophy for liquid flow, this section features a tray column instead. To account for the trays, $\mathrm{K_c}$ was calculated from a typical residence time for a tray column. The number of trays in the stripper (N) is 5, and a typical residence time ($\tau_\mathrm{L,t}$) of 5 seconds was used. $\mathrm{K_c}$ for the stripper section is defined as shown in Equation 2.50.

$$\mathrm{K_L} = \frac{1}{\mathrm{N} \cdot \tau_\mathrm{L,t}} \tag{2.50}$$

2.4.3.5 Complete composition of the product flow

The composition of the product flow was calculated to determine the model's accuracy when compared to product analysis performed by Dynea. As these measurements are given as the overall mole fraction of formaldehyde, water, and methanol in the liquid phase, the total amount of these components, including their presence in the polymers, was calculated. This was achieved by reverting the polymers back to their original reactants through the use of a liquid composition and a weighted coefficient (s). The weighted coefficient is calculated as shown in Equation 2.51. The overall mole fraction in the liquid phase of formaldehyde, water and methanol is given by Equation 2.52, Equation 2.53 and Equation 2.54, respectively. [1].

$$\mathrm{s} = (1 + \mathrm{x_{MG}} + \sum(\mathrm{i} \cdot \mathrm{x_{MG_i}}) + \mathrm{x_{HF}} \sum(\mathrm{i} \cdot \mathrm{x_{HF_i}}))^{-1} \tag{2.51}$$

$$\tilde{\mathrm{x}}_{\mathrm{FA}} = \mathrm{s} \cdot [\mathrm{x_{FA}} + \mathrm{x_{MG}} + \sum(\mathrm{i} \cdot \mathrm{x_{MG_i}}) + \mathrm{x_{HF}} + \sum(\mathrm{i} \cdot \mathrm{x_{HF_i}})] \tag{2.52}$$

$$\tilde{\mathrm{x}}_{\mathrm{W}} = \mathrm{s} \cdot (\mathrm{x_W} + \mathrm{x_{MG}} + \sum(\mathrm{x_{MG_i}})) \tag{2.53}$$

$$\tilde{\mathrm{x}}_{\mathrm{ME}} = \mathrm{s} \cdot (\mathrm{x_{ME}} + \mathrm{x_{HF}} + \sum(\mathrm{x_{HF_i}})) \tag{2.54}$$

2.4.3.6 Activity coefficients using UNIFAC method

The activity coefficients used for the vapour-liquid equilibrium calculations are based on the UNIFAC model. In the UNIFAC model, the activity for each component is based on UNIFAC group contribution. By dividing the components into their respective activity groups, the interactions between different groups are used to find the overall component interactions.

The activity coefficients are determined from the combinatorial and residual activities of the liquid mixture. These are based on the size and surface parameters for the group, as well as the interactions between pure components and mixtures. The calculations of the activity are further described in Appendix B.

CHAPTER

THREE

UNIT MODELLING

3.1 Modelling the vaporiser

The vaporiser was modelled as a closed tank system with an external heating loop. The main model structure was adapted from the model made during the specialisation project.[9] While some parts of the model were kept the same, such as the overall structure, sizes and initial flows, the model required several changes.

The model was closely fitted to the dataset from Dynea, which was also used for the earlier model. The fitting included optimising the valve coefficient (C_v) to provide a more accurate vapour flow to the reactor. The controller gain of the level controller (K_c) was also retuned for smoother control, thereby increasing the stability of the total model. The initial states were also set closer to steady-state values. In addition to the necessary changes, a feedback controller was also implemented to regulate the reactor temperature to the set-point. To account for the inclusion of recycled gas containing hydrogen, carbon dioxide and carbon monoxide, the dynamic mass balances were extended to also include these gases.

The model is made on the assumption that a vapour-liquid equilibrium is always in effect on the vapour and liquid phases. The main gas inlet to the vaporiser consists of cleaned outside air and is mainly comprised of oxygen and nitrogen. Both of these gases have low solubility in liquids at the temperatures and pressures expected inside the vaporiser tank. As a result, it was assumed that these were not included in the components that make up the liquid phase. The model also needed to include the gases that could be introduced through a recycled gas stream from the top of the absorption column. For these gases, the same assumption was made, and they were modelled only to be included in the vapour phase.

The liquid composition of the vaporising components, formaldehyde, water and methanol, was found from the dynamic component mass balances. Similarly, the vapour composition of the components in the vapour feed was determined from their dynamic component balances. The equilibrium between the vapour/liquid phase and the pressure was determined using a simple vapour-liquid equilibrium model and Raoult's law, further described in Section 2.4.1.1. Based on the data from Dynea regarding the liquid phase composition, the concentration of formaldehyde was expected to be low (2-3%). This led to the assumption that the formaldehyde in the liquid could be modelled as water in the vapour-liquid equilibrium, with minimal impact on accuracy. A modelling schematic for the vaporiser model with the heating included is presented in Figure 3.1.1.

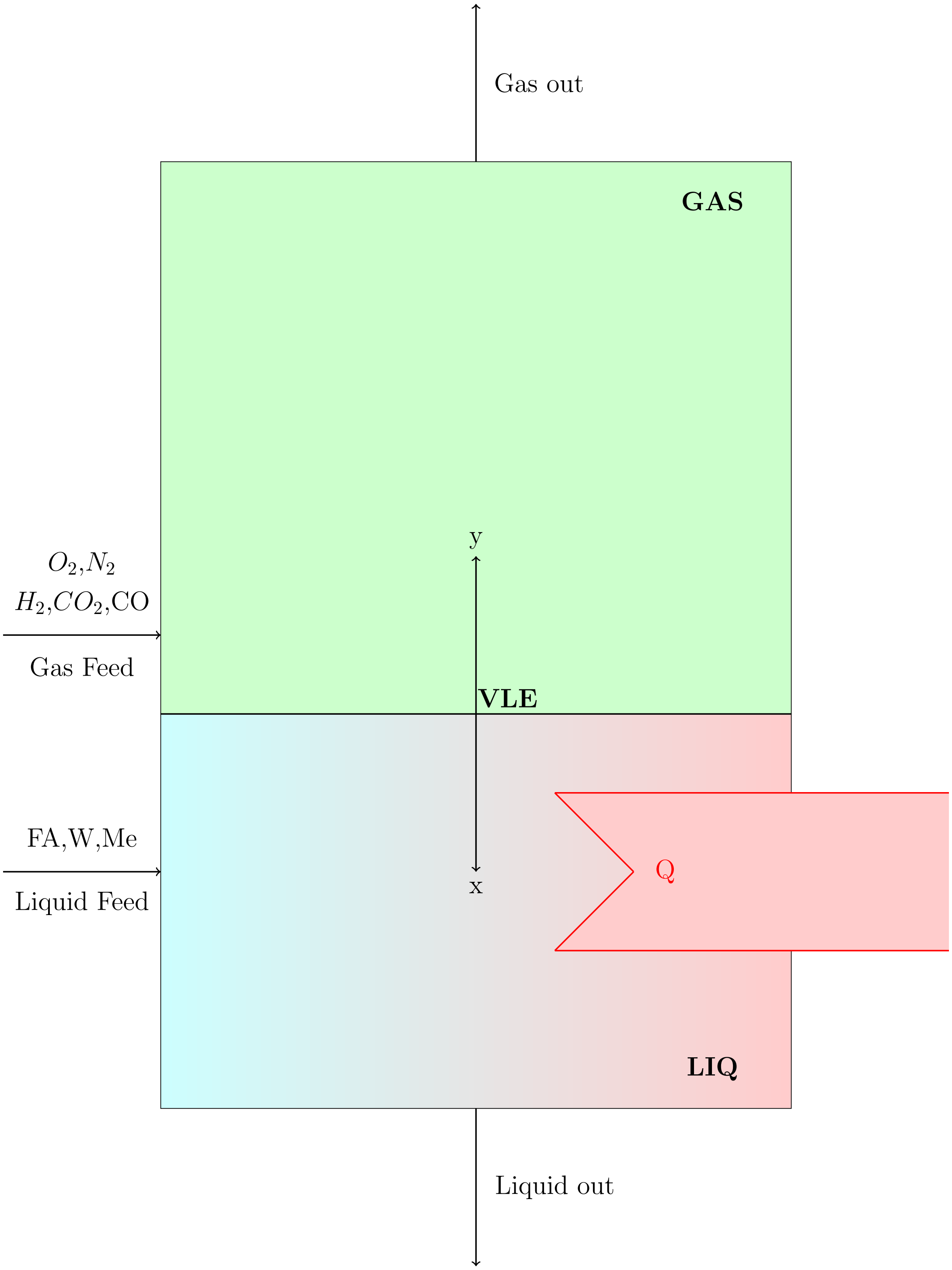

Figure 3.1.1: A modelling schematic of the vaporiser with heating included.

3.2 Modelling the reactor

The reactor model was adapted from the model developed during the specialisation project [9]. As both models are based on the Lillestrøm plant, several assumptions made in the original model were carried over into this one. While the actual plant features two parallel reactors, the model was simplified to include only a single reactor model. Due to the rapid gas-phase dynamics, the conversion in the reactor was assumed to occur instantaneously. As a result, the reactor behaviour is entirely dependent on the dynamics of the vaporiser model.

The model made during the specialisation project was based on the reactor model made by Vo in her master's thesis [10]. The current model, therefore, follows the same modelling principle as this original model. In her thesis, a fixed fraction of oxygen was assumed to react in the first reaction described by Equation 2.1, while the rest of the oxygen was assumed to react in the second reaction, Equation 2.2. With the oxygen conversion known for both reactions, the stoichiometric balances were used to calculate the vapour flow and composition after conversion.

The third and fourth reactions, described by Equation 2.3 and 2.4, were modelled as equilibrium reactions. The extent of these reactions was instead defined by the respective equilibrium constants for each reaction. These were calculated from the Gibbs free energy of reaction, as described in Section 2.4.2.1. In both the specialisation project and Vo's original model, these reactions were solved in sequence.

In the new model, the extents of the first and second reactions are defined similarly, as was also done for the specialisation project [9]. The fraction of oxygen reacted in the first reaction was based on the value found by Fraihat for a similar plant in his master thesis, set to 0.71 [2]. Using the reaction extents, the flow and composition were found from the reaction stoichiometry. However, unlike the previous models, the third and fourth equilibrium reactions are solved simultaneously using a *fmincon* solver. This was done to better reflect the nature of equilibrium reactions, which always react towards equilibrium. Similar to before, the conversion after these reactions is then found from the mass balances based on reaction stoichiometry.

While a *fmincon* solver minimises the residual of the equations to be solved, this proved to be more adaptable than the *fsolve* function that was initially used. Allowing for less accurate initial guesses while still achieving conversion. However, the solver was noticed to be slightly slower, although this may be a result of less accurate initial guesses for the solution.

3.3 Modelling the absorption column

The absorption column was modelled as a combined reactor and vaporiser for each section of the column. The reactions in the column for the formation of higher-order oligomers, further described in Section 2.2.3, are assumed only to be contained in the liquid phase. Methylene glycol and hemiformal are instead considered to form in both the liquid and vapour phases. As a result, the VLE model for the absorption column, further described in Section 2.4.3.1, also includes these components as part of the vapour. A schematic model for the sections with the reactions included is presented in Figure 3.3.1.

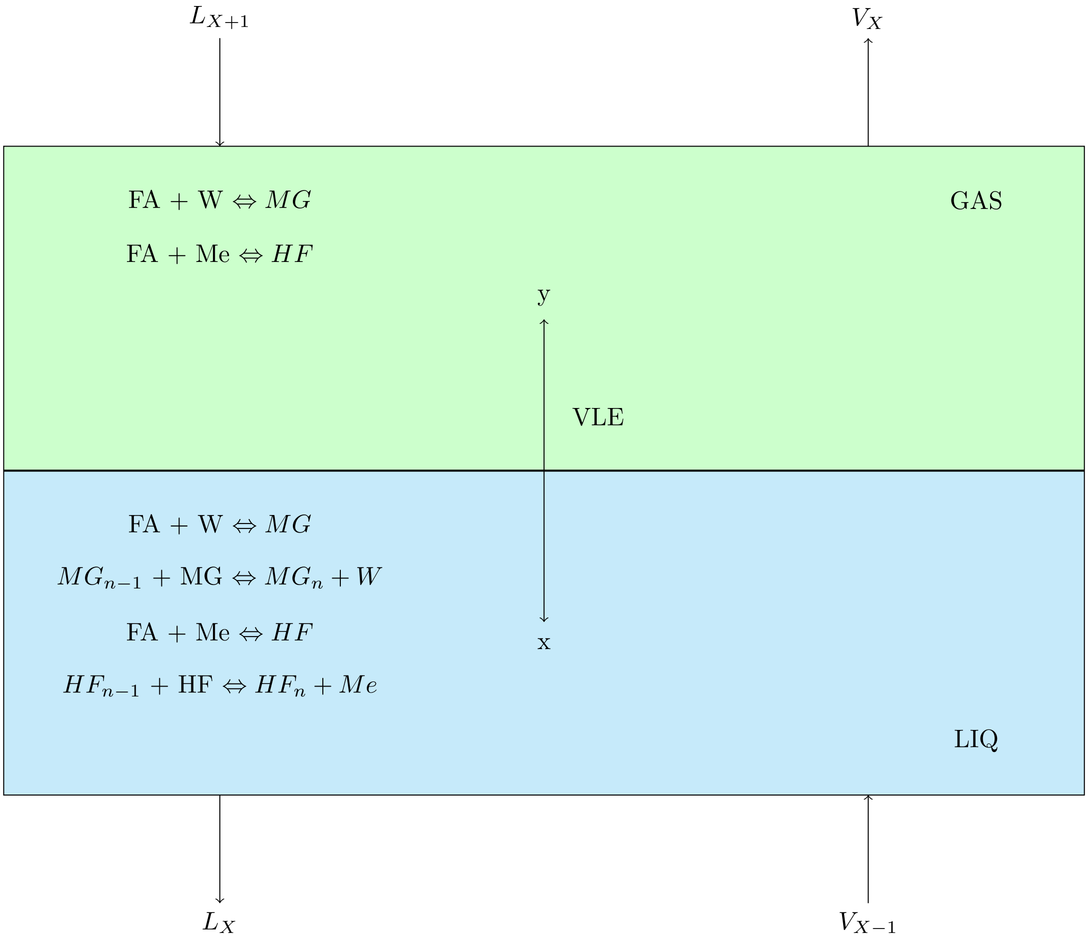

Figure 3.3.1: A schematic model for the sections in the absorption column with the assumed reactions for the vapour and liquid phase.

The column sections were modelled after a similar structure to the vaporiser model. The liquid phase composition was determined from dynamic mass balances, while the corresponding vapour composition was found with the VLE model. As a result, the formation of oligomers was only calculated based on the liquid composition. Due to the equilibrium with the vapour phase, the reactions taking place in both phases will still be accounted for as the vapour composition is dependent on the liquid composition. To model the reactions, the liquid composition found to satisfy the equilibrium constraints for the reactions is calculated separately using a *fsolve* solver. The reactions were assumed to only include oligomers with a maximum chain length of 3. This was decided based on the comparison with a similar model presented in Appendix C.

3.3.1 Validation of the expanded VLE model

While the dynamics in the column were based on the tested vaporiser model, the VLE model and reactions added had to be verified before implementing them into the model.

This validation was performed by comparing it to other known models. The VLE model used is based on a model developed by Maurer for tertiary formaldehyde, water, and methanol systems [1]. This model also accounts for the formation of oligomers and could therefore be used to accurately describe the vapour and liquid compositions in the absorption column.

To describe the interactions between the components, activity coefficients were calculated using the UNIFAC method as described in Section 2.4.3.6. This is also the same method employed in the original model. The method had also previously been used in a model by co-supervisor Susort N. [11], and the calculations were therefore adapted from his model. To verify correct implementation of the method, the calculated activity coefficients were compared to those calculated by the previous model made by co-supervisor Susort N. [11]. With the implementation validated, the vapour composition calculated by the completed VLE model was then compared to the results obtained by the model developed by Maurer [1].

3.3.2 Implementation of reactions in the column

The composition at chemical equilibrium was determined based on the oligomer formation model described in Section 2.4.3.2. The equilibrium constants were used in conjunction with the calculated activity coefficients to determine the fractions of reactants and products in each reaction. The current hold-up was used to define the starting composition for the reactions and determine the required extent of reactions. While this would give the converted hold-up directly, to ensure mass balance over the reactions is upheld, the liquid volume is instead used to calculate the hold-up after reaction.

Similar to the vaporiser model, the liquid hold-up in each section is defined by the molar volumes of each component in the liquid and the total liquid volume. Using known molar volumes for methanol, formaldehyde and water, the molar volumes of the oligomers were defined from the reaction stoichiometry. Although only providing an estimate of the actual molar volumes of the oligomers, this allowed for a similar calculation of the liquid hold-up in the column sections. Consequently, the hold-up of components at equilibrium can be calculated based on these estimations and the composition found from the *fsolve* solver. Assuming that the liquid reactions always reach equilibrium, the reactive flow was defined as the difference in hold-up between the current composition and the composition at equilibrium. Making the model dynamically move towards equilibrium at all times.

3.3.3 Defining vapour and liquid flows in the column

The vapour flow out of the section, defined as V_X in Figure 3.3.1, is calculated using a similar fictitious valve as used in the vaporiser model. The pressure in the section above determines the downstream pressure for the section below, with atmospheric pressure as the downstream pressure at the top of the column.

For the liquid flow out given by L_X in Figure 3.3.1 of the column, two approaches were used. For the top part of the column, consisting of sections 4 and 5, the liquid flow into each section was determined by a level controller. The inflow of liquid into section 5 consisted of pure water from an external system, while the liquid into section 4 was the liquid flow out of section 5. The liquid flow from section 4 is used as the additional liquid feed for the vaporiser. The liquid outflow from the section is therefore indirectly controlled by the level controller in the vaporiser. The liquid flow out of the lower sections was instead calculated through an estimated residence time as described in Section 2.4.3.4. The liquid flow from these sections could then be modelled similarly to a level controller, with an estimated set-point for the liquid hold-up in the section.

3.3.4 The complete column model structure

The column sections were modelled independently, initially being based on the data given by Dynea to define the internal flows of the column. Upon completion of the model, these internal flows were instead determined from the values calculated by the model. As each section of the column is an individual dynamic simulation, the internal flows are not directly exchanged between the sections. Each section will therefore be simulated based on constant inflows over the simulation time.

To facilitate the exchange of calculated data, each section is run independently for the duration of the predetermined simulation time with a set of initial state values. The calculated flows, compositions, and pressures from each simulation are then used as the new initial states for the following simulation. The length of the individual simulations can therefore be considered as the sampling time for the total column simulation. With the values after each "sample" being stored in an upper program layer, making up the total column.

For the 3rd and 4th column section, no liquid is exchanged between the sections, with the inflow of liquid into the 3rd section instead being the liquid bleed from the vaporiser. The liquid outflow from the 4th section is used as the water stream, which makes up part of the total liquid feed to the vaporiser. As the gas from the 3rd section is the only exchange between the upper and lower sections of the column, the upper sections will not affect the lower sections. With the implementation of level controllers for both the 4th and 5th sections, a decision was made to divide the column into two parts. The 3rd section and below made up the lower part of the column, while the 4th and 5th sections made up the upper part of the column.

With each section running independently, only updating flows between individual simulations, this division was made for practical programming reasons. With the two divided parts of the column, each making up a function to be called, this allowed for a more structured model and better control over the input and output from each simulation. A major problem when creating the model was the sensitivity of initial guesses for the solvers defining the equilibrium reactions occurring in the liquid phase. The concentration of reactants in the lower and upper parts of the column varies greatly. The division of the models also enabled improved tuning of the initial guesses, resulting in a more robust model. A schematic model for the program structure of the complete column is presented in Figure 3.3.2.

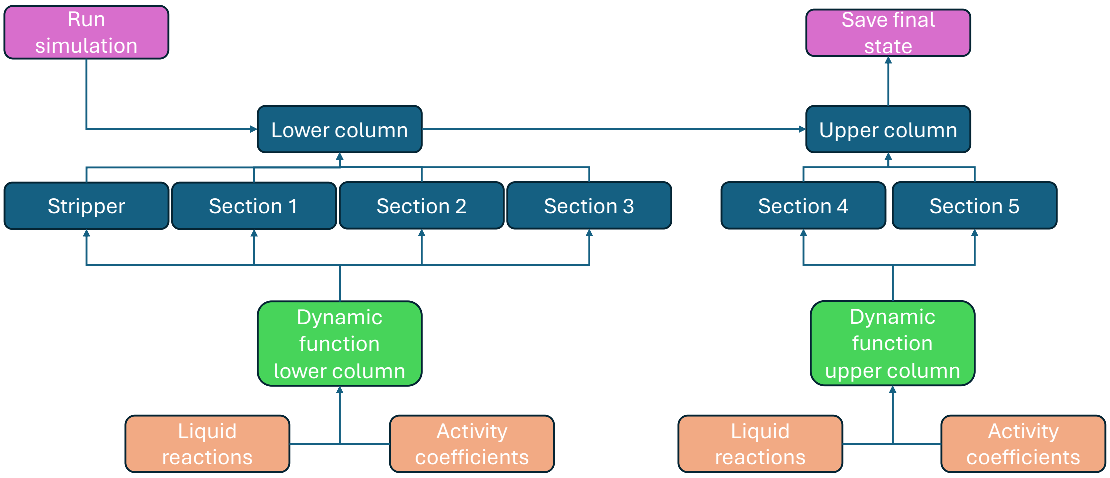

Figure 3.3.2: A schematic representation of the upper column program structure.

While each section consists of a separate dynamic simulation, this approach enabled the internal flows of the column to be updated between individual simulations. It also proved to be a more robust method for modelling the column. With several reactions occurring in the liquid of each section, combined with changing liquid compositions and hold-ups, a single model was deemed too sensitive. This approach also allows for fast modification to adapt the model to new changes. With one of the main problems being the convergence of the reaction solvers that was previously described, this approach also allowed for quicker troubleshooting and better oversight of the model.

3.4 Combined process model

Previously, it was described that the main process models were all modelled as independent simulations rather than as a single large model. While allowing for optimal control over each individual unit in the process, this also introduced a challenge in achieving a plant-wide simulation.

The vaporiser model in the system is given an input for the air feed into the system based on Dynea's measurements. The model will then recalculate all other flows based on the resulting reactor temperature and liquid level inside the vaporiser. The throughput manipulator (TPM) for the system will therefore be the gas feed, or more specifically, the oxygen feed, as the rest of the system is dependent on the vaporiser model's calculations. The reactor consists of a steady-state model based on the assumption that the vapour feed will be converted instantaneously. The reactor can therefore be considered as a conversion step between the dynamic simulation of the vaporiser and the simulation of the absorption column. With the models divided, the combined model needs to integrate the end states of each model into a larger dataset, allowing each model to be dependent on the calculations of the others.

To achieve a continuous simulation, each model was simulated for a specified simulation time while the upstream process determined the flows. The vaporiser was therefore simulated first, with the resulting end flow being used for the reactor to give the resulting reactor temperature and converted gas. While it would be natural to allow the simulation to continue into the absorption column in a connected simulation, that would cause the column to simulate ahead in time after the vaporiser. With the resulting data being after twice the simulated time. While the steady-state values reached would not be affected, this would shift the dynamics and give inconsistent data. To ensure correct timestamps for each model's data, the absorption column would therefore be simulated with the previous values calculated by the reactor and vaporiser. Ensuring that the final states computed by all three units correspond to the same time point.

Through this approach, both the vaporiser and absorption column can be considered as simulating individually over the same time frame, while updating the exchanged flows at the end of the simulation. With the reactor being a steady-state model, it is entirely dependent on the vaporiser dynamics, and these results will therefore match the time frame for the vaporiser data. With each model's end state corresponding to the same time point, an iterative approach can be used to achieve a contentious simulation. The end state after each simulation time for the individual models was therefore saved and used as the new initial state for the next step.

The approach used is similar to a single-shooting approach in which the end state after each integration is saved and used as the initial state for the subsequent integration. To ensure that the model continues to capture the dynamics of the total process, the sample time for all simulations was set to 10 seconds. While the gas dynamics of the system may be faster than this sample time, the overall system dynamics will still be captured. The sample time was chosen based on the estimated liquid dynamics of the column used to define the liquid flows. Another factor that was taken into account was the total time frame of the simulation. A 10-second interval was initially employed between measurements to provide a clear indication of the system's dynamics while allowing for faster simulations.

To simulate the combined model for an extended period, the number of iterations can be increased. As a result, the end state after each completed simulation is saved in a larger dataset, which comprises the total change over time for the entire process. A schematic representation of the program structure for the plant-wide model is given in Figure 3.4.1.

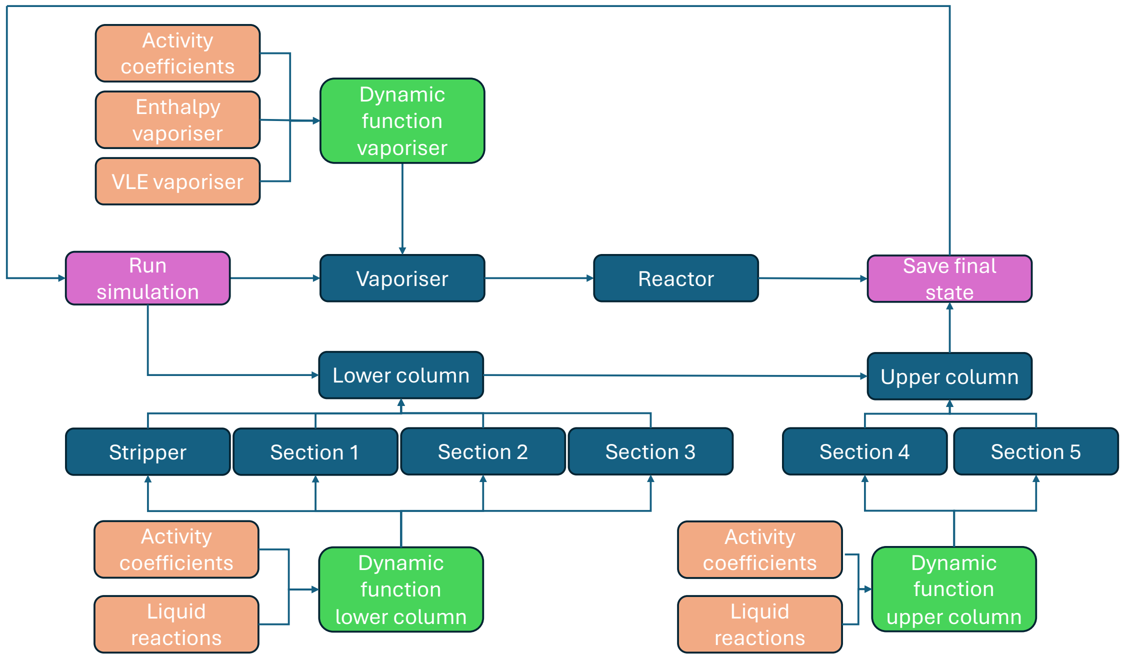

Figure 3.4.1: A schematic representation of the program structure for the plant-wide model.

3.5 Process control structure

The process control structure of the plant was also included in the model. A PFD of the plant with the included control structures is presented in Figure 3.5.1. The control structure used in the program was based on the current control structure used at the Lillestrøm plant.

3.5.1 Vaporiser control structure

The vaporiser model included several control structures to maintain the process at the defined set-points. The level inside the vaporiser was maintained through the use of a P-controller. The inflow of methanol (Flow 1) was used as the manipulated variable for this controller, with the liquid volume inside the tank serving as the controlled variable (CV). To ensure a constant ratio in the liquid feed between the methanol and liquid bleed from the absorption column (Flow 2), a ratio controller was implemented. In the model, the liquid/methanol ratio had a set-point value of 58 w%/w methanol. This ensured that both the liquid level and the ratio of the liquid feed would remain constant.

The liquid bleed to the absorption column was controlled through a flow controller, with a set-point value of 90 kg/h. The mass of the flow was calculated based on the molar mass of the components and the composition inside the vaporiser. As a result, the molar flow of components is dependent on the composition even while the mass flow remains constant.

An additional ratio controller was also included for the gas feed. While the oxygen flow determines the total gas feed to the vaporiser, when recycled gas is implemented, this is defined as a m%/m total gas feed. In the PFD shown in Figure 3.5.1, this is shown as a regular ratio controller. However, this is implemented as a ratio of the total gas feed, and not as a supplementary gas feed in addition to an unchanged air feed. To ensure a constant gas feed, the air feed was adjusted to compensate for the amount of recycled gas used.

The temperature controller for the reactor temperature is also included in the vaporiser model. This was modelled as a feedback PI-controller with the overall heat transfer coefficient (UA) of the heat exchanger (HEX 1) as the manipulated variable (MV). At the same time, the reactor temperature is the controlled variable (CV). The real process includes internal steam heating coils and cooling loops in addition to the heating loops. When additional heating or cooling is required, this is instead performed by the external heating and cooling loops rather than changing the heat provided by the heat exchanger. This is done to maintain a near-constant flow from the first section of the absorption column to the heat exchanger, as this section also serves as the cooling loop for the section. To simplify this structure, a decision was made to model this system as an increase or decrease in the UA value, while maintaining a constant heating flow. As previously described in Section 2.2.2 an increase in the methanol content in the vapour feed to the reactor will reduce temperature based on the reactions taking place. As a result, the temperature in the vaporiser and the temperature in the reactor will have inverse responses.

3.5.2 Reactor control structure

The reactor model includes the temperature control of the vapour through the "Superheater". The heat exchanger (HEX 2) is not modelled, and perfect temperature control is assumed. The temperature of the vapour feed into the reactor is therefore calculated from the temperature of the vaporiser with a 10 °C increase to simulate the heat exchanger. It also provides the temperature of the reactor's outflow to the vaporiser, allowing the feedback controller to regulate the reactor temperature, as previously described in Section 3.5.1.

3.5.3 Absorption column control structure

The absorption column features several cooling loops, in addition to level controllers, for the top sections of the column. These cooling loops were assumed to have perfect temperature control and were not modelled, instead, the temperature in each section remained at a constant set-point temperature. As a result of the liquid from the 4th section being determined by the vaporiser, level controllers were implemented for both the 4th and 5th sections of the column. For the 4th section, the flow of liquid from the 5th section was used as the MV to control the liquid volume. For the 5th section, the flow into the section, consisting of pure water from an external process, was used instead. This allowed the model to account for the increase or decrease in liquid feed to the vaporiser and its effect on the gas cleaning sections at the top of the column.

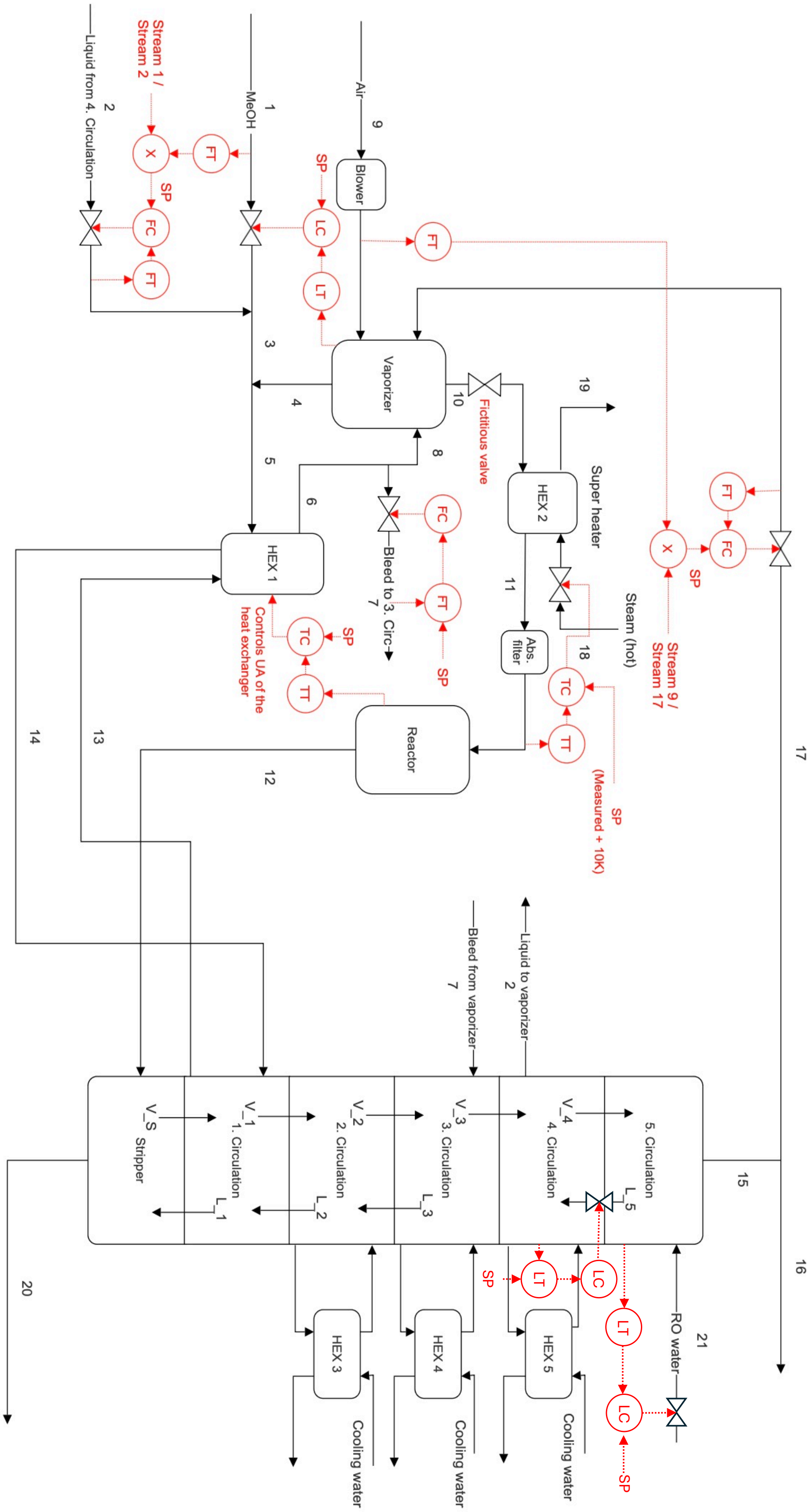

Figure 3.5.1: A PFD showing the process control structure for the plant included in the model.

CHAPTER

FOUR

MODEL VALIDATION AND CONTROLLER TUNING

4.1 Model validation

4.1.1 Validation of the activity coefficients calculated by the column model

The activity coefficients used by the column model are calculated based on the UNIFAC method, as described in Section B.2. The method and coefficients used in the calculation are further explained and presented in Appendix B. Due to the non-ideality of the liquid phase in all parts of the column, correct calculation of the activity coefficients is paramount with regard to VLE calculations. The reactions taking place in the column are also dependent on these coefficients, and miscalculations could have a significant impact on the resulting liquid compositions.

To ensure the correct implementation of the method, the calculated activity coefficients were compared with the results for activity coefficients obtained from another model developed by Susort N. [11]. This model had previously been used to calculate the conversion of oligomers based on a known initial liquid composition and had been proven to depict this conversion accurately. While the comparison was done for several initial compositions and temperatures, one of the comparisons for the calculated activity coefficients is presented in Table 4.1.1. This comparison was made for a temperature of 363.2 K and the shown overall composition. The results were selected based on the temperature being close to the operating temperatures of the lower parts of the column (343-363 K). All comparisons are further presented in Appendix D, and achieved similar results.

Table 4.1.1: Comparison of activity coefficients (γ) found by the model and the model developed by Susort N. for a temperature of 363 K [11].

Component	$\tilde{x}_{\mathbf{liquid}}$	$x_{\mathbf{liquid}}$	$\gamma_{\mathbf{Model}}$	$\gamma_{\mathbf{Sosort}}$	$\Delta\gamma$
FA	0.0089	1.5843e-05	1.4808	1.4808	0.0
W	0.4785	0.4825	1.2273	1.2273	0.0
Me	0.5126	0.5085	1.1202	1.1202	0.0
MG	0	2.5648e-04	0.5768	0.5768	0.0
HF	0	0.0087	0.9702	0.9702	0.0
MG2	0	1.8799e-06	0.2166	0.2166	0.0
MG3	0	3.1253e-09	0.1496	0.1496	0.0
MG4	0	5.0334e-12	0.1053	0.1053	0.0
MG5	0	7.9708e-15	0.0758	0.0758	0.0
HF2	0	2.1449e-05	0.9086	0.9086	0.0
HF3	0	5.6644e-08	0.7980	0.7980	0.0
HF4	0	1.5564e-10	0.6736	0.6736	0.0
HF5	0	4.3941e-13	0.5534	0.5534	0.0

From the comparison, it can be observed that the activity coefficients calculated by both models are identical for a maximum oligomer chain formation length of 5. While not included, the same result was achieved for all chain lengths up to a maximum length of 10. While it is possible to extend the method to include further chain lengths, this is the maximum the activity coefficient function can handle in its current form. With both models being based on the UNIFAC calculation model, achieving identical results is expected. These comparisons therefore demonstrate that the method was correctly implemented and that the model will provide accurate calculations for the interactions between the liquid components. As previously mentioned, both the vapour-liquid equilibrium and the reactions are dependent on these activity coefficients. Based on the comparison results, these calculations are indicated to be accurate.

4.1.2 Validation of the vapour-liquid equilibrium model with oligomer formation

While the model performed well in calculating the activity coefficients, as demonstrated by the comparison in Section 4.1.1, a direct validation of the VLE model was also conducted. The reactions and VLE model were based on a previous model developed by Maurer, using similar coefficients as the original model to calculate the resulting compositions [1]. The activity coefficients used in that model are also calculated using the UNIFAC method. As a result of these similarities, both models should yield nearly identical calculations for the vapour phase based on a fixed liquid composition. To determine the validity of the model, the vapour composition reached by the model was compared to the results obtained by the original model [1].

The comparison was performed using a similar liquid composition and temperature to those used in the original results. The liquid phase in the study is defined as the overall liquid composition, comprising the total formaldehyde, water, and methanol in the liquid

[1]. These were calculated as described in Section 2.4.3.5 from the actual liquid composition, including the oligomers. The comparison could therefore also be used as a direct measurement to validate the model's calculations of the liquid reactions.

The comparison was made for different compositions and temperatures, as described in Section 3.3. The maximum length of oligomers that are formed in the reactions varies between 3 and 5 for each comparison. The results from the comparisons at a temperature of 363.2 K for a maximum oligomer length of 3 and 5 are presented in Table 4.1.2 and 4.1.3, respectively.

Table 4.1.2: The resulting vapour composition for the model and the model proposed by Maurer at 363.2 K and a polymer length of 3.[1]

Component	$\mathbf{x_{liquid}}$	$\mathbf{y_{Model}}$	$\mathbf{y_{Maurer}}$	$\mathbf{\Delta y}$	$\mathbf{\Delta y_{relative}\%}$
Formaldehyde	0.0058	0.0078	0.0077	0.0001	1.3163
Methanol	0.0098	0.0693	0.0691	0.0002	0.2634
Water	0.9844	0.9229	0.9232	-0.0003	-0.0307
Formaldehyde	0.0089	0.0028	0.0028	0.0000	-0.7789
Methanol	0.5126	0.7768	0.7768	0.0000	-0.0026
Water	0.4785	0.2204	0.2204	0.0000	0.0189
Formaldehyde	0.0996	0.1001	0.0988	0.0013	1.2740
Methanol	0.0341	0.1108	0.1114	-0.0006	-0.5218
Water	0.8663	0.7891	0.7898	-0.0007	-0.0858
Formaldehyde	0.1259	0.0528	0.0528	0.0000	0.0211
Methanol	0.4060	0.6688	0.6689	-0.0001	-0.0200
Water	0.4681	0.2784	0.2783	0.0001	0.0440

Table 4.1.3: The resulting vapour composition for the model and the model proposed by Maurer at 363.2 K and a polymer length of 5.[1]

Component	$\mathbf{x_{liquid}}$	$\mathbf{y_{Model}}$	$\mathbf{y_{Maurer}}$	$\mathbf{\Delta y}$	$\mathbf{\Delta y_{relative}\%}$
Formaldehyde	0.0058	0.0078	0.0077	0.0001	1.3156
Methanol	0.0098	0.0693	0.0691	0.0002	0.2635
Water	0.9844	0.9229	0.9232	-0.0003	-0.0307
Formaldehyde	0.0089	0.0028	0.0028	0.0000	.0.7789
Methanol	0.5126	0.7768	0.7768	0.0000	-0.0026
Water	0.4785	0.2204	0.2204	0.0000	0.0189
Formaldehyde	0.0996	0.0988	0.0988	0.0000	0.0467
Methanol	0.0341	0.1113	0.1114	-0.0001	-0.1062
Water	0.8663	0.7899	0.7898	0.0001	0.0091
Formaldehyde	0.1259	0.0528	0.0528	0.0000	-0.0456
Methanol	0.4060	0.6688	0.6689	-0.0001	-0.0137
Water	0.4681	0.2784	0.2783	0.0001	0.0416

From the comparison, it can be observed that the increase in maximum formation length of the polymers generally has a limited effect on model accuracy for the compared compositions. The most significant impact can be seen in the 3rd composition, with a formaldehyde concentration of approximately 10%, and a methanol concentration of 3.4%. For this composition, increasing the formation length to 5 slightly improves the accuracy, both concerning the formaldehyde and the water content in the vapour.

Comparing these results further, the notable increase in accuracy is achieved for the composition with the highest formaldehyde/methanol ratio in the liquid phase. With the assumption that the composition of the liquid mixture reaches chemical equilibrium, this may be expected. The increased formaldehyde concentration in the liquid mixture leads to a higher formation of longer-chain oligomers. Since these oligomers are not accounted for in the vapour phase by the model, formaldehyde concentration in the vapour should consequently appear lower. Comparing the two cases, this effect is also observable. The formaldehyde concentration in the vapour phase is noticeably lower in the results with a higher maximum oligomer formation length.

From the reactions in the column, described in Section 2.2.3, the increased accuracy regarding water is also expected. When a maximum formation length of 3 was used in the comparison, the water content in the vapour was lower than the original model, while increasing with increased oligomer length. This may be caused by the water being a product of continued poly(oxymethylene) glycol reactions. Allowing for more water to be formed as a result of the increased concentration of higher-order oligomers in the liquid. The reduction of formaldehyde in the vapour phase will also increase the fraction of the vapour composition made up of water and methanol. This is also observed through the increased fraction of methanol, which follows similar reaction mechanisms to water in these reactions.

While there is an increase in accuracy for this scenario, the general trend for the comparisons is only a limited improvement. In the comparisons of activity coefficients shown in Table 4.1.1, the actual composition of the liquid phase is also given. From this composition, it can be observed that the fractions of higher-order oligomers are low, with a trend of a 1×10^{-3} reduction in composition for each increased length above 2. From these results, it can be deduced that only minor improvements can be made by increasing the maximum length. Where the increase in length required for any meaningful increase in accuracy will be in the hundreds. Increasing the length will also increase the numerical complexity of the system, as these reactions must be solved continuously, which may reduce stability and solver convergence. The use of a maximum length of 3 can therefore be concluded as providing sufficient accuracy based on the model comparison, while maintaining higher stability and simulation speed.

4.2 Controller tuning

The controllers in the system were tuned based on the SIMC rules developed by Skogestad S [12]. The level controllers for each section were tuned based on the response to a 5 % step increase in the flow used as the manipulated variable for the controller. The tuning variables were found from the subsequent response in the liquid volume. For the temperature controller to the reactor temperature, the tuning for the controller was calculated based on the response in reactor temperature to a 5 % step increase in the UA value of the heat exchanger.

The vaporiser level is controlled by the inflow of methanol into the system. The methanol flow is also in a ratio controller with the liquid bleed from the absorption column. This controller is just defined as a split ratio between the flows and calculated by the model, the bleed will therefore mirror the methanol response, and no further tuning is needed. The response in the level of the vaporiser for a 5% step in the methanol feed at t = 200 is shown in Figure 4.2.2, with the calculated tuning parameters presented in Table 4.2.1.

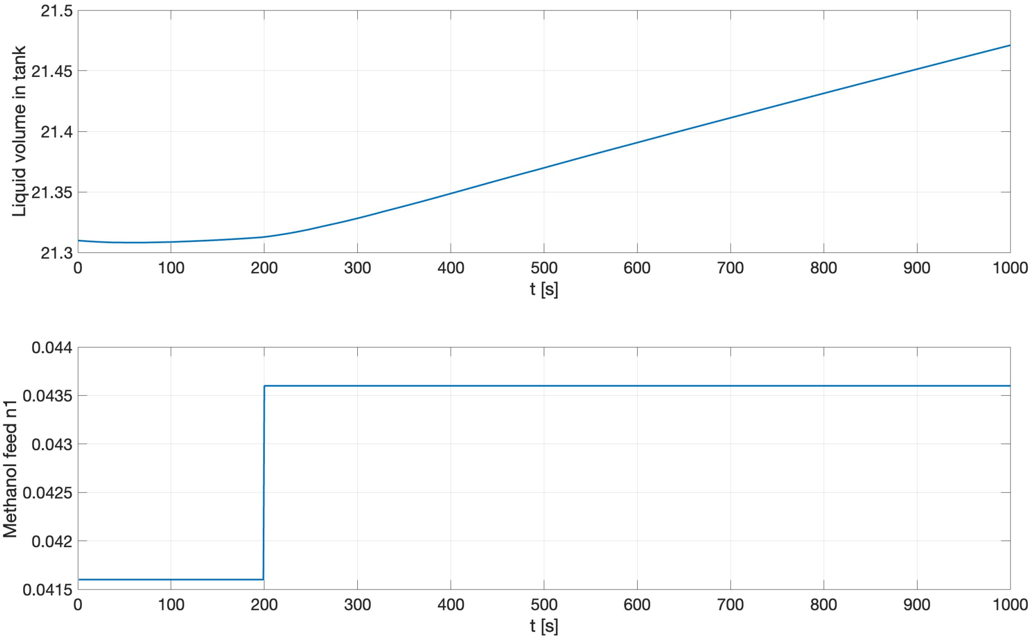

Figure 4.2.1: The response in the liquid level of the vaporiser to a 5% step in the methanol feed.

Table 4.2.1: The measured response from the liquid level in the vaporiser and calculated tuning parameters for a step in the methanol feed of 5%.

Parameter	**Response**
Δ y	0.0205
Δ u	0.002
Δ t	100
Tuning parameters	**Value**
k'	0.1025
τ_c	5
K_c	1.95

The reactor temperature in the process is also controlled. The control is based on increasing or decreasing the vaporisation of methanol and water in the vaporiser. In the actual process, this is achieved through a heat exchanger with a heating circulation leading from the 1st section for the absorption column. It is therefore desirable to maintain this flow constant, as it is also considered to be the cooling for the column section. To regulate the temperature of the vaporiser, further separate external systems are instead used. These include steam coils inside the vaporiser for additional heating, and an external cooling loop to reduce the temperature. To simplify the control structure, the model controls the temperature by adjusting the heat transfer rate (UA) from the heat exchanger, thereby simulating the effect of external heating or cooling loops. The controller, therefore, manipulates the heat transfer rate (MV) to control the reactor temperature (CV). To achieve adequate control, the controller was tuned using the complete system model. The tuning was based on the response in the reactor temperature to a 5% step increase in the UA value. The resulting response is given in Figure 4.2.2 with the calculated tuning parameters presented in Table 4.2.2. For the tuning, the closed-loop time constant (τ_c) was set to 10 seconds.

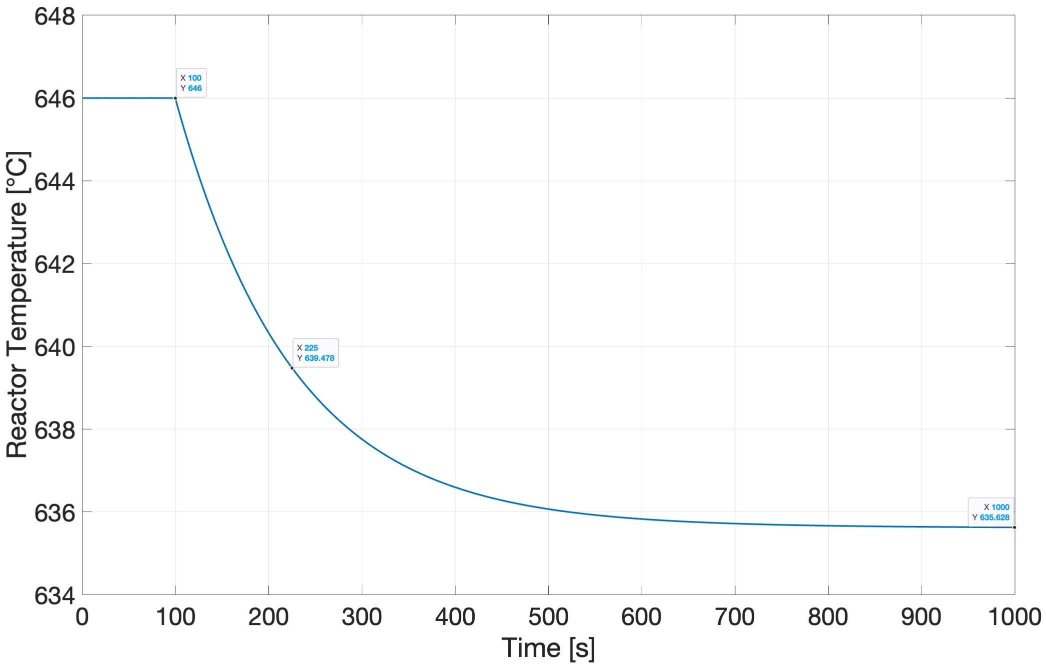

Figure 4.2.2: The response in the reactor temperature to a 5% step in the heat transfer rate (UA).

Parameter	Response
Δ y	-10.372
Δ u	26444
Tuning parameters	**Value**
k	-3.9×10^{-4}
θ	1
τ_1	125
τ_c	10
τ_I	40
K_c	-32051

Table 4.2.2: The measured response from reactor temperature and calculated tuning parameters for a 5% step increase in the UA value of the heat exchanger.

To determine the accuracy of the tuning, the response for the tuned temperature controller to a 5% increase in the air feed is shown in Figure 4.2.3.

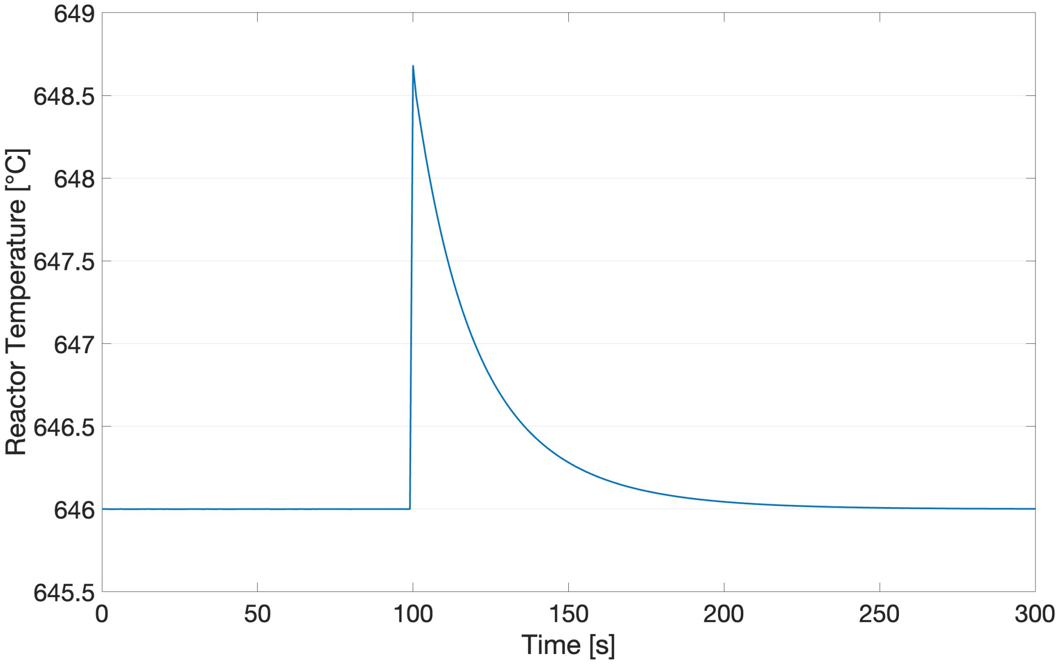

Figure 4.2.3: The response in the reactor temperature to a 5% step increase in the air feed with the tuned controller active.

The response indicated that the controller quickly reverts to the set-point when a disturbance is introduced. The response is also smooth, without undershooting the set point. While the initial peak is higher than desired, the model's limited implementation of gas dynamics means that it is not possible to reduce it by better tuning.

CHAPTER

FIVE

RESULTS AND DISCUSSION

For all simulations performed with the model, the temperatures of the absorption column were kept at their original set-point value. The complete model was constructed as explained in Section 3.4. For the simulations, a sample length of 1 second was set. This implies that each single dynamic model was simulated for 1 second per iteration of the combined model. The model was run for 3000 iterations, with flows being updated each iteration, resulting in a total simulation length of 3000 seconds.

5.1 Simulation of the system model to steady-state

The structure for the completed model used to make the simulations is described in Section 3.4. For the simulation, the air inlet into the vaporiser model was set to 7712 kg/h, based on Dynea data used as the design basis, as presented in Section 2.3. The rest of the feeds into the vaporiser and the flows both internally and shared between units were calculated by the model. For this simulation, the gas recycle was not implemented, as it was not active in the plant at the time of the measurements in the dataset.

The data provided by Dynea may be inaccurate for certain parts of the system, as it is based on calculations rather than measurements. This includes the flow and composition of internal flows in the absorption column and flows between process units. However, the dataset still provides valuable insight into expected results for the simulation. The flow and composition of the product stream are also known based on measurements and chemical analysis. The product is also dependent on several factors, such as temperature profile in the column, the conversion in the reactor and the vaporisation of liquid in the vaporiser. A comparison with the product flow may therefore serve as an important reference point for evaluating the overall model at the chosen parameters.

The achieved product composition when the model is at steady-state is presented in Table 5.1.1 with the compositions given as the overall compositions ($\bar{x}$) of formaldehyde, water and methanol. The flow rate of the product stream is presented in Table 5.1.2.

Table 5.1.1: Comparison between the steady-state results from the model and the data given by Dynea for the product composition. With all compositions given as the overall composition.

Components	$\bar{x}_{\textbf{model}}$	$\bar{x}_{\textbf{data}}$	$\Delta\bar{x}$	**relative error**
Formaldehyde	51.87%	51.69%	+0.18%	+0.35%
Water	46.87%	47.46%	-0.59%	-1.24%
Methanol	1.26 %	0.85%	+0.41%	+48.24%

Table 5.1.2: Comparison between the steady-state results from the model and the data given by Dynea for the product flow.

Parameter	**Model**	**Data**	**Δ flow**	**relative error**
Product flow	7724 kg/h	7708 kg/h	+16 kg/h	+0.21 %

The resulting product composition presented in Table 5.1.1 shows that the concentration of formaldehyde in the product is higher than expected, with a relative error of +0.35% from the concentration given in the dataset. The methanol content can also be observed to be higher with a relative error of +48.24%. The error in the values may be a result of the assumptions made when modelling the process, particularly regarding the assumption that chemical equilibrium is always maintained in every unit. With varying temperatures and pressures between the column sections, achieving perfect equilibrium may not be possible in reality.

The equilibrium constant used in the process may also not be entirely correct. Based on the same coefficients employed in the model developed by Maurer [1]. The constants were found experimentally, however, the experiments consisted of lower formaldehyde concentrations than what is expected in the product. This may have affected the validity of the constants at increasing concentration.

While several factors may have contributed to the final composition error, particularly regarding the methanol concentration, the numerical error in the values is minimal. Due to the low concentration of methanol in comparison to the other components, minor errors in either of the other compositions will have a larger impact on the relative error of methanol. This is also evident from the difference between the compositions given by the model and the data from Dynea, where there are only minor numerical errors in the values.

This implies that, although not perfect, the model performs well in predicting the process, providing a relatively accurate representation of the flow and composition of the product stream. With the product being determined by many parameters in the process, as previously discussed, it can be argued that the model will give an acceptable representation of the process for all parts of the model.

5.2 Simulations utilising recycled gas with constant gas flow

To determine the effect of recycle gas on the system, the system was simulated with the implementation recycle gas from the top of the absorption column while the total gas flow was kept constant. The implementation was performed stepwise with a 0.1% increase in the fraction of recycled gas per step. This was done to ensure stability throughout the simulation. The total fraction of the total gas feed containing recycled gas was simulated up to 10% with the first step starting at t = 100 seconds.

In the real process plant, gas recycle can be used to increase or decrease the formalin concentration of the product. The tail gas from the absorption column is nitrogen- and hydrogen-rich because the oxygen in the air feed acts as a reactant in the formation of formaldehyde. The implementation of recycled gas will therefore have consequences on the reactor temperature. Nitrogen is inert for all reactions, as can be seen from the reaction equations presented in Section 2.2.2. The increased nitrogen concentration in the vapour feed to the reactor will therefore reduce the temperature. As a result of the temperature control, a corresponding decrease in the vaporiser temperature should be observed to maintain the reactor temperature at its set-point.

The dynamic response to the implementation of the recycled gas stream for the overall heat transfer rate of the heat exchanger and the temperature in the vaporiser are shown in Figure 5.2.1 and Figure 5.2.2 respectively. The steady-state values before and after the implementation of recycle gas are presented in Table 5.2.1.

Table 5.2.1: The overall heat transfer rate (UA) and vaporiser temperature before and after the implementation of recycled gas to a total of 10% of the total gas feed.

Parameter	**Before**	**After**	Δ value
T	74.79 °C	72.63 °C	-2.16 °C
UA	528.88×10^3 W/K	316.59×10^3 W/K	-212.29×10^3 W/K

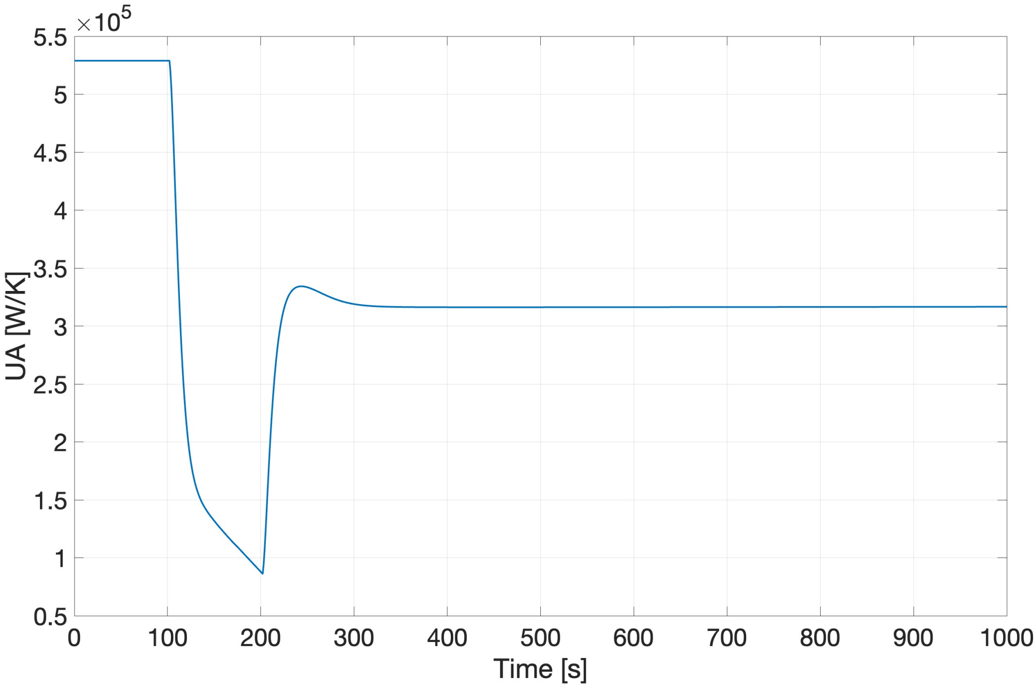

Figure 5.2.1: The response in UA as a result of implementing recycled gas stepwise to a total of 10% of the total gas feed with constant gas feed to the vaporiser.

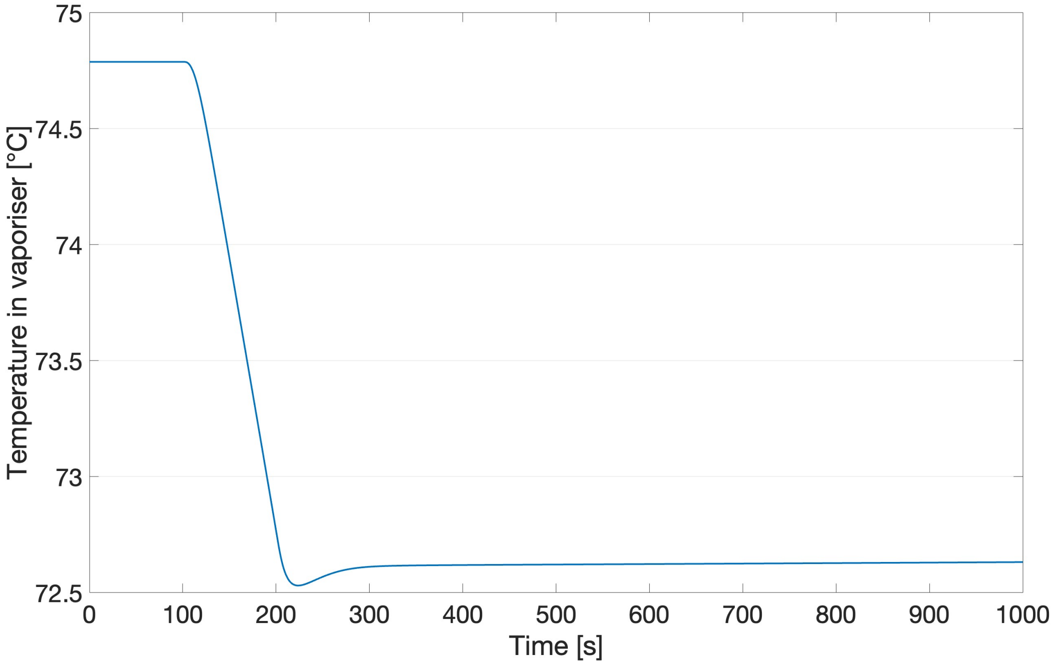

Figure 5.2.2: The response in vaporiser temperature as a result of implementing recycled gas stepwise to a total of 10% of the total gas feed with constant gas feed to the vaporiser.

From the response shown in Figure 5.2.1 of the heat supplied to the vaporiser, given by the heat transfer rate (UA), a significant drop is observed. This coincides with the expected dynamics in the system when an increased amount of nitrogen is introduced into the reactor, as previously mentioned. However, while a drop is expected, the heat is reduced by around 40 %. From the temperature of the vaporiser given by Figure 5.2.2, only a slight decrease in temperature is observable. The larger reduction in heat could be a result of a reduction in the liquid feed into the vaporiser. This is expected due to the level controller, which determines the liquid feed flows. With a lower temperature in the vaporiser, less liquid will be vaporised into the vapour phase. Leading to a reduction in the liquid feed.

To simplify the model, the vaporiser system was assumed not to lose any heat over time. The reduction in the liquid feed, in addition to the lower vaporiser temperature, could therefore explain the significant decrease in the heating required.

With a reduction in both oxygen and methanol in the vapour as a result of both lower air feed and reduction of vaporiser temperature, the methanol/oxygen ratio in the vapour should be affected. The response in methanol/oxygen ratio is presented in Figure 5.2.3, with the values before and after the implementation of recycle gas given in Table 5.2.2.

Table 5.2.2: The methanol/oxygen ratio in the vapour feed to the reactor before and after the implementation of recycled gas to a total of 10% of the total gas feed.

Parameter	**Before**	**After**	**Δ**
Methanol/oxygen	2.736	2.665	-0.071

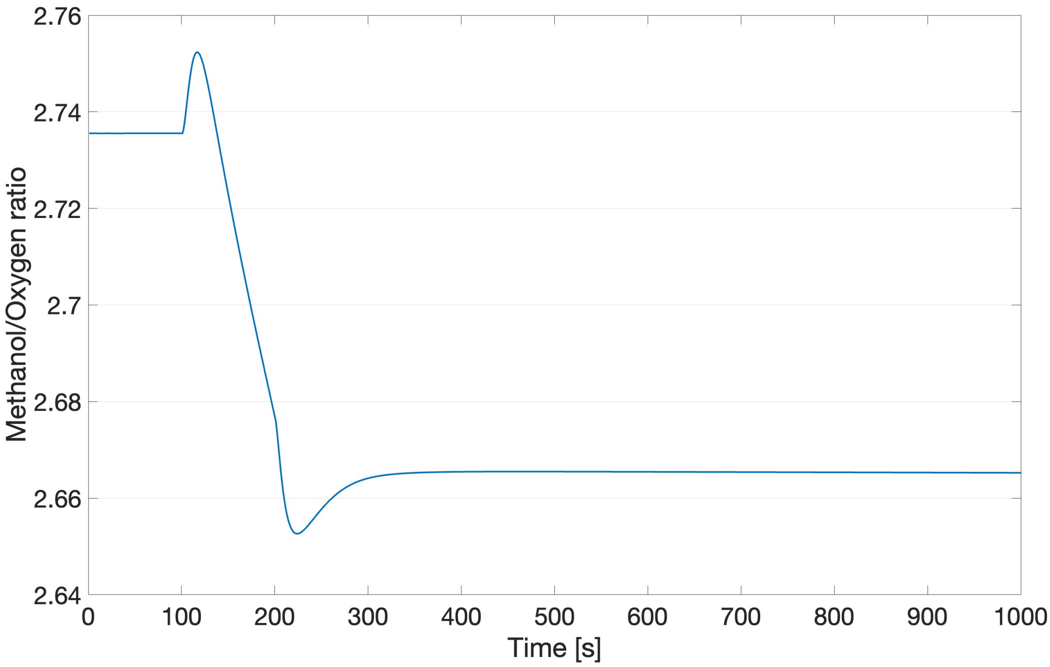

Figure 5.2.3: The response in the methanol/oxygen as a result of implementing recycled gas stepwise to a total of 10% of the total gas feed.

From the results in Table 5.2.2, it can be observed that the methanol/oxygen ratio in the vapour is slightly reduced. Methanol is reduced by both the reduction of air into the system, and also from the lower temperature in the vaporiser. However, the ratio is not significantly affected, indicating that the relationship between the two components is still maintained by the system. As previously discussed in Section 2.2.2, increasing the amount of oxygen in the vapour will increase the reactor temperature based on the reactions. A slight reduction in the methanol/oxygen ratio is therefore expected to account for the increased heat needed to maintain the temperature. With the minimal change, possibly explained by the additional reduction in methanol.

The reactions taking place in the reactor are described in Section 2.2.2. As can be seen from the stoichiometry, both reactions, including the formation of formaldehyde, are dependent on the presence or deficit of oxygen. While the reaction between methanol and oxygen is irreversible, the reaction in the absence of oxygen is instead an equilibrium reaction. Variations in this ratio should therefore have an apparent effect on the product composition.

To investigate this effect further, the response in the product flow and composition to the implementation of gas recycle is presented in Figure 5.2.4 and Figure 5.2.5, respectively. The steady-state values for the product flow before and after implementation are given in Table 5.2.3, while the values for the product composition are presented in Table 5.2.4. The composition is given as the overall composition of formaldehyde, water and methanol in the liquid, calculated as described in Section 2.4.3.5.

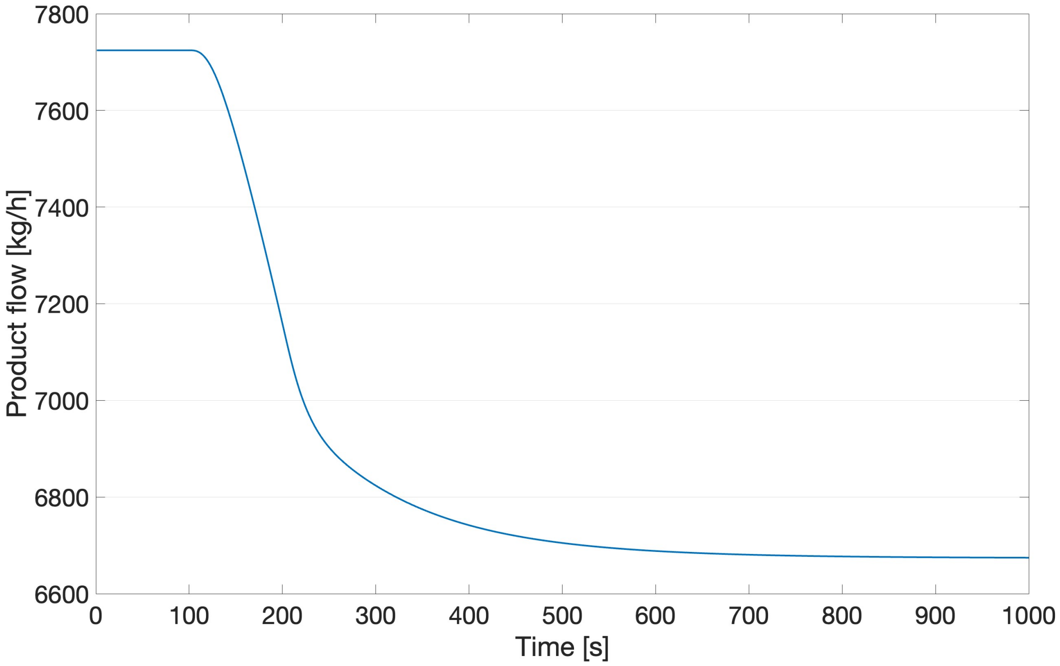

Figure 5.2.4: The response in the product flow as a result of implementing recycled gas stepwise to a total of 10% of the total gas feed.

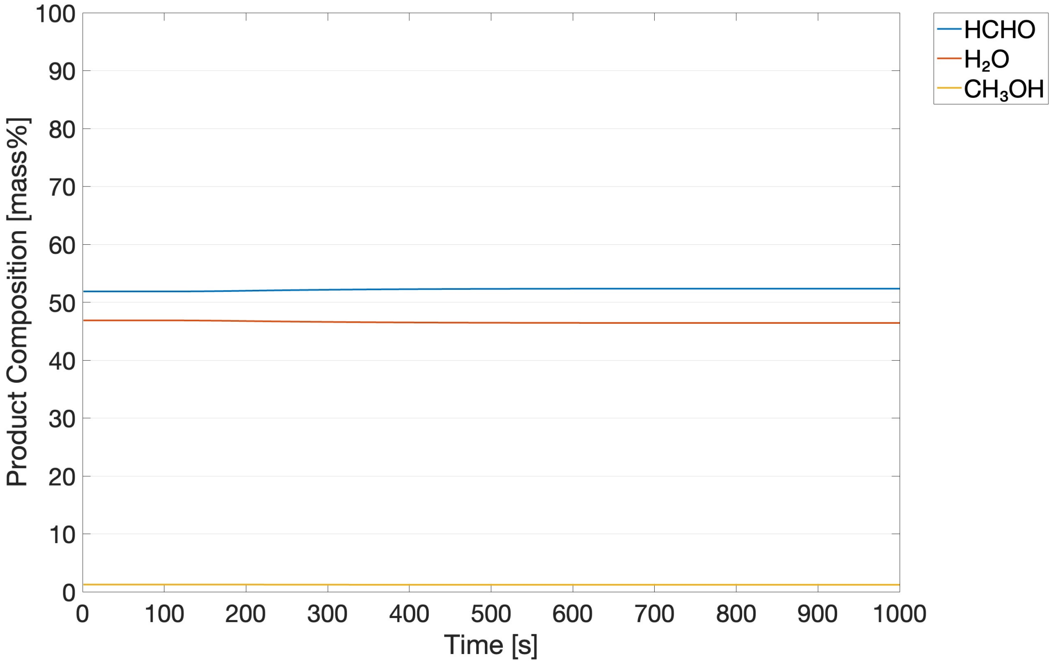

Figure 5.2.5: The response in the product composition as a result of implementing recycled gas stepwise to a total of 10% of the total gas feed.

Table 5.2.3: The flow of the product stream from the bottom of the column before and after the implementation of recycled gas to a total of 10% of the total gas feed.

Parameter	**Before**	**After**	**Δ**
Product flow	7724 kg/h	6675 kg/h	-1049 kg/h

Table 5.2.4: The composition of the product stream given as the complete composition of components before and after the implementation of recycled gas to a total of 10% of the total gas feed. The composition is given as the overall liquid composition.

Component	$\bar{x}_{\text{before}}$ **[m%]**	$\bar{x}_{\text{after}}$ **[m%]**	$\Delta\bar{x}$
Formaldehyde	51.87	52.36	+0.49
Water	46.87	46.43	-0.44
Methanol	1.26	1.21	-0.05

From the response in the product flow presented in Table 5.2.3, a decrease of around 4% is observed as a result of implementing recycled gas into the system. With less liquid entering the system due to the reduction in liquid feed, a corresponding decrease in product flow is expected. However, with an increase in gas feed proportional to the introduction of gas recycle, it should be possible to maintain the product flow at its original value. At the Dynea plant, this is also typically done when introducing gas recycle into the system.

From the response in the composition presented in Table 5.2.4, an increase in formaldehyde concentration in the product is observed. Additionally, a reduction in the methanol concentration in the product is also observable. These results align with the actual plant response previously mentioned. With a reduction in the methanol-to-oxygen ratio, a decrease in methanol content in the product could be expected. The further increase in formaldehyde concentration may be explained by the lower temperature in the vaporiser. With a reduction in temperature, the water content in the vapour will also be reduced along with methanol. The concentration of formaldehyde in the product may therefore be further increased due to the reduction of vaporised water.

5.3 Simulations utilising recycled gas with constant air feed

A simulation in which the air feed was kept constant while implementing gas recycle was performed to determine if similar effects would be observed as for the simulation in Section 5.2. The gas recycle was implemented similarly to the previous simulation, but the total gas feed was instead increased to accommodate for the fraction made up of recycled gas. To compare the responses in the system, similar results for this simulation are presented.

The response to the implementation of the recycled gas stream for the overall heat transfer rate of the heat exchanger and the temperature in the vaporiser is shown in Figure 5.3.1 and Figure 5.3.2, respectively. The steady-state values before and after the implementation of the recycle gas are presented in Table 5.3.1.

Table 5.3.1: The overall heat transfer rate (UA) and vaporiser temperature before and after the implementation of recycled gas to a total of 10% of the total gas feed.

Parameter	**Before**	**After**	**Δ**
T	74.79 °C	72.75 °C	-2.04 °C
UA	528.88×10^3 W/K	371.46×10^3 W/K	-157.42×10^3 W/K

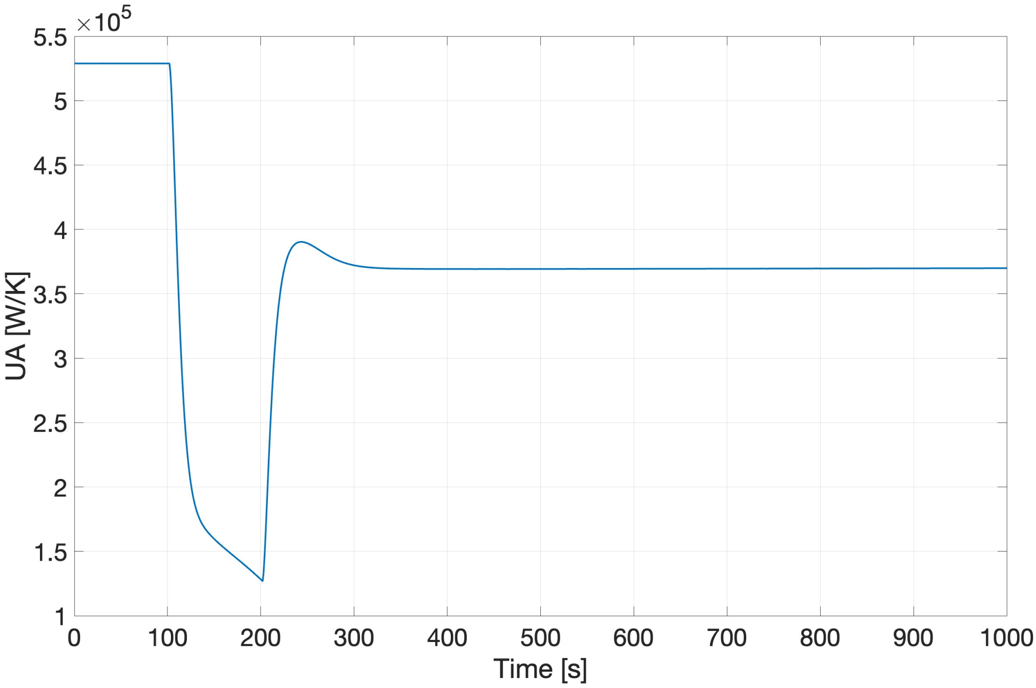

Figure 5.3.1: The response in UA as a result of implementing recycled gas stepwise to a total of 10% of the total gas feed.

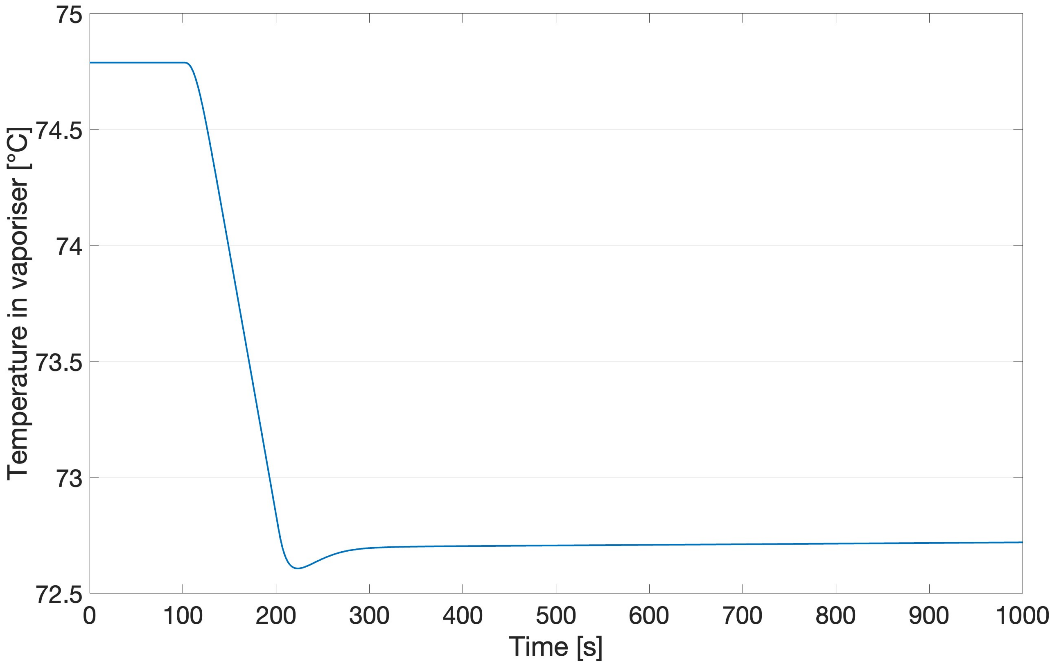

Figure 5.3.2: The response in vaporiser temperature as a result of implementing recycled gas stepwise to a total of 10% of the total gas feed.

A reduction in the overall heat transfer rate is still observed from the results. However, the reduction is lower compared to the previous simulation in which the total gas feed was kept constant. With a larger air flow, the effect on reactor temperature should be reduced, resulting in a higher vaporiser temperature than previously. While the temperature increase is minimal, as observed from the results presented in Table 5.3.1, the liquid feed will also increase. Consequently, the heat supplied to the vaporiser must also be higher. Similarly to what was discussed in the previous simulation, this could be a factor in the larger increase observed in the heat supplied, despite the minimal temperature difference between the simulations.

The response in methanol/oxygen ratio is presented in Figure 5.3.3, with the values before and after the implementation of recycle gas given in Table 5.3.2.

Table 5.3.2: The methanol/oxygen ratio in the vapour feed to the reactor before and after the implementation of recycled gas to a total of 10% of the total gas feed.

Parameter	**Before**	**After**	**Δ**
Methanol/oxygen	2.736	2.665	-0.071

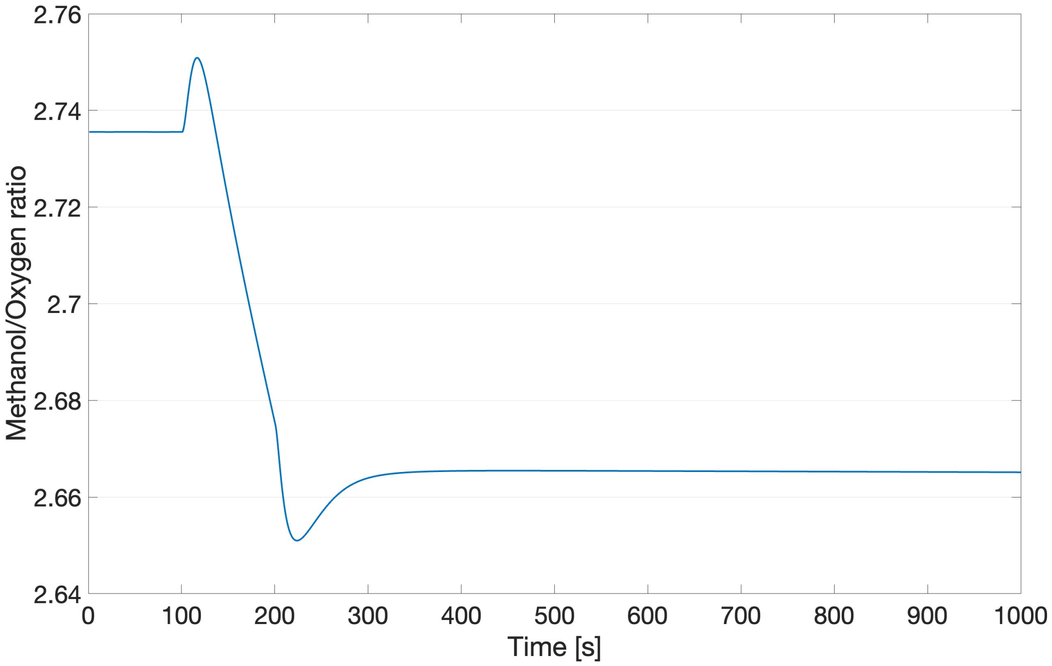

Figure 5.3.3: The response in the methanol/oxygen as a result of implementing recycled gas stepwise to a total of 10% of the total gas feed.

The methanol to oxygen ratio can be observed to be reduced by around 3% compared to the initial value. Compared to the previous simulation, the results are also identical. With all other parameters remaining constant except for the total gas feed, only minor differences in the vapour phase are expected due to the fast vapour dynamics. For the liquid phase, more noticeable differences may be observed due to the slow liquid dynamics of the system.

The response in the product flow and composition to the implementation of gas recycle is presented in Figure 5.3.4 and Figure 5.3.5, respectively. The steady-state values for the product flow before and after implementation are given in Table 5.3.4, while the values for the product composition are presented in Table 5.3.3. The composition is given as the total composition of formaldehyde, water and methanol, calculated as described in Section 2.4.3.5.

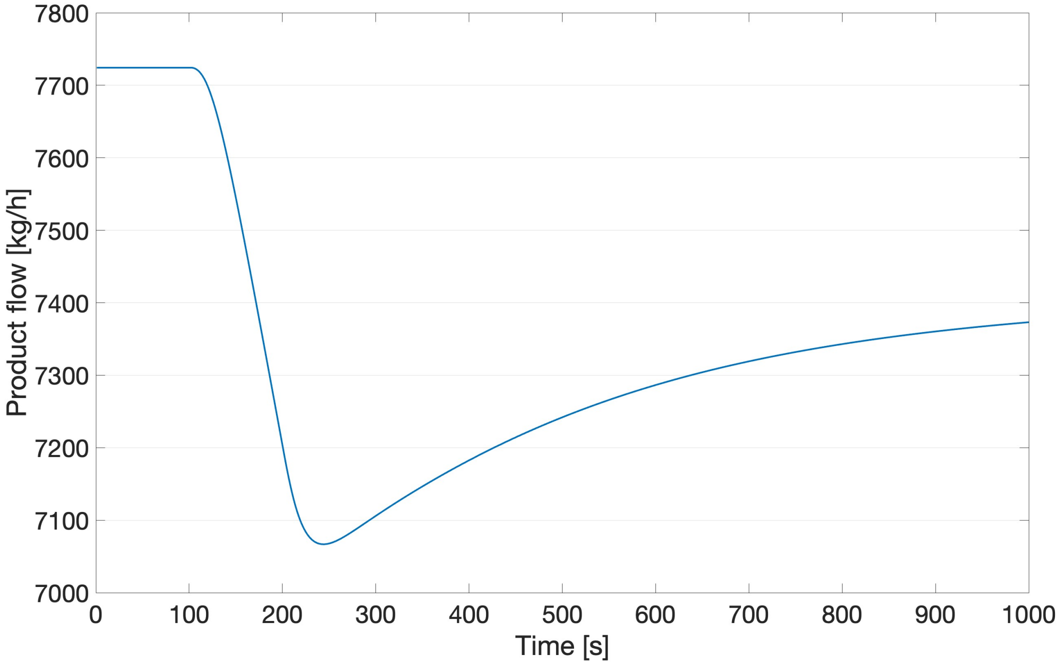

Figure 5.3.4: The response in the product flow as a result of implementing recycled gas stepwise to a total of 10% of the total gas feed.

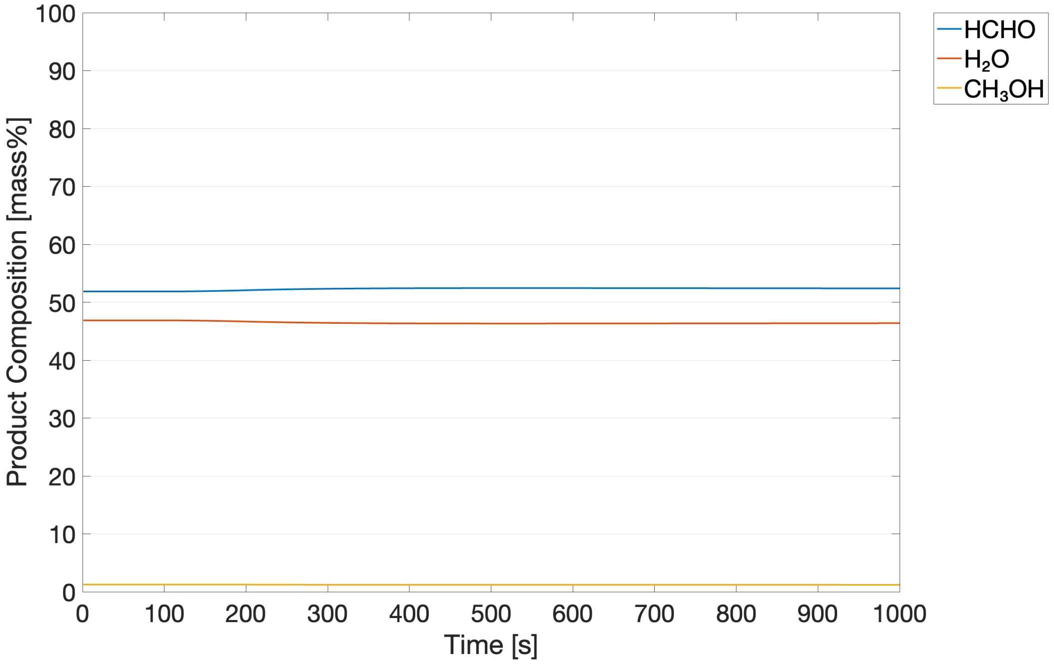

Figure 5.3.5: The response in the product composition as a result of implementing recycled gas stepwise to a total of 10% of the total gas feed.

Table 5.3.3: The flow of the product stream from the bottom of the column before and after the implementation of recycled gas to a total of 10% of the total gas feed.

Parameter	**Before**	**After**	**Δ**
Product flow	7724 kg/h	7411 kg/h	-313 kg/h

Table 5.3.4: The composition of the product stream given as the complete composition of components before and after the implementation of recycled gas to a total of 10% of the total gas feed.

Component	$\bar{x}_{\textbf{before}}$ **[m%]**	$\bar{x}_{\textbf{after}}$ **[m%]**	$\Delta\bar{x}$
Formaldehyde	51.87	52.33	+0.46
Water	46.87	46.48	-0.39
Methanol	1.26	1.20	-0.06

As seen from the resulting product flow presented in Table 5.3.3, a decrease in the product flow rate is observed. Although the oxygen feed is constant for this simulation, the additional nitrogen will still affect the reactor temperature. This is also observed through the response in UA and vaporiser temperature, which are reduced. As a result, the liquid feed will still be lower after the implementation, and a drop in product flow rate can be expected.

While higher than for the previous simulation, this implies that a further increase in total gas feed is required to maintain the product flow at the initial rate. However, the reduction is only around 4% for this simulation, and so only a minor increase in total gas feed is needed when a variable total gas feed is used to accommodate the recycled gas stream.

From the resulting product composition, the concentration of formaldehyde has been increased by around 0.5% with a reduction in methanol of 0.06%. These results are similar to those found in the previous simulation, indicating that the increase in gas feed will still have a comparable effect on the product composition. Given that both simulations have an identical methanol-to-oxygen ratio, this result also demonstrates how the ratio is a key factor in determining the product composition.

5.4 Simulations utilising recycled gas with reduction in reactor temperature set-point

With the implementation of recycled gas while maintaining the air feed to the vaporiser constant, it was observed that the formaldehyde concentration in the product increased. The increase was also similar to when the recycled gas comprised part of a constant total gas feed. By increasing the total gas flow instead of keeping it constant, the drop in product flow was also reduced, while the effect on product composition remained.

Another factor that will affect the process is the set-point for the reactor temperature. With a reduction in the set-point, the temperature in the vaporiser will be higher. As a result, the vapour feed to the reactor will have an increased concentration of methanol. This will result in a higher methanol-to-oxygen ratio than in the previous simulations.

To investigate this effect on the product composition, the gas recycle was implemented as described in Section 5.3. Additionally, the reactor temperature set-point was also reduced by 0.8 °C per % recycle gas in the total gas feed. The temperature reduction was based on discussions with co-supervisor Susort N. about what is performed in the actual plant [11].

The response in the UA value for the heat exchanger in the vaporiser heating loop with the implementation of a 10% increase in recycle gas and a reduction in the reactor temperature set-point is presented in Figure 5.4.1. The values before implementation and for the new steady-state of the system are presented in Table 5.4.1

Table 5.4.1: The overall heat transfer rate (UA) and vaporiser temperature before and after the implementation of recycled gas to a total of 10% of the total gas feed.

Parameter	Before	After	Δ
T	74.79 °C	72.9 °C	-1.89 °C
UA	528.88×10^3 W/K	385.83×10^3 W/K	-143.05×10^3 W/K

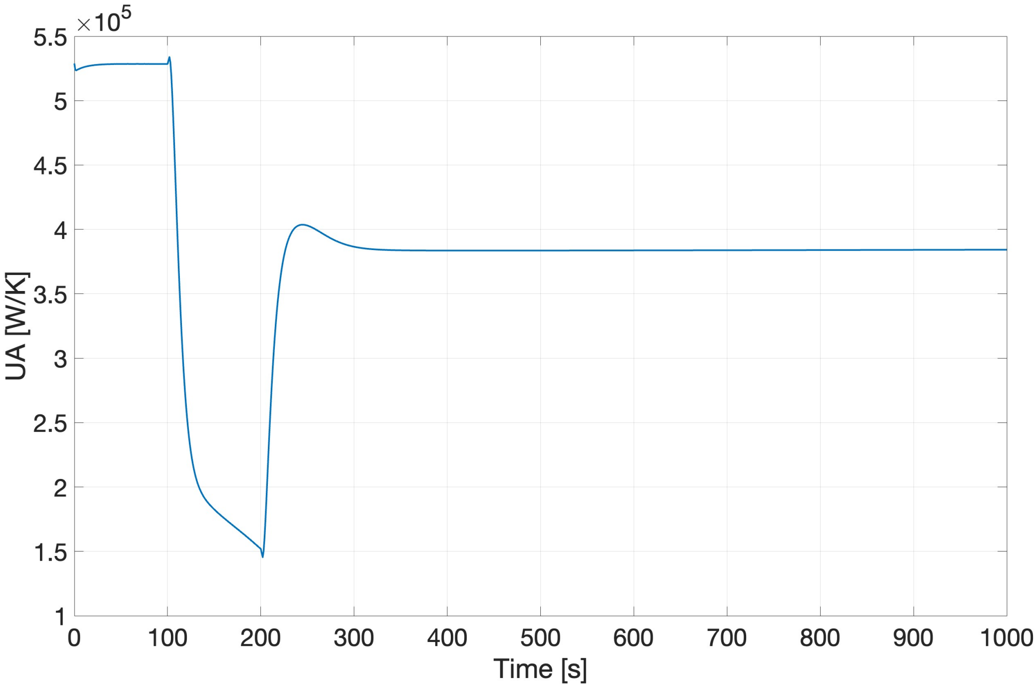

Figure 5.4.1: The response in the UA value when recycled gas is 10% of the total gas feed and the temperature set-point in the reactor is reduced.

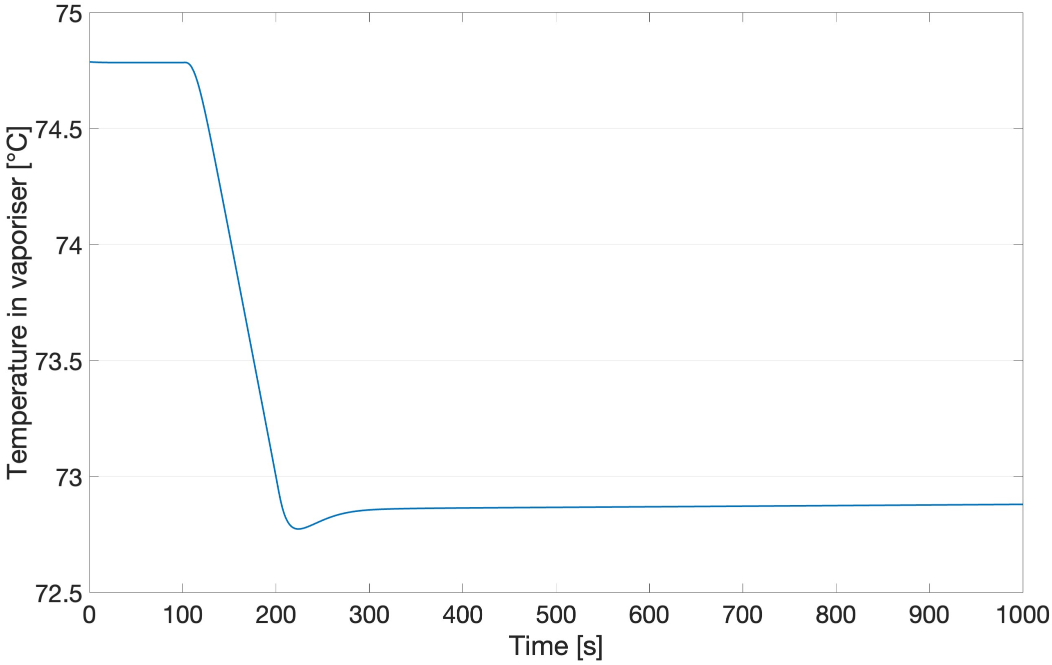

Figure 5.4.2: The response in the UA value when recycled gas is 10% of the total gas feed and the temperature set-point in the reactor is reduced.

With the reduction in set-point for reactor temperature, the heating supplied to the vaporiser presented in Table 5.4.1 shows an increase compared to the previous simulation.

As previously discussed, this is expected as a result of the temperature controller. With a lower temperature in the reactor, the vapour contains an increased amount of methanol to maintain the set-point. Due to increased vaporisation, more energy is required, and the required heating will be higher.

The response in methanol/oxygen ratio is presented in Figure 5.4.3, with the values before and after the implementation of recycle gas given in Table 5.4.2.

Table 5.4.2: The methanol/oxygen ratio in the vapour feed to the reactor before and after the implementation of recycled gas to a total of 10% of the total gas feed.

Parameter	**Before**	**After**	**Δ**
Methanol/oxygen	2.736	2.697	-0.039

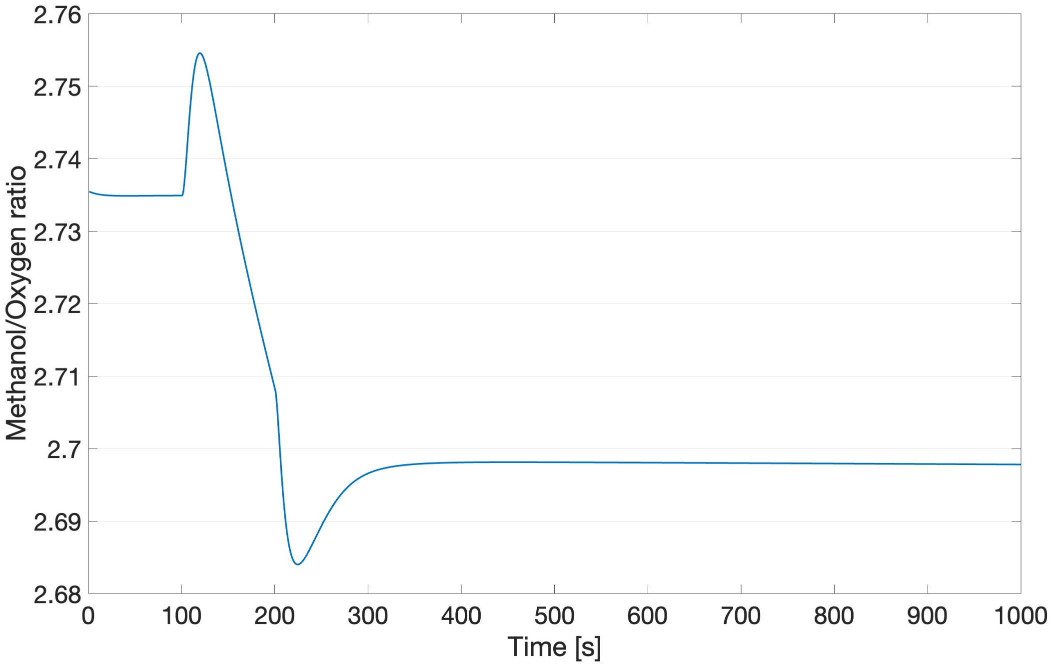

Figure 5.4.3: The response in the methanol/oxygen as a result of implementing recycled gas stepwise to a total of 10% of the total gas feed.

With the increase in methanol in the vapour compared to the previous simulation, a higher methanol-to-oxygen ratio is expected. This is also observable from the results presented in Table 5.4.2. In the first two simulations, where the total gas feed and the air feed were kept constant, it was observed that the reduction in this ratio determined the product concentration. With all other parameters kept constant except for the temperature set-point, the effect of the increased ratio should be more pronounced on the product. However, the temperature change will affect the equilibrium reaction for the dehydrogenation of methanol in the reactor, potentially impacting the resulting composition.

The response in the flow and composition of the product stream for the simulation are presented in Figure 5.4.4 and Figure 5.4.5, respectively. The calculated flow and composition before and after implementation are presented in Table 5.4.3 and Table 5.4.4.

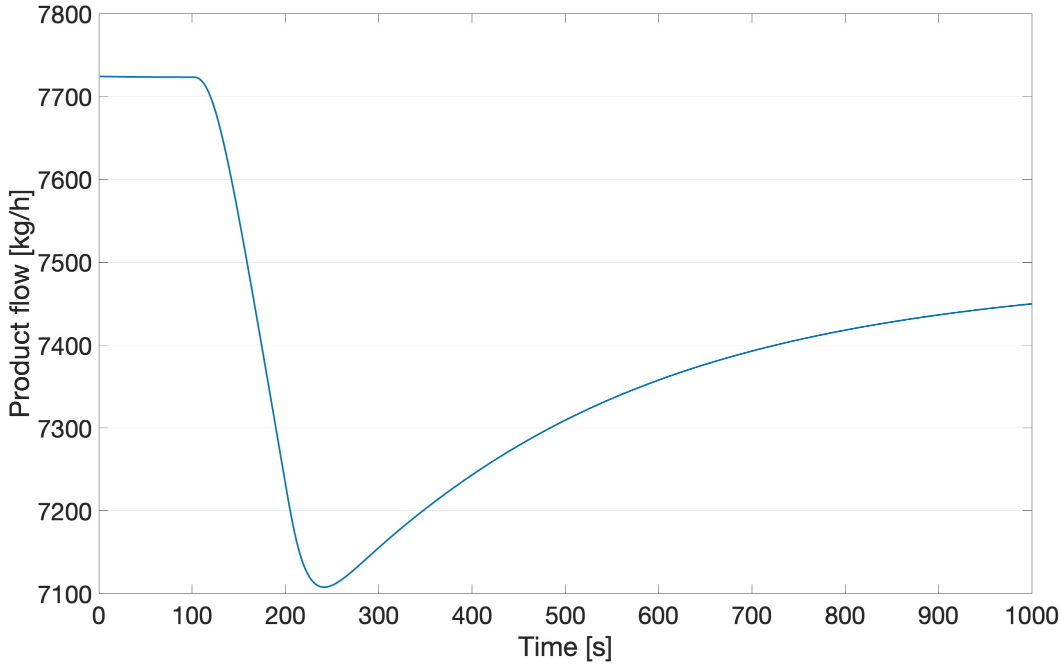

Figure 5.4.4: The flow of the product stream when recycled gas is 10% of the total gas feed and the temperature set-point in the reactor is reduced.

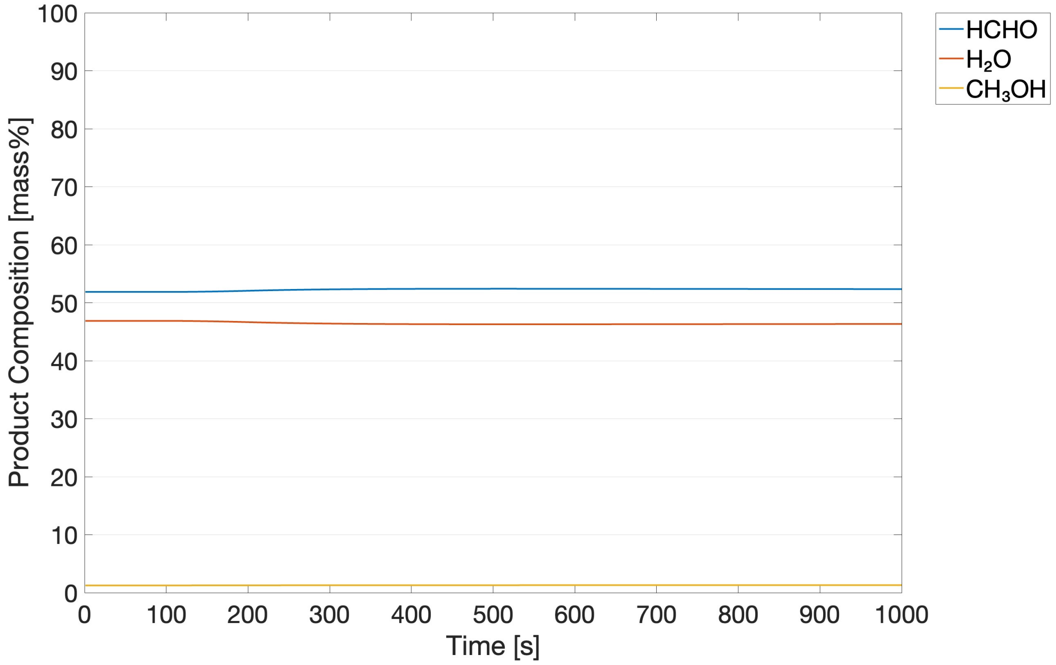

Figure 5.4.5: The liquid composition of the product stream when recycled gas is 10% of the total gas feed and the temperature set-point in the reactor is reduced.

Table 5.4.3: The flow of the product stream from the bottom of the column before and after the implementation of recycled gas to a total of 10% of the total gas feed.

Parameter	**Before**	**After**	**Δ**
Product flow	7724 kg/h	7489 kg/h	-235 kg/h

Table 5.4.4: The composition of the product stream given as the complete composition of components before and after the implementation of recycled gas to a total of 10% of the total gas feed.

Component	**$\bar{x}_{\text{before}}$ [m%]**	**$\bar{x}_{\text{after}}$ [m%]**	**$\Delta\bar{x}$**
Formaldehyde	51.87	52.27	+0.40
Water	46.87	46.42	-0.45
Methanol	1.26	1.31	+0.05

From the flow rate of the product stream presented in Table 5.4.3, a reduction in the product flow is still observed. This is expected due to the lowering of the reactor temperature, which allows for higher vaporisation of the liquid and increases the liquid feed. For the composition presented in Table 5.4.4, an increase in the formaldehyde concentration is also observed.

Interestingly, the methanol concentration in the product increases. With a lower product flow, a reduction in the liquid feeds can be assumed. The increase in methanol, therefore, seems to indicate lower conversion of methanol to formaldehyde through dehydrogenation. As seen from Equation 2.3, this reaction is an endothermic process. As endothermic reactions are more thermodynamically preferred at high temperatures, the temperature reduction can shift the equilibrium towards a higher methanol concentration. With the slight decrease in temperature, this shift is unlikely to account for the entire temperature increase. The rest of the increase is therefore likely caused by the methanol/oxygen ratio in the vapour.

Although a reduction in the ratio is noticeable, it remains higher than in the previous simulations. This would have less effect on the methanol content in the product. With the shift of the equilibrium reaction due to the change in temperature set-point, the combination of both factors could be a likely cause. This result also clearly displays the complexity of the system, in which several factors will affect the final product.

5.5 Comparison of the recycled gas simulations

To determine the optimal control strategy based on the results from each simulation, a comparison was conducted to assess the effects on the system resulting from each parameter change. This also provides a clear overview of the separate simulation results.

The comparison was first made between the resulting heating from the heat exchanger, as determined from the UA value. The comparison is presented in Table 5.5.1.

Table 5.5.1: Comparison between the heat supplied by the heat exchangers for each of the simulations utilising gas recycle.

Simulation	
Initial steady-state	528.88×10^3 W/K
Constant gas feed	316.59×10^3 W/K
Constant air feed	371.46×10^3 W/K
Varying temperature set-point	385.83×10^3 W/K

A factor previously identified as a major contributor to the product's composition is the methanol-to-oxygen ratio in the vapour entering the reactor, with results indicating that a lower methanol-to-oxygen ratio may be preferred for optimal product concentration. The comparison between the ratios obtained in each simulation is presented in Table 5.5.2.

Table 5.5.2: Comparison between the methanol/oxygen ratio in the vapour to the reactor for each of the simulations utilising gas recycle.

Simulation	
Initial steady-state	2.736
Constant gas feed	2.665
Constant air feed	2.665
Varying temperature set-point	2.697

From the results, it can be seen that the first two simulations, which involve implementing gas recycle with a constant gas feed or increasing the gas feed while implementing the recycle gas, give a similar ratio. As a result of the gas composition remaining similar in both cases, with a possible change in the composition of the recycled gas, a similar ratio is probable. Although a slight reduction was observed, this may be due to numerical factors in the model or variations in system dynamics between the two cases. For the simulation where the set-point temperature was also reduced, a higher ratio is observed. With the increased amount of methanol possible in the vapour as a result of the reduction in temperature set-point, this is an expected result.

With some variations between the simulations regarding energy supplied to the vaporiser and the resulting methanol/oxygen ratio, the final effect on the product is most important. The comparison of product flow rates is presented in Table 5.5.3, with the composition for the three cases listed in Table 5.5.4.

Table 5.5.3: Comparison of the product flow rate obtained from each simulation when implementing at the new steady-state for the model.

Simulation	Product flow rate
Initial steady-state	7724 kg/h
Constant gas feed	6675 kg/h
Constant air feed	7411 kg/h
Varying temperature set-point	7489 kg/h

Table 5.5.4: Comparison of the product composition obtained from each simulation at the new steady-state for the model. The composition is given as the overall composition ($\bar{x}$) in the liquid.

Simulation	$\bar{x}$ FA	$\bar{x}$ W	$\bar{x}$ Me
Initial steady-state	51.87 m%	46.87 m%	1.26 m%
Constant gas feed	52.36 m%	46.43 m%	1.21 m%
Constant air feed	52.33 m%	46.48 m%	1.20 m%
Varying temperature set-point	52.27 m%	46.42 m%	1.31 m%

By comparing the product flow rates for the simulations presented in Table 5.5.3, it can be observed that all simulations experience a drop in the total product flow compared to the initial simulation. For the first simulation, the air feed into the system was reduced to accommodate the increasing gas recycle. With the liquid feed into the process being determined by the level controller in the vaporiser, the only free production rate parameter is the air feed into the system. The air feed will therefore determine the throughput in the system and can be considered the throughput performance measure (TPM) for the process. With a reduction in the air feed, a drop in product flow rate is therefore expected based on the mass balance for the process.

Similarly, in the second simulation, where the air flow is kept constant, the drop in production rate for the process is less significant. However, a clear drop is still observed and is likely the result of increased nitrogen and hydrogen gas in the vapour phase. Since nitrogen is inert in all reactions, an increased nitrogen concentration will reduce the reactor temperature. In response, the methanol content in the vapour must be reduced to maintain the reactor temperature, leading to a lower methanol feed rate and, consequently, a reduced production rate.

To mitigate the effect of the increased nitrogen, the set-point for the reaction temperature was reduced in the final simulation. This will allow for a higher concentration of methanol in the vapour, further increasing the production rate. This is also observed from the results in Table 5.5.3, where an increase in production rate is noticeable compared to the second simulation. As both simulations have the same total gas flow, this increase can be attributed to the change in temperature set-point.

From the comparison of product compositions presented in Table 5.5.4, it is observed that while reducing the temperature set-point led to a higher production rate, it also reduced the effect on product concentration. The same results show that, in both the simulations where only recirculated gas was implemented, the impact on product composition persisted even as the total gas feed was increased. This suggests that recycled gas could be used as a manipulated variable in a future product composition controller. However, this would require adjusting the total gas flow proportionally to the amount of recycled gas used.

The similar results for the simulations where only gas recycle was implemented are also noticed for the methanol/oxygen ratio presented in Table 5.5.2, which are identical. For the simulation with reduced temperature set-point, this ratio is higher than for the other simulations. Although previously discussed, this further implies that this ratio is the main contributor to changes in product composition. As a reduction in the ratio leads to a more concentrated product, this suggests that a methanol concentration in the vapour below the steady-state value will result in a more favourable product composition.

It should be noted that, for the model, a constant fraction of oxygen reacting in the first reaction described by Equation 2.1 was used. It has previously been found that with the implementation of gas recycle, the fraction may change. As a result, the total impact on the process may not have been captured. With the implementation of lower reactor temperatures, exothermic reactions are more favoured, and the fraction could be reduced further.

5.6 Simulation varying the methanol to water feed ratio

A possible parameter for controlling the product composition is the ratio between the bleed from the 4th section of the absorption column and the pure methanol feed. While the methanol feed is determined from the level controller in the vaporiser, the liquid bleed is instead controlled in a ratio to the methanol. With the flow of methanol controlled, the ratio controller is integrated into the already existing control structure. This would make it ideal for further control of the product composition, as the flows are already dependent on the rest of the system. To investigate the response in the process of manipulating the ratio, the system was simulated for a reduction of 2% in the water/methanol ratio. Increasing the amount of water in the liquid feed to the vaporiser.

The resulting change in UA value for the simulation is presented in Table 5.6.1.

Table 5.6.1: The overall heat transfer rate (UA) and vaporiser temperature before and after the increase in the water/methanol ratio.

Parameter	**Before**	**After**	**Δ**
T	74.79 °C	75.05 °C	+0.26 °C
UA	528.88×10^3 W/K	561.24×10^3 W/K	$+32.36 \times 10^3$ W/K

From the resulting UA value presented in Table 5.6.1, an increase in the heating supplied to the vaporiser is observed. The liquid from the 4th section of the absorption column is mainly comprised of water. An increase in the liquid feed to the vaporiser, consisting of this liquid, will therefore increase the water content in the vaporiser. With water having a higher heat capacity than methanol, an increase in energy required to maintain the vaporisation of product is expected. As the liquid composition changes, the temperature in the vaporiser must also increase to maintain the reactor temperature. This will increase the vaporisation of liquid, leading to a higher liquid feed. As a result, the heat supplied to the vaporiser must increase to maintain vaporisation. The increase in energy required is therefore an expected result of increasing the water content in the vaporiser liquid.

The resulting product flow and composition are presented in Table 5.6.2 and Table 5.6.3, respectively.

Table 5.6.2: The flow of the product stream from the bottom of the column before and after the implementation of recycled gas to a total of 10% of the total gas feed.

Parameter	**Before**	**After**	**Δ**
Product flow	7724 kg/h	7754 kg/h	+30 kg/h

Table 5.6.3: The composition of the product stream given as the complete composition of components before and after the implementation of recycled gas to a total of 10% of the total gas feed.

Component	$\bar{x}_{\text{before}}$ **[m%]**	$\bar{x}_{\text{after}}$ **[m%]**	$\Delta\bar{x}$
Formaldehyde	51.87	51.60	-0.27
Water	46.87	47.15	+0.28
Methanol	1.26	1.24	-0.02

With a higher liquid feed resulting from a lower methanol concentration in the liquid, an increase in the product flow rate is expected. This can also be observed from the results presented in Table 5.6.2. With lower methanol concentration in the liquid, the reactor temperature will increase. In order to maintain the temperature, further vaporisation of liquid is needed. This was also previously observed from the increased temperature and heat supplied to the vaporiser. The increased water content is also observable from the product composition given in Table 5.6.3. An apparent reduction in formaldehyde concentration is noticed, which may be attributed to the higher water concentration in the vapour entering the reactor as a result of the higher vaporiser temperature.

While the methanol concentration in the liquid phase is reduced, the methanol in the vapour phase may remain similar to the initial concentration. This is due to the increased feed and temperature in the vaporiser, which will vaporise more of the liquid feed. However, with the presence of an increased amount of water in the vapour phase contributing to a reduction in reactor temperature, a drop in methanol is still likely to occur. This will slightly affect the methanol-to-oxygen ratio in the vapour, which has been shown to affect the methanol in the product. As a result of these factors, the reduction of methanol in the product may be attributed to the increased water content rather than a decrease in methanol. As seen from the results presented in Table 5.6.3, this is also supported by the increase in water.

Based on the overall results, the water-to-methanol ratio in the liquid feed appears to be a viable parameter for composition control. The methanol-to-oxygen ratio has been found to be a crucial parameter in controlling the product composition. With the control using only the methanol-to-water ratio of the liquid feed, the controller will be part of the liquid phase. Due to the considerable liquid hold-up in the vaporiser and the inherently slow liquid dynamics in the system, this may lead to a slow controller response. While using the methanol-to-water ratio may be the simplest solution for controlling composition, it may be more effective when paired with other control parameters. As seen from previous analysis during the implementation of recycled gas, the response in the system to changes in the vapour phase is fast. A combination of the two control structures could therefore be a possibility.

CHAPTER

SIX

CONCLUSION

While previous models have been developed to accurately depict the tertiary formaldehyde-, methanol- and water system, these have been limited to smaller-scale experiments. The extension of these models into a plant-wide model for a formaldehyde production plant is therefore not a direct process. A plant-wide model can be an important tool to assist in decision-making regarding upgrades or changes to the plant. This can be achieved through quicker calculations and predictions for suggested changes, in addition to the possibility of implementing optimisation routines.

During this master's thesis, a plant-wide model of the Dynea formaldehyde production plant in Lillestrøm was constructed. The model was compared with models developed by Maurer and Susort. From the comparisons, it was determined that the model performs well in describing the vapour-liquid equilibrium of tertiary formaldehyde, water and methanol systems. Additionally, the same comparison was used to validate the calculation of the liquid reactions for oligomer formation used in the absorption column model. Based on the results from the comparisons, the model was determined to be accurate in its solution of the oligomer fractions in the liquid phase. It was also concluded that the decided maximum oligomer length of 3 was a valid assumption based on the low concentration of higher-order oligomers.

The complete model was simulated to steady state, and the product composition and flow were compared to data given by Dynea. From the comparison, it was found that the model performed well in predicting the dynamics and gave an acceptable representation of the process for all parts of the model.

The model was used to analyse the prospect of utilising the tail gas from the absorption column as a gas recycle to control the composition of the liquid product stream. From the analysis, the main parameter for controlling the composition was concluded to be the methanol-to-oxygen ratio in the vapour feed to the reactor. With gas recycle having an apparent effect on this ratio, it was determined that the use of gas recycle can be used to control the product composition. With the changes affecting the vapour phase, the rapid gas dynamics in the system would allow for a fast controller response. However, it was noted that to maintain the production rate, a secondary control is required to adjust the total gas feed into the system to compensate for the loss in the product flow rate. It was also found that for the process, a methanol-to-oxygen ratio in the vapour feed to the reactor of around 2.665 yielded the best results and the highest concentration of formaldehyde in the product stream.

The possibility of using the methanol-to-water ratio in the liquid feed to control product composition was also briefly explored in this thesis. The results showed a clear correlation between the ratio in the liquid feed and the product composition. However, due to the considerable liquid hold-up and slow liquid dynamics, the system's response was slow. It was therefore concluded that a pairing with other parameters, such as gas recycle, could be a solution for improving control.

CHAPTER

SEVEN

FURTHER WORK

Although the model developed during this master's thesis can be considered complete, further work can be done to improve the simulation and identify an optimal control structure for regulating the product composition.

This includes the possible use of optimisation routines in order to determine the optimal process parameters for the product composition. While the model in its current form has performed well in the simulations of the system, the possible adaption to symbolic variables may improve the speed of the simulation while allowing for the use of several optimization routines.

Further additions to the model could also be implemented, these include modelling the heat exchangers in the sections of the absorption column, allowing for a temperature gradient between the liquid and gas phases in the column. The implementation of a variable fraction of oxygen to react in the reactor dependent on the amount of gas recycle could also improve the model.

With the model currently being divided into several models, the adaption of the model into a single continuos simulation may also improve accuracy. This would also make it easier to determine control parameters for a product composition controller.

These improvements would allow for a faster, and more accurate model to generate better data and determine optimal process parameters and control structures.

BIBLIOGRAPHY

[1] Michael Albert et al. “Vapor–liquid equilibrium of aqueous solutions of formaldehyde and methanol”. en. In: *AIChE Journal* 46.8 (2000), pp. 1676–1687. DOI: `10.1002/aic.690460818`.

[2] Jonas Fraihat. “Control of the formaldehyde reactor section validated using dynamic simulations”. MA thesis. NTNU, 2024.

[3] Noel de Nevers. *Physical and Chemical Equilibrium for Chemical Engineers - Appendix A: Useful Tables and Charts.* John Wiley & Sons, 2012.

[4] T Chang, R M Rousseau, and J K Ferrell. *Vapor/liquid equilibria of constituents from coal gasification in refrigerated methanol.* North Carolina State Univ., Raleigh (USA). Dept. of Chemical Engineering, 1987.

[5] Sigurd Skogestad. *Prosessteknikk Masse- og energibalanser.* 3rd. Tapir Akademiske Forlag, 2009.

[6] Allan G. Blackman and Lawrence R. Gahan. *Aylward and Findlay’s SI Chemical Data,* 7th edition. John Wiley & Sons Australia, 2014.

[7] Ray Sinnott Gavin Towler. *Chemical engineering design, Appendix C - Physical Property Data Bank.* Butterworth-Heinemann, 2011.

[8] A. Kayode Coker. *Ludwig’s Applied Process Design for Chemical and Petrochemical Plants, Appendix C - PHYSICAL PROPERTIES OF LIQUIDS AND GASES.* 4th. Gulf Professional Publishing, 2007, pp. 827–862. DOI: `10.1016/B978-075067766-0/50019-1`.

[9] Håvard Fromreide. *Dynamic modelling of silver formaldehyde process.* NTNU, 2024.

[10] Phuong Ny Lillian Nguyen Vo. “Control of formaldehyde silver catalyst reactor system”. MA thesis. NTNU, 2023.

[11] Nils Arne Susort. “Meetings with Co-supervisor Nils Arne Susort from Dyena”. 2025.

[12] Sigurd Skogestad and Chriss Grimholt. *The SIMC Method for Smooth PID Controller Tuning.* London: Springer London, 2012, pp. 147–175. DOI: `10.1007/978-1-4471-2425-2_5`.

APPENDIX

A Calculation of UNIQUAC activity coefficients for vaporiser

For a system composed of water and methanol, the structural parameters and the adjustable Δu are given in Table A.1

Table A.1: Size and surface parameters for calculation of activity coefficients for a binary methanol-water mixture.

Component	**r**	**q**	**q'**	**Δu**
Methanol	1.43	1.43	0.96	-10.652
Water	0.92	1.40	1	15.107

With a liquid mixture consisting of (N) components, the coefficients required to calculate the activity of component (i) are provided in Equations A.1 through A.5. The coordination number is denoted by z and is typically assumed to be equal to 10. With r_i representing the structural size parameter of component i, q_i and q'_i are the structural area and modified structural area parameters of the component. The parameters r_i, q_i and q'_i are all pure component physical properties. While Δu is an adjustable binary parameter found from experimental data.[4]

$$l_i = \frac{z \cdot (r_i - q_i)}{2} - (r_i - 1) \tag{A.1}$$

$$\Phi_i = \frac{r_i \cdot x_i}{\sum_k^N r_k \cdot x_k} \tag{A.2}$$

$$\Theta_i = \frac{q_i \cdot x_i}{\sum_k^N q_k \cdot x_k} \tag{A.3}$$

$$\Theta'_{\mathrm{i}} = \frac{\mathrm{q}'_{\mathrm{i}} \cdot \mathrm{x}_{\mathrm{i}}}{\sum\limits_{\mathrm{k}}^{\mathrm{N}} \mathrm{q}'_{\mathrm{k}} \cdot \mathrm{x}_{\mathrm{k}}} \tag{A.4}$$

$$\tau_{\mathrm{i,k}} = \exp\left[-\frac{\Delta \mathrm{u}_{\mathrm{i,k}}}{\mathrm{RT}}\right] \tag{A.5}$$

For a binary mixture, γ_i is given by Equation A.6 and A.7.

$$\begin{aligned} \gamma_1 = {} & \ln\left(\frac{\Phi_1}{x_1}\right) + \left(\frac{\mathrm{z} \cdot \mathrm{q}_1}{2}\right) \cdot \ln\left(\frac{\Theta_1}{\Phi_1}\right) + \Phi_2 \cdot \left[\mathrm{l}_1 - \left(\frac{\mathrm{l}_2 \cdot \mathrm{r}_1}{\mathrm{r}_2}\right)\right] \\ & + \mathrm{q}'_1 \cdot \left[\ln\left(\theta'_1 + \theta'_2 \cdot \tau_{21}\right) + \frac{\theta'_2 \cdot \tau_{21}}{\theta'_1 + \theta'_2 \cdot \tau_{21}} \quad - \frac{\theta'_2 \cdot \tau_{12}}{\theta'_2 + \theta'_1 \cdot \tau_{12}}\right] \end{aligned} \tag{A.6}$$

$$\begin{aligned} \gamma_2 = {} & \ln\left(\frac{\Phi_2}{\mathrm{x}_2}\right) + \left(\frac{\mathrm{z} \cdot \mathrm{q}_2}{2}\right) \cdot \ln\left(\frac{\Theta_2}{\Phi_2}\right) + \Phi_1 \cdot \left[\mathrm{l}_2 - \left(\frac{\mathrm{l}_1 \cdot \mathrm{r}_2}{\mathrm{r}_1}\right)\right] \\ & + \mathrm{q}'_2 \cdot \left[\ln\left(\theta'_2 + \theta'_1 \cdot \tau_{12}\right) + \frac{\theta'_1 \cdot \tau_{12}}{\theta'_2 + \theta'_1 \cdot \tau_{12}} \quad - \frac{\theta'_1 \cdot \tau_{21}}{\theta'_1 + \theta'_2 \cdot \tau_{21}}\right] \end{aligned} \tag{A.7}$$

B Calculation of UNIFAC activity coefficients for absorption column

The components that existed in the liquid phase were divided into UNIFAC groups and UNIFAC parameters (size and surface parameters). The division of the components into groups is given in Table B.1 with the size and surface parameters for each group given in Table B.2. Methylene glycol is considered as a single group, while hemiformal, poly(oxymethylene) glycol and poly(oxymethylene) hemiformal were divided into several groups.

Table B.1: Division of components in UNIFAC groups.

Component	**UNIFAC group**	
Formaldehyde	1 CH_2O	
Water	1 H_2O	
Methanol	1 CH_3OH	
Methylene Glycol	1 $HO(CH_2O)H$	
Hemiformal	1 CH_2O, 1 CH_3OH	
Poly(oxymethylene) glycol	(n-1) CH2O, 2 OH, 1 CH2	$n > 1$
Poly(oxymethylene) hemiformal	(n-1) CH2O, 2 CH3OH, 1 CH2OH	$n > 1$

Table B.2: Size and surface parameters for the UNIFAC groups.

Group	**No.**	**R**	**Q**
CH_2O	1	0.9183	0.780
H_2O	2	0.9200	1.400
$HO(CH_2O)H$	3	2.6744	2.940
OH	4	1.0000	1.200
CH_2	5	0.6744	0.540
CH_3O	6	1.1450	1.088
CH_3OH	7	1.4311	1.432
CH_2OH	8	1.2044	1.124

The UNIFAC interaction parameters $a_{i,j}$ that were used to describe the interactions in the liquid are given in Table B.3. Where i,j denote the group numbers for the groups listed in Table B.2.

Table B.3: UNIFAC interaction parameters, $a_{i,j}$, [K].

i	**j = 1**	**2**	**3**	**4**	**5**	**6**	**7**	**8**
1	-	774.81	189.21	237.7	83.36	0.0	238.4	238.4
2	-142.35	-	189.52	-229.1	300.0	-219.29	289.6	$_{2,8}$
3	59.20	-191.82	-	-229.1	300.0	-142.35	289.6	289.6
4	28.06	353.5	353.5	-	156.4	112.82	-137.1	-137.1
5	251.5	1318.0	1318.0	986.5	-	447.77	697.2	697.2
6	0.0	423.75	774.81	1164.81	272.96	-	238.4	238.4
7	-128.6	-181.0	-181.0	249.1	16.51	-128.6	-	0.0
8	-128.6	$a_{8,2}$	-181.0	249.1	16.51	-128.6	0.0	-

The interaction parameters for $a_{8,2}$ and $a_{2,8}$ were fitted to experimental data and were therefore calculated separately. This was done using Equation B.1 with the coefficients shown in Table B.4, with T being the temperature of the liquid in Kelvin.

$$a_{i,j} = A + B/T \tag{B.1}$$

Table B.4: Coefficients for the fitted interaction parameters $a_{2,8}$ and $a_{8,2}$.

Function	**A**	**B**
$a_{2,8}$	$4.516 \cdot 10^3$	$-1.141 \cdot 10^5$
$a_{8,2}$	$-1.018 \cdot 10^3$	$3.299 \cdot 10^5$

The UNIFAC model follows the ASOG model, in which the activity coefficients of a liquid are described based on the group contribution of the liquid components. Using data given in the tables above, this allows for the calculation of the activity coefficients from the liquid composition.

The UNIFAC equation for a molecular liquid component i is given in Equation B.2. In which the activity coefficient(γ_i) is found from the sum of the combinatorial coefficient($\gamma_{i,c}$) given by Equation B.3 and the residual coefficient($\gamma_{i,R}$) given by Equation B.9.

$$\ln \gamma_i = \ln \gamma_{i,c} + \ln \gamma_{i,R} \tag{B.2}$$

$$\ln \gamma_{i,c} = \ln \frac{\Phi_i}{x_i} + \frac{z}{2} \cdot q_i \cdot \ln \frac{\theta_i}{\Phi_i} + l_i - \frac{\Phi_i}{x_i} \cdot \Sigma_j x_j \cdot l_j \tag{B.3}$$

Here Φ_i is given by Equation B.4, θ_i is given by Equation B.5 and l_i is given by Equation B.6, while z is the coordination factor assumed to equal 10 and x_i is the fraction of component i. This is similar to the UNIQUAC calculations done in Appendix A.

$$\Phi_{\mathrm{i}} = \frac{\mathrm{q_i x_i}}{\Sigma_{\mathrm{j}} \mathrm{q_j x_j}} \tag{B.4}$$

$$\theta_{\mathrm{i}} = \frac{\mathrm{r_i x_i}}{\Sigma_{\mathrm{j}} \mathrm{r_j x_j}} \tag{B.5}$$

$$\mathrm{l_i} = \frac{\mathrm{z}}{2} \cdot (\mathrm{r_i} - \mathrm{q_i}) - (\mathrm{r_i} - 1) \tag{B.6}$$

For the UNIFAC model, the combinatorial part of the activity is used directly, with only pure component properties being used in the equation. The parameters $\mathrm{q_i}$ and $\mathrm{r_i}$ are calculated as the sum of the group volume ($\mathrm{R_k}$) and group area ($\mathrm{Q_k}$) parameters, as shown in Equation B.7 and Equation B.8. Where $\mathrm{v_k}$ is the number of groups k in molecule i. The group size and surface parameters R and Q are given in Table B.2.

$$\mathrm{r_i} = \Sigma_{\mathrm{k}} \mathrm{v_k} \cdot \mathrm{R_k} \tag{B.7}$$

$$\mathrm{q_i} = \Sigma_{\mathrm{k}} \mathrm{v_k} \cdot \mathrm{Q_k} \tag{B.8}$$

The residual part of the activity coefficient is calculated from the solution-of-group concept given in Equation B.9.

$$\ln \mathrm{y_i^R} = \Sigma_{\mathrm{k}} \mathrm{v_k^{(i)}} [\ln \Gamma_{\mathrm{k}} - \ln \Gamma_{\mathrm{k}}^{(\mathrm{i})}] \tag{B.9}$$

Where Γ_{k} is the group residual activity coefficient and $\Gamma_{\mathrm{k}}^{(\mathrm{i})}$ is the residual activity coefficient of group k in a reference solution containing only molecule i ($\mathrm{x_i} = 1$). The group activity coefficient Γ_{k} is found from Equation B.10.

$$\ln \Gamma_{\mathrm{k}} = \mathrm{Q_k}[1 - \ln(\Sigma_{\mathrm{m}} \Theta_{\mathrm{m}} \Psi_{\mathrm{mk}}) - \Sigma_{\mathrm{m}}(\frac{\Theta_{\mathrm{m}} \Psi_{\mathrm{km}}}{\Sigma_{\mathrm{n}} \Theta_{\mathrm{n}} \Psi_{\mathrm{nm}}})] \tag{B.10}$$

Θ_{m} is the area fraction of group m, and the sums are over all different groups. Θ_{m} is calculated in the same way as θ_{i} as shown in Equation B.11. The group interaction parameter Ψ_{mn} is calculated from the group-interaction parameters $\mathrm{a_{mn}}$ listed in Table B.4 as shown in Equation B.12.

$$\Theta_{\mathrm{m}} = \frac{\mathrm{Q_m X_m}}{\Sigma_{\mathrm{n}} \mathrm{Q_n X_n}} \tag{B.11}$$

$$\Psi_{\mathrm{mn}} = \exp - (\frac{\mathrm{a_{mn}}}{\mathrm{T}}) \tag{B.12}$$

C Comparison of vapour composition between the VLE model and results obtained by Maurer's model for similar total liquid compositions

The VLE model including formaldehyde polymer formation was compared with the model developed by Maurer [1]. In the paper "Vapour–Liquid Equilibrium of Aqueous Solutions of Formaldehyde and Methanol", several vapour compositions calculated from total liquid composition by the model are given.[1] The comparison was made between the resulting vapour composition of both models, based on the given liquid composition of formaldehyde and methanol. The remaining liquid phase consisted of water.

For the comparison, the polymer formation model was given the total liquid composition, giving the true composition of the liquid phase, including the polymers. The activity coefficients were then calculated based on the true liquid composition and used in the VLE model to define the vapour phase. The model includes methylene glycol and hemiformal in the vapour, similar to the VLE model used by Maurer [1]. As the vapour composition in the paper is given as the total composition of formaldehyde, methanol and water, the total vapour composition was calculated.

The comparison was made with various compositions at temperatures 333.1 K, 363.2 K and 383.1 K taken from the same paper. The comparison was made for the same compositions with a both polymer length of 3 and 5. The results for a temperature of 333.1 K are given in Table C.1 and Table C.2. For 363.2 K, the results from the comparison for both polymer lengths are shown in Table C.3 and Table C.4. The final comparisons for a temperature of 383.1 K are shown in Table C.5 and Table C.6.

Table C.1: The resulting vapour composition for the model and the model proposed by Maurer at 333.1 K and a polymer length of 3 [1].

Component	$\mathbf{x_{liquid}}$	$\mathbf{y_{Model}}$	$\mathbf{y_{Maurer}}$	$\Delta\mathbf{y}$	$\Delta\mathbf{y_{relative}}\%$
Formaldehyde	0.0057	0.0051	0.0052	-0.0001	-0.9829
Methanol	0.0084	0.0696	0.0695	0.0001	0.1945
Water	0.9859	0.9252	0.9253	-0.0001	-0.0091
Formaldehyde	0.0082	0.0024	0.0024	0.0000	0.5845
Methanol	0.4144	0.7531	0.7531	0.0000	0.0028
Water	0.5774	0.2445	0.2445	0.0000	-0.0142
Formaldehyde	0.0436	0.0096	0.0096	0.0000	-0.4117
Methanol	0.6343	0.8528	0.8528	0.0000	-0.0005
Water	0.3221	0.1376	0.1376	0.0000	0.0319
Formaldehyde	0.1053	0.0645	0.0643	0.0002	0.3507
Methanol	0.1345	0.3914	0.3916	-0.0002	-0.0539
Water	0.7602	0.5441	0.5441	0.0000	-0.0026

Table C.2: The resulting vapour composition for the model and the model proposed by Maurer at 333.1 K and a polymer length of 5 [1].

Component	x_{liquid}	y_{Model}	y_{Maurer}	Δy	$\Delta y_{relative}\%$
Formaldehyde	0.0057	0.0051	0.0052	-0.0001	-0.9838
Methanol	0.0084	0.0696	0.0695	0.0001	0.1945
Water	0.9859	0.9252	0.9253	-0.0001	-0.0091
Formaldehyde	0.0082	0.0024	0.0024	0.0000	0.5845
Methanol	0.4144	0.7531	0.7531	0.0000	0.0028
Water	0.5774	0.2445	0.2445	0.0000	-0.0142
Formaldehyde	0.0436	0.0096	0.0096	0.0000	-0.4123
Methanol	0.6343	0.8528	0.8528	0.0000	-0.0005
Water	0.3221	0.1376	0.1376	0.0000	0.0319
Formaldehyde	0.1053	0.0643	0.0643	0.0000	-0.0770
Methanol	0.1345	0.3918	0.3916	0.0002	0.0417
Water	0.7602	0.5440	0.5441	-0.0001	-0.0209

Table C.3: The resulting vapour composition for the model and the model proposed by Maurer at 363.2 K and a polymer length of 3 [1].

Component	x_{liquid}	y_{Model}	y_{Maurer}	Δy	$\Delta y_{relative}\%$
Formaldehyde	0.0058	0.0078	0.0077	0.0001	1.3163
Methanol	0.0098	0.0693	0.0691	0.0002	0.2634
Water	0.9844	0.9229	0.9232	-0.0003	-0.0307
Formaldehyde	0.0089	0.0028	0.0028	0.0000	-0.7789
Methanol	0.5126	0.7768	0.7768	0.0000	-0.0026
Water	0.4785	0.2204	0.2204	0.0000	0.0189
Formaldehyde	0.0996	0.1001	0.0988	0.0013	1.2740
Methanol	0.0341	0.1108	0.1114	-0.0006	-0.5218
Water	0.8663	0.7891	0.7898	-0.0007	-0.0858
Formaldehyde	0.1259	0.0528	0.0528	0.0000	0.0211
Methanol	0.4060	0.6688	0.6689	-0.0001	-0.0200
Water	0.4681	0.2784	0.2783	0.0001	0.0440

Table C.4: The resulting vapour composition for the model and the model proposed by Maurer at 363.2 K and a polymer length of 5 [1].

Component	$\mathbf{x_{liquid}}$	$\mathbf{y_{Model}}$	$\mathbf{y_{Maurer}}$	$\mathbf{\Delta y}$	$\mathbf{\Delta y_{relative}}$%
Formaldehyde	0.0058	0.0078	0.0077	0.0001	1.3156
Methanol	0.0098	0.0693	0.0691	0.0002	0.2635
Water	0.9844	0.9229	0.9232	-0.0003	-0.0307
Formaldehyde	0.0089	0.0028	0.0028	0.0000	.0.7789
Methanol	0.5126	0.7768	0.7768	0.0000	-0.0026
Water	0.4785	0.2204	0.2204	0.0000	0.0189
Formaldehyde	0.0996	0.0988	0.0988	0.0000	0.0467
Methanol	0.0341	0.1113	0.1114	-0.0001	-0.1062
Water	0.8663	0.7799	0.7898	0.0001	0.0091
Formaldehyde	0.1259	0.0528	0.0528	0.0000	-0.0456
Methanol	0.4060	0.6688	0.6689	-0.0001	-0.0137
Water	0.4681	0.2784	0.2783	0.0001	0.0416

Table C.5: The resulting vapour composition for the model and the model proposed by Maurer at 383.1 K and a polymer length of 3 [1].

Component	$\mathbf{x_{liquid}}$	$\mathbf{y_{Model}}$	$\mathbf{y_{Maurer}}$	$\mathbf{\Delta y}$	$\mathbf{\Delta y_{relative}}$%
Formaldehyde	0.0059	0.0101	0.0101	0.0000	0.3222
Methanol	0.0099	0.0643	0.0644	-0.0002	-0.0833
Water	0.9842	0.9255	0.9255	0.0000	0.0023
Formaldehyde	0.0063	0.0085	0.0085	0.0000	-0.2043
Methanol	0.0475	0.2428	0.2426	0.0002	0.0791
Water	0.9462	0.7487	0.7489	-0.0002	-0.0233
Formaldehyde	0.0073	0.0050	0.0050	0.0000	0.1855
Methanol	0.1984	0.5431	0.5431	0.0000	0.0041
Water	0.7943	0.4519	0.4519	0.0000	-0.0069
Formaldehyde	0.0101	0.0041	0.0041	0.0000	0.2138
Methanol	0.4269	0.7157	0.7158	-0.0001	-0.0075
Water	0.5630	0.2801	0.2801	0.0000	0.0159

Table C.6: The resulting vapour composition for the model and the model proposed by Maurer at 383.1 K and a polymer length of 5 [1].

Component	$\mathbf{x_{liquid}}$	$\mathbf{y_{Model}}$	$\mathbf{y_{Maurer}}$	$\mathbf{\Delta y}$	$\mathbf{\Delta y_{relative}\%}$
Formaldehyde	0.0059	0.0101	0.0101	0.0000	0.3216
Methanol	0.0099	0.0643	0.0644	-0.0001	-0.0832
Water	0.9842	0.9255	0.9255	0.0000	0.0023
Formaldehyde	0.0063	0.0085	0.0085	0.0000	-0.2045
Methanol	0.0475	0.2428	0.2426	0.0002	0.0791
Water	0.9462	0.7487	0.7489	-0.0002	-0.0233
Formaldehyde	0.0073	0.0050	0.0050	0.0000	0.1855
Methanol	0.1984	0.5431	0.5431	0.0000	0.0041
Water	0.7943	0.4519	0.4519	0.0000	-0.0069
Formaldehyde	0.0101	0.0041	0.0041	0.0000	0.2138
Methanol	0.4269	0.7157	0.7158	-0.0001	-0.0075
Water	0.5630	0.2801	0.2801	0.0000	0.0159

D Calculated activity coefficients compared to Susort N. calculations

The activity coefficients calculated by the model developed in this thesis were compared to the activities found by an earlier model developed by co-supervisor Susort N. from Dynea [11]. The found activities at different temperatures and total compositions were compared. Both of these models use the UNIFAC model described in Appendix B to find the component activity. The composition of the liquid is defined as the outcome after selected complete liquid compositions have reacted. These were taken from the comparison between the VLE of the model developed in this thesis and the VLE of the model by Maurer shown in Appendix C. The activity coefficients reached by the models were compared for different compositions at temperatures of 333.1 K, 363.2 K and 383.1 K. All comparisons were performed with a maximum polymer formation length of 5.

Table D.1: Comparison of activity coefficients (γ) found by the model and the model by Susort N. for a temperature of 333 K [11].

Component	$\tilde{\mathbf{x}}_{\mathbf{liquid}}$	$\mathbf{x}_{\mathbf{liquid}}$	$\gamma_{\mathbf{Model}}$	$\gamma_{\mathbf{Sosort}}$	$\Delta\gamma$
FA	0.0057	3.2844e-05	3.1536	3.1536	0.0
W	0.9859	0.9870	1.0002	1.0002	0.0
Me	0.0084	0.0073	2.2053	2.2053	0.0
MG	0	0.0044	0.5536	0.5536	0.0
HF	0	0.0011	2.9650	2.9650	0.0
MG2	0	6.3199e-05	1.3276	1.3276	0.0
MG3	0	7.3343e-07	1.4908	1.4908	0.0
MG4	0	8.2097e-09	1.7357	1.7357	0.0
MG5	0	9.0094e-11	2.0613	2.0613	0.0
HF2	0	1.9290e-05	4.6199	4.6199	0.0
HF3	0	3.6523e-07	6.7522	6.7522	0.0
HF4	0	7.1936e-09	9.4870	9.4870	0.0
HF5	0	1.4555e-10	12.9755	12.9755	0.0

Table D.2: Comparison of activity coefficients (γ) found by the model and the model by Susort N. for a temperature of 363 K [11].

Component	$\tilde{\mathbf{x}}_{\mathbf{liquid}}$	$\mathbf{x}_{\mathbf{liquid}}$	$\gamma_{\mathbf{Model}}$	$\gamma_{\mathbf{Sosort}}$	$\Delta\gamma$
FA	0.0089	1.5843e-05	1.4808	1.4808	0.0
W	0.4785	0.4825	1.2273	1.2273	0.0
Me	0.5126	0.5085	1.1202	1.1202	0.0
MG	0	2.5648e-04	0.5768	0.5768	0.0
HF	0	0.0087	0.9702	0.9702	0.0
MG2	0	1.8799e-06	0.2166	0.2166	0.0
MG3	0	3.1253e-09	0.1496	0.1496	0.0
MG4	0	5.0334e-12	0.1053	0.1053	0.0
MG5	0	7.9708e-15	0.0758	0.0758	0.0
HF2	0	2.1449e-05	0.9086	0.9086	0.0
HF3	0	5.6644e-08	0.7980	0.7980	0.0
HF4	0	1.5564e-10	0.6736	0.6736	0.0
HF5	0	4.3941e-13	0.5534	0.5534	0.0

Table D.3: Comparison of activity coefficients (γ) found by the model and the model by Susort N. for a temperature of 383 K [11].

Component	$\tilde{\mathbf{x}}_{\mathbf{liquid}}$	$\mathbf{x}_{\mathbf{liquid}}$	$\gamma_{\mathbf{Model}}$	$\gamma_{\mathbf{Sosort}}$	$\Delta\gamma$
FA	0.0101	3.5906e-05	1.6248	1.6248	0.0
W	0.5630	0.5683	1.1676	1.1676	0.0
Me	0.4269	0.4216	1.1892	1.1892	0.0
MG	0	4.4789e-04	0.5627	0.5627	0.0
HF	0	0.0096	0.9838	0.9838	0.0
MG2	0	3.5921e-06	0.2591	0.2591	0.0
MG3	0	7.8517e-09	0.1902	0.1902	0.0
MG4	0	1.6670e-11	0.1437	0.1437	0.0
MG5	0	3.4863e-14	0.1102	0.1102	0.0
HF2	0	3.1085e-05	0.9758	0.9758	0.0
HF3	0	1.0680e-07	0.9075	0.9075	0.0
HF4	0	3.8182e-10	0.8111	0.8111	0.0
HF5	0	1.4028e-12	0.7054	0.7054	0.0

E Volumes and sizes

The sizes and dimensions used in the modelling of the process were taken from mechanical drawings, PFDs and P&IDs from Dynea. Some dimensions were not explicitly defined by the drawings and were instead based on assumed values.

The sizes for the vaporiser and its connected system were determined based on a technical construction drawing for the vaporiser. The volumes of the main tank, inner steam coil, gas pipe and the heating circulation pipes are listed in Table E.1

Table E.1: Volume of the equipment making up the vaporiser.

Equipment	**Volume [m^3]**
Vaporiser tank	37.164
Steam coil	0.314
Gas pipe	0.2826
Heat circulation pipes	1.4523

The sizes and dimensions for the different parts of the absorption column were determined based on the construction drawings from Dynea. Internal documents, which determined the volume and dimensions of the packing for each section, were also used to calculate the total volume of each section. For all sections, the liquid volume inside the packed parts of the column was set as 7.5% of the packing volume.

The stripper section only contains trays, and therefore, the total volume is solely dependent on the total volume of the section. The dimensions and volume for the stripper section are given in Table E.2.

Table E.2: Dimensions, number of trays and the total volume of the stripper section.

Tray column	
Diameter [mm]	2980
Hight [mm]	4000
Number of trays	5
Volume	
Total section [m^3]	27.9

Section 1 consists of a packed column with a sump below which holds the liquid to be circulated and cooled. Additionally, 4 gas risers reach from the section below to above the sump height. The dimensions for both the packed section and the sump are given in Table E.3.

Table E.3: Dimensions and volume of the packed column and sump, and the volume of the pipes for section 1.

Packing	
Diameter [mm]	2980
Hight [mm]	4000
Sump	
Diameter [mm]	2980
Hight [mm]	1100
Circulation pipes [m^3]	
Gas riser volume [m^3]	1.94
Volume	
Packing [m^3]	27.9
Sump [m^3]	7.67
Total section [m^3]	35.57

Similar to section 1, section 2 consists of a packed column with a sump below, which holds the liquid to be circulated and cooled. There are also 4 gas risers that reach from the section below to above the sump height. The dimensions for both the packed section and the sump are given in Table E.4.

Table E.4: Dimensions and volume of the packed column and sump, and the volume of the pipes for section 2.

Packing	
Diameter [mm]	2688
Hight [mm]	4000
Sump	
Diameter [mm]	2688
Hight [mm]	950
Gas riser volume [m^3]	1.77
Volume	
Packing [m^3]	22.7
Sump [m^3]	5.4
Total section [m^3]	28.1

Section 3 instead only consists of a packed column, without a sump below. There are also no circulation pipes connected to this section of the absorption column. The pipe with the liquid feed from the vaporiser is not included in the section volume. The dimensions and volumes of section 3 are given in Table E.5

Table E.5: The dimensions of the packed area and total volumes of the 3rd section.

Packing	
Diameter [mm]	1992
Hight [mm]	6000
Volume	
Packing [m^3]	18.7
Total section [m^3]	18.7

Section 4 contains a packed column with a sump below. There is also the pipe leading to the vaporiser that has been included as the volume for this section. The dimensions and volumes of section 4 are given in Table E.6

Table E.6: The dimensions of the packed area and total volumes of the 4th section.

Packing	
Diameter [mm]	1992
Hight [mm]	3000
Volume	
Packing [m^3]	9.35
Total section [m^3]	9.35

Section 5 contains a packed column with a sump below. The liquid enters from an external water source, and the piping is not included in the section volume. However, the pipe containing the vapour out of the section was included. The dimensions and volumes of this section are given in Table E.7

Table E.7: The dimensions of the packed area and total volumes of the 5th section.

Packing	
Diameter [mm]	1494
Hight [mm]	2050
Volume	
Packing [m^3]	3.6
Total section [m^3]	3.6

F Data from Lillestrøm plant

Dynea provided process data based on plant measurements recorded on February 22nd, 2023. This dataset was selected because the plant had been operating under relatively stable conditions for an extended period. As such, the data were considered to reflect steady-state operation accurately and were deemed suitable for use in the modelling work.

Target		Upstream	SplitCirc4	MixME
Stream #		2	3	3
Phase		L	L	L
Reaction enthalpy	MJ/h			
Cp correction	kJ/kg K			
		1	2	3
		Methanol feed	Aqueous bleed from absorber	Liquid feed to vaporizer
Temperature	°C	3,0	26,3	14,7
Pressure	barg	Hold	Hold	Hold
Density	kg/m3	807	1009	895
Molar mass	kg/kmol	32,0	19,5	25,5
Enthalpy	MJ/h	-261	-391	-386
Specific heat capacity	kJ/kg K	2,41	3,99	3,03
Total flow	kg/h	4793	2780	7572
Formaldehyde	kg/h	0	153	153
Water	kg/h	0	2546	2546
Methanol	kg/h	4793	81	4873
Nitrogen	kg/h	0	0	0
Oxygen	kg/h	0	0	0
Hydrogen	kg/h	0	0	0
CarbonDioxide	kg/h	0	0	0
CarbonMonoxide	kg/h	0	0	0
Ethylene Glycol	kg/h	0	0	0
Formaldehyde	kg/kg	0,0 %	5,5 %	2,0 %
Water	kg/kg	0,0 %	91,6 %	33,6 %
Methanol	kg/kg	100,0 %	2,9 %	64,4 %
Nitrogen	kg/kg	0,0 %	0,0 %	0,0 %
Oxygen	kg/kg	0,0 %	0,0 %	0,0 %
Hydrogen	kg/kg	0,0 %	0,0 %	0,0 %
CarbonDioxide	kg/kg	0,0 %	0,0 %	0,0 %
CarbonMonoxide	kg/kg	0,0 %	0,0 %	0,0 %
Ethylene Glycol	kg/kg	0,0 %	0,0 %	0,0 %
Total flow	kmol/h	149,6	148,9	298,5
Formaldehyde	kmol/h	0,0	5,1	5,1
Water	kmol/h	0,0	141,3	141,3
Methanol	kmol/h	149,6	2,5	152,1
Nitrogen	kmol/h	0,0	0,0	0,0
Oxygen	kmol/h	0,0	0,0	0,0
Hydrogen	kmol/h	0,0	0,0	0,0
CarbonDioxide	kmol/h	0,0	0,0	0,0
CarbonMonoxide	kmol/h	0,0	0,0	0,0
Ethylene Glycol	kmol/h	0,0	0,0	0,0
Formaldehyde	kmol/kmol	0,0 %	3,4 %	1,7 %
Water	kmol/kmol	0,0 %	94,9 %	47,3 %
Methanol	kmol/kmol	100,0 %	1,7 %	50,9 %
Nitrogen	kmol/kmol	0,0 %	0,0 %	0,0 %
Oxygen	kmol/kmol	0,0 %	0,0 %	0,0 %
Hydrogen	kmol/kmol	0,0 %	0,0 %	0,0 %
CarbonDioxide	kmol/kmol	0,0 %	0,0 %	0,0 %
CarbonMonoxide	kmol/kmol	0,0 %	0,0 %	0,0 %
Ethylene Glycol	kmol/kmol	0,0 %	0,0 %	0,0 %

SplitVap 3 L	Scrubber 4 L	Vaporizer 4 L	MixVapBtm 3 L
23 Aqueous bleed from vaporizer	22 Scrubber liquid to 3rd circ.	Liquid below vaporizer packing	6 Vaporizer circ. after mixing with feed
73,6	73,6	74,0	73,6
Hold	Hold	0,00	Hold
938	938	939	938
21,4	21,4	21,3	21,4
9	9	99286	98586
3,69	4,21	3,72	3,69
90	90	992428	1000000
5	5	51847	52000
63	63	694454	697000
23	23	246127	251000
0	0	0	0
0	0	0	0
0	0	0	0
0	0	0	0
0	0	0	0
0	0	0	0
5,2 %	5,2 %	5,2 %	5,2 %
69,7 %	69,7 %	70,0 %	69,7 %
25,1 %	25,1 %	24,8 %	25,1 %
0,0 %	0,0 %	0,0 %	0,0 %
0,0 %	0,0 %	0,0 %	0,0 %
0,0 %	0,0 %	0,0 %	0,0 %
0,0 %	0,0 %	0,0 %	0,0 %
0,0 %	0,0 %	0,0 %	0,0 %
0,0 %	0,0 %	0,0 %	0,0 %
4,3	4,3	47956,2	48254,7

0,2	0,2	1726,7	1731,8
3,5	3,5	38548,1	38689,4
0,7	0,7	7681,3	7833,4
0,0	0,0	0,0	0,0
0,0	0,0	0,0	0,0
0,0	0,0	0,0	0,0
0,0	0,0	0,0	0,0
0,0	0,0	0,0	0,0
0,0	0,0	0,0	0,0
3,6 %	3,6 %	3,6 %	3,6 %
80,2 %	80,2 %	80,4 %	80,2 %
16,2 %	16,2 %	16,0 %	16,2 %
0,0 %	0,0 %	0,0 %	0,0 %
0,0 %	0,0 %	0,0 %	0,0 %
0,0 %	0,0 %	0,0 %	0,0 %
0,0 %	0,0 %	0,0 %	0,0 %
0,0 %	0,0 %	0,0 %	0,0 %
0,0 %	0,0 %	0,0 %	0,0 %

SplitVap	SplitHX1	SplitHX1	HX1
2	2	3	2
L	L	L	L
			-27
4,05	4,05		4,05
Vaporizer circ. cold side	Vaporizer circ. heat exchanger inlet	Vaporizer circ. heat exchanger bypass	Vaporizer circ. heat exchanger outlet
73,6	73,6	73,6	77,1
0,00	0,00	0,00	0,00
938	938	938	936
21,4	21,4	21,4	21,4
98577	90691	7886	103635
4,05	4,05	3,69	4,05
999910	919917	79993	919917
51995	47836	4160	47836
696937	641182	55755	641182
250977	230899	20078	230899
0	0	0	0
0	0	0	0
0	0	0	0
0	0	0	0
0	0	0	0
0	0	0	0
5,2 %	5,2 %	5,2 %	5,2 %
69,7 %	69,7 %	69,7 %	69,7 %
25,1 %	25,1 %	25,1 %	25,1 %
0,0 %	0,0 %	0,0 %	0,0 %
0,0 %	0,0 %	0,0 %	0,0 %
0,0 %	0,0 %	0,0 %	0,0 %
0,0 %	0,0 %	0,0 %	0,0 %
0,0 %	0,0 %	0,0 %	0,0 %
0,0 %	0,0 %	0,0 %	0,0 %
48250,3	44390,3	3860,0	44390,3

1731,7	1593,1	138,5	1593,1
38685,9	35591,0	3094,9	35591,0
7832,7	7206,1	626,6	7206,1
0,0	0,0	0,0	0,0
0,0	0,0	0,0	0,0
0,0	0,0	0,0	0,0
0,0	0,0	0,0	0,0
0,0	0,0	0,0	0,0
0,0	0,0	0,0	0,0
3,6 %	3,6 %	3,6 %	3,6 %
80,2 %	80,2 %	80,2 %	80,2 %
16,2 %	16,2 %	16,2 %	16,2 %
0,0 %	0,0 %	0,0 %	0,0 %
0,0 %	0,0 %	0,0 %	0,0 %
0,0 %	0,0 %	0,0 %	0,0 %
0,0 %	0,0 %	0,0 %	0,0 %
0,0 %	0,0 %	0,0 %	0,0 %
0,0 %	0,0 %	0,0 %	0,0 %

MixHX1	Upstream	Blower	HXAir
3	1	2	2
L	V	V	V
4,05			
7	4	54	64
Vaporizer circ. hot side	Process air	Process air to preheater	Process air to air scrubber
76,8	3,0	47,0	47,0
Hold	0,00	0,35	0,35
936	1,272	1,470	1,470
21,4	28,8	28,8	28,8
111521	-127	217	217
4,05	1,03	1,03	1,04
999910	7712	7712	7712
51995	0	0	0
696937	18	18	18
250977	0	0	0
0	5909	5909	5909
0	1780	1780	1780
0	0	0	0
0	5	5	5
0	0	0	0
0	0	0	0
5,2 %	0,0 %	0,0 %	0,0 %
69,7 %	0,2 %	0,2 %	0,2 %
25,1 %	0,0 %	0,0 %	0,0 %
0,0 %	76,6 %	76,6 %	76,6 %
0,0 %	23,1 %	23,1 %	23,1 %
0,0 %	0,0 %	0,0 %	0,0 %
0,0 %	0,1 %	0,1 %	0,1 %
0,0 %	0,0 %	0,0 %	0,0 %
0,0 %	0,0 %	0,0 %	0,0 %
48250,3	267,7	267,7	267,7

1731,7	0,0	0,0	0,0
38685,9	1,0	1,0	1,0
7832,7	0,0	0,0	0,0
0,0	210,9	210,9	210,9
0,0	55,6	55,6	55,6
0,0	0,0	0,0	0,0
0,0	0,1	0,1	0,1
0,0	0,0	0,0	0,0
0,0	0,0	0,0	0,0
3,6 %	0,0 %	0,0 %	0,0 %
80,2 %	0,4 %	0,4 %	0,4 %
16,2 %	0,0 %	0,0 %	0,0 %
0,0 %	78,8 %	78,8 %	78,8 %
0,0 %	20,8 %	20,8 %	20,8 %
0,0 %	0,0 %	0,0 %	0,0 %
0,0 %	0,0 %	0,0 %	0,0 %
0,0 %	0,0 %	0,0 %	0,0 %
0,0 %	0,0 %	0,0 %	0,0 %

Scrubber	SplitDirAir	SplitDirAir	Vaporizer
2	2	3	2
V	V	V	V
Scrubbed air	13 Process gas to vaporizer	Process gas in bypass vaporizer	Process gas above vaporizer packing
47,0	47,0	47,0	74,0
0,34	0,34	0,34	0,27
1,460	1,460	1,460	1,213
28,8	28,8	28,8	27,3
217	217	0	12500
1,06	1,06	1,06	1,40
7712	7712	0	15195
0	0	0	148
18	18	0	2502
0	0	0	4851
5909	5909	0	5909
1780	1780	0	1780
0	0	0	0
5	5	0	5
0	0	0	0
0	0	0	0
0,0 %	0,0 %	0,0 %	1,0 %
0,2 %	0,2 %	0,2 %	16,5 %
0,0 %	0,0 %	0,0 %	31,9 %
76,6 %	76,6 %	76,6 %	38,9 %
23,1 %	23,1 %	23,1 %	11,7 %
0,0 %	0,0 %	0,0 %	0,0 %
0,1 %	0,1 %	0,1 %	0,0 %
0,0 %	0,0 %	0,0 %	0,0 %
0,0 %	0,0 %	0,0 %	0,0 %
267,7	267,7	0,0	561,9

0,0	0,0	0,0	4,9
1,0	1,0	0,0	138,9
0,0	0,0	0,0	151,4
210,9	210,9	0,0	210,9
55,6	55,6	0,0	55,6
0,0	0,0	0,0	0,0
0,1	0,1	0,0	0,1
0,0	0,0	0,0	0,0
0,0	0,0	0,0	0,0
0,0 %	0,0 %	0,0 %	0,9 %
0,4 %	0,4 %	0,4 %	24,7 %
0,0 %	0,0 %	0,0 %	26,9 %
78,8 %	78,8 %	78,8 %	37,5 %
20,8 %	20,8 %	20,8 %	9,9 %
0,0 %	0,0 %	0,0 %	0,0 %
0,0 %	0,0 %	0,0 %	0,0 %
0,0 %	0,0 %	0,0 %	0,0 %
0,0 %	0,0 %	0,0 %	0,0 %

MixRecirc 3 V	MixVapTop 3 V	UpstreamSteam 5 V	MixSteamInj 3 V
Process gas after mixing with recirc. gas	Process gas prior steam injection	Post-vaporization steam injection	55 Process gas superheater inlet
74,0	74,0	132,0	74,0
0,27	0,27	0,27	0,27
1,201	1,201	1,583	1,201
27,0	27,0	18,0	27,0
12790	12790	0	12790
1,39	1,39	2,03	1,39
15195	15195	0	15195
148	148	0	148
2502	2502	0	2502
4851	4851	0	4851
5909	5909	0	5909
1780	1780	0	1780
0	0	0	0
5	5	0	5
0	0	0	0
0	0	0	0
1,0 %	1,0 %	0,0 %	1,0 %
16,5 %	16,5 %	100,0 %	16,5 %
31,9 %	31,9 %	0,0 %	31,9 %
38,9 %	38,9 %	0,0 %	38,9 %
11,7 %	11,7 %	0,0 %	11,7 %
0,0 %	0,0 %	0,0 %	0,0 %
0,0 %	0,0 %	0,0 %	0,0 %
0,0 %	0,0 %	0,0 %	0,0 %
0,0 %	0,0 %	0,0 %	0,0 %
561,9	561,9	0,0	561,9

4,9	4,9	0,0	4,9
138,9	138,9	0,0	138,9
151,4	151,4	0,0	151,4
210,9	210,9	0,0	210,9
55,6	55,6	0,0	55,6
0,0	0,0	0,0	0,0
0,1	0,1	0,0	0,1
0,0	0,0	0,0	0,0
0,0	0,0	0,0	0,0
0,9 %	0,9 %	0,0 %	0,9 %
24,7 %	24,7 %	100,0 %	24,7 %
26,9 %	26,9 %	0,0 %	26,9 %
37,5 %	37,5 %	0,0 %	37,5 %
9,9 %	9,9 %	0,0 %	9,9 %
0,0 %	0,0 %	0,0 %	0,0 %
0,0 %	0,0 %	0,0 %	0,0 %
0,0 %	0,0 %	0,0 %	0,0 %
0,0 %	0,0 %	0,0 %	0,0 %

HXSup 2 V	Reactor 2 V	WHB 4 V	WHBeco 4 V
9 Feed gas to converter	Post-reaction gas	Product gas after waste heat boiler	10 Product gas to stripper before quenching
84,0	646,0	220,0	220,0
0,25	0,16	0,14	0,14
1,151	0,348	0,640	0,640
27,0	22,8	22,8	22,8
13000	25823	14963	14963
1,36	1,83	1,51	1,51
15195	15195	15195	15195
148	4134	4134	4134
2502	4277	4277	4277
4851	139	139	139
5909	5909	5909	5909
1780	0	0	0
0	127	127	127
5	565	565	565
0	44	44	44
0	0	0	0
1,0 %	27,2 %	27,2 %	27,2 %
16,5 %	28,1 %	28,1 %	28,1 %
31,9 %	0,9 %	0,9 %	0,9 %
38,9 %	38,9 %	38,9 %	38,9 %
11,7 %	0,0 %	0,0 %	0,0 %
0,0 %	0,8 %	0,8 %	0,8 %
0,0 %	3,7 %	3,7 %	3,7 %
0,0 %	0,3 %	0,3 %	0,3 %
0,0 %	0,0 %	0,0 %	0,0 %
561,9	667,6	667,6	667,6

4,9	137,7	137,7	137,7
138,9	237,4	237,4	237,4
151,4	4,3	4,3	4,3
210,9	210,9	210,9	210,9
55,6	0,0	0,0	0,0
0,0	62,8	62,8	62,8
0,1	12,8	12,8	12,8
0,0	1,6	1,6	1,6
0,0	0,0	0,0	0,0
0,9 %	20,6 %	20,6 %	20,6 %
24,7 %	35,6 %	35,6 %	35,6 %
26,9 %	0,6 %	0,6 %	0,6 %
37,5 %	31,6 %	31,6 %	31,6 %
9,9 %	0,0 %	0,0 %	0,0 %
0,0 %	9,4 %	9,4 %	9,4 %
0,0 %	1,9 %	1,9 %	1,9 %
0,0 %	0,2 %	0,2 %	0,2 %
0,0 %	0,0 %	0,0 %	0,0 %

NTNU

Norwegian University of
Science and Technology